STUDY AND ANALYSIS OF SEMG SIGNAL FOR ENHANCEMENT OF ABOVE SHOULDER MYOELECTRIC ARM FUNCTIONALITY

A Thesis

In fulfilment of the requirement for the award of degree of

DOCTOR OF PHILOSOPHY

Submitted by

Amanpreet Kaur
(Registration No. 950906044)

Under the supervision of

Dr. Ravinder Agarwal
Professor, EIED
Thapar University, Patiala

Dr. Amod Kumar
Chief Scientist,
CSIO, Chandigarh

Submitted to

DEPARTMENT OF ELECTRONICS AND COMMUNICATION ENGINEERING
THAPAR UNIVERSITY, PATIALA-147004
PUNJAB (INDIA)

JULY 2017

Certificate

It is certified that the work contained in the thesis titled, "**Study and Analysis of sEMG Signal for Enhancement of above Shoulder Myoelectric Arm Functionality**", for the award of degree of **Doctor of Philosophy** in Electronics and Communication Engineering Department (ECED), Thapar University, Patiala, has been carried out under our ssupervision and the results presented in this thesis has not been submitted elsewhere for any other degree.

Dr. Ravinder Agarwal
Professor and Head, EIED
Thapar University,
Patiala.

Dr. Amod Kumar
Chief Scientist
CSIO, Chandigarh

ਨਹੀਂ ਕੋਈ ਤੁਮ ਬਿਨੁ ਅਵਰੁ ਹਮਾਰਾ॥

ਜੋ ਕੁਰ ਹੈ ਹਮਰੀ ਪ੍ਰੀਤਪਾਰਾ॥ (ਭਾਈ ਗੁਰਦਾਸ ਜੀ)

Oh my Generous Guru ! without You, I have no body, I am foolish and ignorant; I seek Your Shelter. Please be Merciful and unite me with the Almighty Lord.

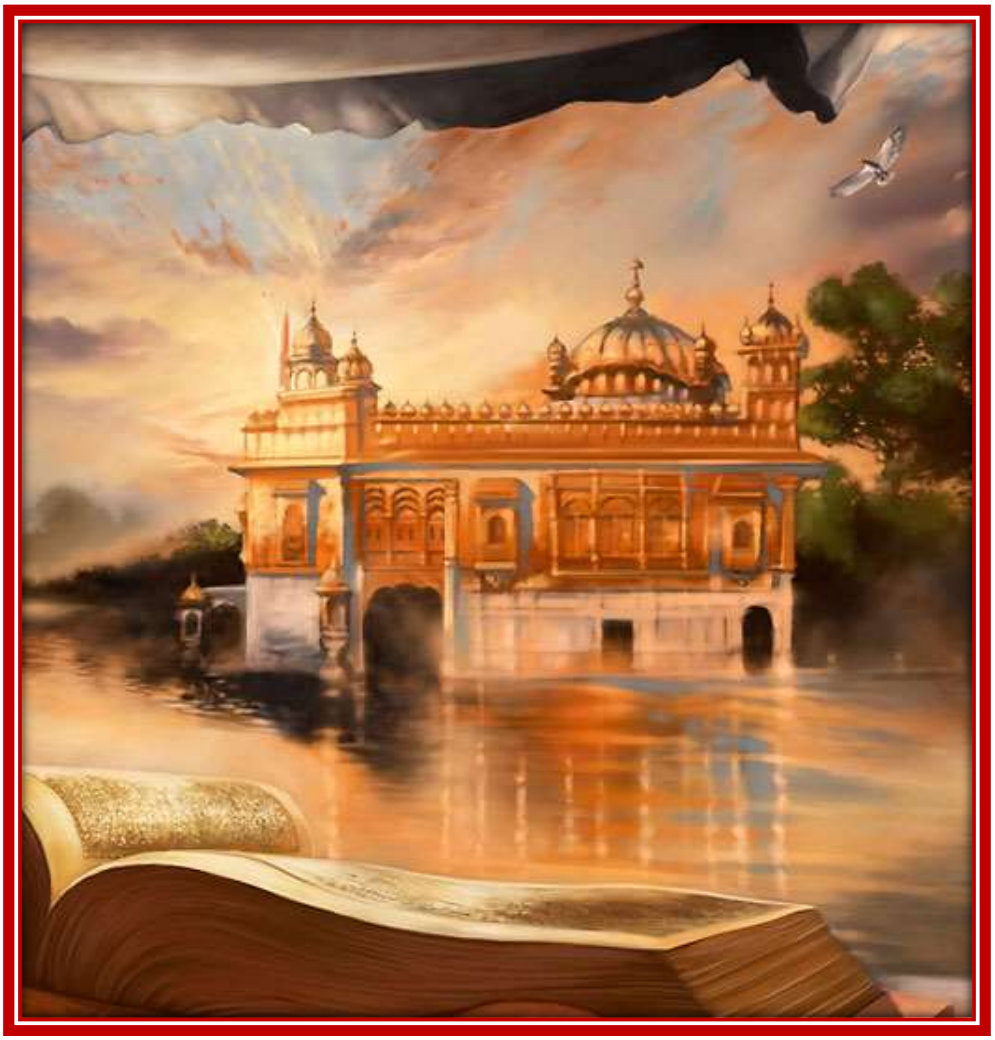

Dhan Shri Guru Granth Sahib Ji

Acknowledgement

This thesis is the culmination of my journey of Ph.D. which was just like climbing a high peak step by step accompanied with encouragement, hardship, trust and frustration. When I found myself at top experiencing the feeling of fulfilment, I realized though only my name appears on the cover of this dissertation, a great many people have contributed to accomplish this huge task.

First and foremost, I bow my head humbly before my greatest teacher, Almighty Dhan Shri Guru Granth Sahib Ji for making me capable of completing my Ph.D. Thesis; with HIS blessings only I have accomplished this huge task. I could have never done this without HIS blessings. I feel very fortunate to have HIS blessings during all these years of my life. HE is the true shepherd of my life. HIS hold on me is stronger than my hold on HIM.

I owe a deep debt of gratitude to my university 'Thapar University, Patiala' for giving me an opportunity to complete this work.

I express deep sense of gratitude and thankfulness to my research advisors, Dr. Ravinder Agarwal and Dr. Amod Kumar for their support and guidance during the course of my study. They are always there for me and had my best interest at heart. They always pointed me when I lost the path and supported me when I was in right path inspite of their busy schedule. I found their guidance to be extremely valuable. I am very thankful to Dr. Ravinder Agarwal who made me introduce to Dr. Amod Kumar when I started my journey of Ph.D. I have not seen such a person in my life who is very easy in technical discussion via telephone. He has helped me at each and every point of my research work with patience and enthusiasm. The discussion at every step felt very energetic and full of energy. He ensuring that the fire keeps burning and being there at times, when I required motivation and propelling me on the course of this thesis. Lastly, I would like to add that my mentors are such persons that are willing to give me insight and pointers to tackle the problem. My respect for them will always grow throughout my life.

I am extremely thankful to my head of department Dr. Alpana Agarwal, senior faculty members Dr. Sanjay Sharma, Dr. A.K Chatterjee and Dr. Rajesh Khanna for encouraging me

throughout my research work. I also thanks to Dr. Kulbir Singh and Dr. Mandeep Singh being on my Ph.D committee members. Their suggestions and comments have really helped me in bringing this thesis to the present shape. I would like to thank my colleagues Mr. A.K Chatterjee, Dr. Hardeep Singh, Dr. Rahul Upadhyay, Dr. Ravi Kumar, Dr. Parshant Singh Rana and Dr. Ajayinder Singh Jawanda for supporting me and helping me in different stages of work.

I express my gratitude to my friend Ms. Sakshi who have helped me in different stages. She has, kept me going on my path to success, assisting me as per their abilities, in whatever manner possible and for ensuring that good times keep flowing. Her support, encouragement and credible ideas have been great contributors in the completion of the thesis. I never forgot the help given me by Mr. Shivam, Mr. Rohit and Ms. Geetali for their fruitful discussion at various stages.

My acknowledgement would be incomplete without thanking the biggest source of my strength, my family. I owe thanks to a very special person, my husband, S. Jaspreet Singh for his continued and unfailing love, support and understanding during my pursuit of Ph.D degree that made the completion of thesis possible. He was always around at times I thought that it is impossible to continue, he helped me to keep things in perspective. He has been my source of inspiration and motivation and helped me in both practical and theoretical aspect of thesis work. I greatly value his contribution, deeply appreciate his belief in me and also thank him for sending his holy spirit to my heart. I appreciate my baby, my little cute daughter Jotroop Kaur for abiding my ignorance and the patience she showed during my thesis work. Words would never say how grateful I am to both of you. I consider myself the luckiest in the world to have such a lovely and caring husband standing beside me with their love and unconditional support. He is one of my greatest blessing from GOD.

I would like to thank my family for standing by me through all the joys and sorrows that life had to offer. My heartfelt thanks and life-long gratitude go to my parents who has raised me and wanted me to study more and more and do best in the life. They made things seem a lot easier than they were, with their tireless support and lot of blessing and support. A very special thanks to my brother and sister-in -law for their cooperation and support. The presence of my parents-in law and in every endeavour of my life is also very supporting and

appreciative for all of sacrifices that they have made on my behalf. I am really grateful for them giving up so much time to look after my daughter. I am very thankful to my father- in law for their blessings and support. I am also very grateful to my sister-in *–law who has provided me the dedicated study space and giving special support to me in these days. A very special thanks to my niece Divjot, nephew Taran and niece- in- law Seerat for giving company to my daughter during my thesis writing.*

No research is possible without the Library, I take this time to express my gratitude to all the library staff for their services and special thanks to Ms. Archan Nanda and Mr Rakesh who have helped me in solving different issues regarding the Ph.D. thesis work. I would also like to thank non- teaching staff of ECED department for their kind help.

.

I am grateful to you the different authors of the Literature I have gone through without which it would have been impossible for me to carry out this exciting research. I have tried to express my gratitude to every person who contributed in this work directly or indirectly, there may still be someone hiding behind the veils of my forgetful part of memory. Last but not the least; I would like to thank all such great souls.

Amanpreet Kaur
Thapar University,
Patiala

Abstract

Upper limb amputation is a traumatic event that can seriously affect the person's capacity to perform regular tasks and can lead individuals to lose their confidence and autonomy. Prosthetic devices can give relief by acting as substitute the function of missing limb which can help to improve the quality of life of the amputees. In recent years, myoelectric devices have received extensive attraction to provide enhanced degree of freedom over traditional devices. Myoelectric prosthesis is controlled via the acquisition and processing of electromyogram signal produced at the muscles fibre from the surface of body with an array of electrode placed on the residual limb. The acquired signal is a complex one being dependent on the physiological and anatomical property of muscles. The electrodes convert muscles-activity from the torso into information that can be processed by different techniques. The unwanted noise contributes from the electrolyte skin surface, while travelling through the muscles. To make the noisy signal useful, advancement in the detection and processing of the signal becomes a very important requirement in biomedical engineering. The signal has to undergo pre-processing stage consisting of amplification, filtering and adaptive peak detection etc. to reduce the noise level in the raw signal. The different signal processing techniques such as time domain techniques, wavelet coefficients and autoregressive coefficients have been applied to increase the information yield from the EMG signal. Different algorithms to identify the intended movements are available that rely on the feature extraction that provide the user with access to multiple degrees of freedom and have shown great promise in research literature. The identified information of movements is translated into control signal to drive the artificial limb and the force generated by the artificial limb can be varied by the user's muscles intensity.

The commercially available myoelectric prostheses do not allow to control the transhumeral level and shoulder disarticulation level of amputation. For transhumeral amputee with no muscles-activity or very less muscles-activity in the residual limb there is no intuitive control source for either elbow or hand, therefore controlling the prosthetic device is impossible with existing techniques. As a result, better strategy is required to control a prosthesis for a high-level amputation. Further studies are required to improve the training protocol and analysis of the signal for development of the prosthetic devices for these applications. The main contribution of this thesis to implement the prosthesis based on the EMG signal from the set of shoulder muscles intact in the transhumeral amputee. For this, an overview of the human

shoulder muscles anatomy was carried out. The acquired SEMG data with the different shoulder movement are described. Various pre-processing techniques and adaptive peak detection techniques were explored. A new threshold method was developed and applied to filter the unwanted peaks in the pre-processing stage of the SEMG signal. Next step was to investigate the shoulder movements of amputees and non-amputees and compare the EMG activity based on the amplitude level of the signal. Different signal analysis methods such as Fourier transform, short time Fourier transform and wavelet transform were investigated and wavelet transform was applied successfully. The proposed detection scheme focuses on the discrete Daubechies wavelet transform with four decomposition levels. A systematic approach for selecting the optimal wavelet transform method was proposed and demonstrated. A pattern based recognition technique was used with immediate access to four different movements at a time. A set of features was extracted from shoulder muscles of the transhumeral amputee by transforming the wavelet reconstructed coefficients to the new transformed coefficients by using the new proposed transformation method. Subsequently, investigation of classification is presented through various experiments conducted on amputees. The work was carried out with the aim to enhance the robustness in the pattern recognition system to classify different shoulder movements so that it is helpful for making a more reliable and useful device. To classify the different shoulder motions, various machine learning algorithms were compared to select the optimal and efficient algorithm. A data mining Random forest classifier was utilized in this work which was found better than other classifiers. These classification results were evaluated and validated by a prototype using Arduino motor controller for elbow and hand movement.

Myoelectric signal is one of the control signals for controlling the powered prosthesis. A number of commercial products have been developed for these prostheses. But these devices are still insufficient to satisfy the needs of amputee. The precise measurement and analysis of human movements and muscles activity are essential processes in rehabilitation. In India, the maximum amputation rate is for below elbow which is about 52% of the total amputation. Transhumeral amputation is the second largest in upper limb amputation which is about 24% the total. The available literature and systems mostly focus on below elbow amputees and limited work is available on prosthetic design for the shoulder amputees. The researchers have largely ignored the real time SEMG signal for the transhumeral amputees with no activation in the triceps and biceps muscles with the result that a prosthetic device for such amputees is not available off the shelf. The system developed in this work is based on the data from the

amputee's muscles activation from different arm movements which allows one to have independent signals required for independent motion of elbow and hand. The system performance has been validated through an actual arm which will be worn by the amputee. The performance of arm has been checked under actual environment. The developed system promises an overall accuracy of more than 90% for correct motion of elbow and hand which shows that its functionality is very close to natural human arm.

This work presents a successful design of an affordable SEMG platform. The effort to achieve this goal will always encourage the researchers into the field of SEMG technologies. Mechanical fabrication using light composite material and electronic assembly using advanced processors can be implemented to make the arm ready for large scale clinical trials. If required, high mechanical functionality in electrode grid to follow the skin surface can be achieved by connecting the wireless sensor to produce better results. High end DSP chip system can be used to handle the large data set and the code that presently exists in MATLAB. The use of energy efficient motors, driving circuits and couplings can further improve the degree of functionalities of the arm.

The main idea of this research is to provide a set of guidelines for researchers and engineers aiming to develop their own low-cost EMG systems applicable in biomechanical, clinical, rehabilitation, sport, and research contexts. EMG signals can be used to generate device control commands for rehabilitation equipment such as robotic prostheses and can be useful in many clinical and industrial applications.

Table of Contents

List of Figures

List of Tables

Acronyms

ADP	Adaptive Denoising function
AMT	Amplitude Thresholding Method
coif	Coiflet
CWT	Continuous Wavelet Transform
db	Daubechies
dmey	Discrete Meyer
DT	Decision Tree
DWT	Discrete Wavelet Transform
FDF	Frequency Domain Features
FN	False Negative
FPR	False Positive Rate
HAR	Hard function of threshold method
Infra	Infraspinatus muscle
KNN	K Nearest Neighbour
MSE	Mean Square Error
NB	Naïve Bayes
Pect	Pectoralis muscle
RF	Random Forest
ROC	Receiver Operating Curve
sEMG	Surface Electromyogram Signal
SOF	Soft function of threshold method
STFT	Short Time Fourier Transform
SURE	Stein's Unbiased Risk Estimate thresholding rule method
SVM	Support Vector Machine
sym	Symlets
TDF	Time Domain Features
TEO	Teager Energy Operator
TFDF	Time-Frequency domain Features
TN	True Negative
TPR	True Positive Rate
WAV	Weighted averaging function
WT	Wavelet Transform

Chapter 1
Introduction

1.1 Amputation Statistics

Millions of people are suffering from the limb amputation worldwide due to accidents or because of the number of diseases. These physical impairments resulting from a complete or partial removal of the limb can hamper their ability to carry out daily activities. This amputation can be of lower limb (from gluteal to toe) or upper extremity (deltoid region to hand). The primary causes of extremity include traumatic accident, laceration from tools and machinery, cardiovascular disease, cancer etc. Lambert and Sciore [1] found that the trauma is the most common cause of amputation (loss of any part of the body due to accident or injury) in the USA accounting for 52% of all amputations [2]. Diseases cause the majority of the amputation in the UK. According to the Centre for Health Statistics, every year new amputations to the tune of 61000 partial amputations and 25000 resulting in loss of one arm take place in USA. By a crude estimate, 30% amputation is upper limb loss, transradial amputations make up 60% while 10% covers the wrist and hand amputation. Going by age statistics, 60% of amputees are between the age of 21-64 years and only 10% are under the age of 21 years [1]. The age ranges from 21 to 30 years accounting for 32% of all the amputees, the amputee in the age group 31-40 years account for 23.3% of all amputations and below the age of 20 years, the percentage is 14.2%. Gender-wise, almost 86% amputees are men. In one of the studies described by Ghosh *et al.*, [3] for Kolkata (India), out of 155 amputations, 70.3% were a victim of trauma and 27.7% were due to peripheral vascular disease shown in Figure 1.1 [4].

The upper extremity loss can broadly be classified into different types such as trans-radial, transhumeral, transcarpal, forequarter and elbow/wrist/shoulder disarticulation (Figure 1.1). The maximum amputation rate is below elbow and is about 52% of the total amputation which is the combination of trans-radial, trancarpal and wrist disarticulation [3]. The second largest part of amputation is the transhumeral amputation with 24% of the total.

1.2 Amputee Quality of Life through Prosthetics

The statistics in the last section has provided the knowledge about the need of the prosthesis for the amputees so that they can be capable of performing daily routine and social activities. A prosthetic is an artificial externally provided medical device that helps to replace the lost

arm, and its function should be near to the natural arm. Many approaches to prosthesis have been developed for cosmetic appearance, role in human life and to provide psychological advantage.

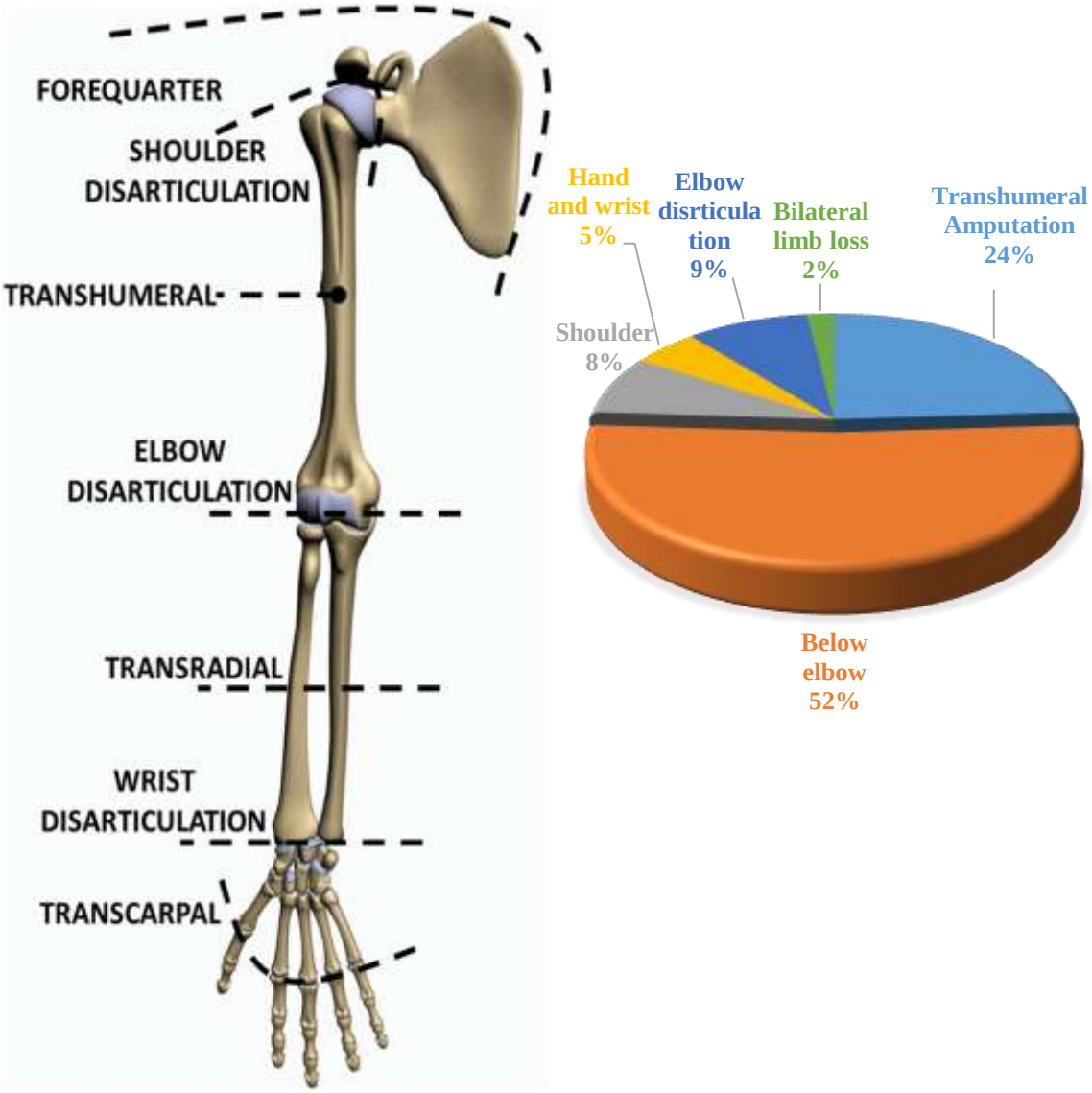

Figure 1.1: Different level of arm amputation and statistics of amputation in India [4]

Worldwide, a lot of efforts have been made to improve the activity in the working range of the prosthetic hand. The history of prosthetics started in 484 BC by Heroduts when the prosthetic was made up of little crutches, wood and leather cups [5]. Then in 1536, Ambroise Pare designed an iron prosthetic for their soldiers. In 1852, the prosthetic function was controlled by using straps connected to the shoulder to control the movement of arm and hand. However, these straps were heavy and unnatural in performance. After the American civil war, upper limb prosthetic development picked up the attention, and they refined the earlier arm by adding

more functional features. In recent years, disabled persons have been provided with a prosthetic hand that was actuated by different motors. Engineers developed a neuromuscular stimulation system to control the neuro prostheses using mathematical model but causes problem in clinical solution[6],[7]. However, a significant number of individuals do not use their prosthetic hand regularly because the hands are unpleasantly thick, strange in appearance and movements [5]. The most traditional approach, the ***cosmetic prosthesis*** replaces the missing part of the body [5], does not provide the functionality but improves the person's appearance. These are made up of silicon and PVC globe but there is no mobility in hand and arm (Figure 1.2).

Figure 1.2: Otto bock Cosmetic prosthetic hand [8]

Body powered prosthesis are a type of functional prosthesis that consists of socket, hooks, harness, wrist unit, terminal device, triceps cuff (below elbow amputee) and elbow (above elbow amputee). Bowden cables are anchored on the back of the arm between the elbow and the shoulder and are free to move within the sleeve cable. In the below elbow model, the terminal device can be opened and close by the shoulder shrug. However, the above elbow system is quite complicated because an additional cable has to control the elbow flexion [9]. In this kind of prosthesis, high energy is required to do any task and this is its main limitation [9]. O Bock *et al.*, invented an arm with an elbow arm unit that just required the terminal device (Hook and Hand). These were lightweight and low-cost prosthesis but were uncomfortable, had restricted range of motion, poor appearance, and somewhat ungainly control movement.

In electrical prosthesis, system operated devices have high efficiency with minimum loss of energy, low power consumption and reduction in battery dimensions. Primitive models of this prostheses were built with the pair of touch switches with flexor and extensors. The arm carries

the control circuitry with SET and RESET limit switches and the relay that controls the motors according to the switches thus closing and opening the hand structure. The Otto Bock power elbow structure was the most attractive externally powered prosthesis.

Hybrid model provides the combination of body powered and electrical prosthesis. These are normally used in the prosthetic limb of a person who has above elbow amputation or bilateral arm amputation. These types of prosthetic are most appropriate for a particular task. This system is hard to carry because of the body powered terminal device with heavy weight.

The next approach was the ***Myoelectric Arm*** prosthesis, implemented with the muscles signal by Reiters in 1945, specially designed for the amputee workers in Germany. The movement of any part of the body causes the activation of the muscles and produce the signal called electromyography (EMG) signal. At that time the prosthetic was not easily portable as it had a large number of vacuum tubes with a complicated wiring system. Through the late 1950s to early 1960, the previous study was continued in the same field with funding from British National Fund and designed a better myoelectric system. The control system was made that could amplify the muscles signal from two different rhythms of contractions and could control the two movements of the hand (Figure 1.3)[10] .

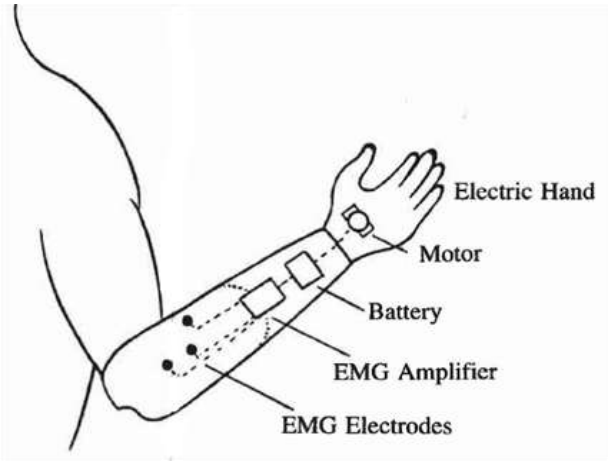

Figure 1.3: Myoelectric prosthesis contains the inbuilt amplifiers, motor and battery [10]

In the UK, Battya and Nightingale were developed the myoelectric control system for an artificial hand. At Academy of Science in USSR, Kabrinski's group designed the myoelectric control system from two different muscles and used one to control hand opening and other to monitor closing. In 1964, Sauzki developed a servo motor system with a small electrode

sensing device which was a controlled muscle system that could control more different function of the prosthesis. O Bock developed a new electric hand and arm under the leadership of Nader, so that an individual could select the arm which suits him best. Afterwards, O Bock concentrated on myoelectric control and improving the signal processing techniques used in the myoelectric hand. The biomedical signal processing came as a stepping stone for developing a diagnostic system which seemed like a successful extraction tool for the hidden information in the signal [11]. Later on, O Bock *et al.*, published their work on the hand opening and closing of the myoelectric system and started the development of the myoelectric prosthesis in 1986.

1.3 Electrodes

The prosthetic system uses the electrodes to detect the minute activity of the muscles and convert it into the electrical signal. Many different types of electrodes have used for acquiring the signal [12]. The two kinds of electrodes viz. Intramuscular electrode and Body-surface bio-potential electrodes.

Figure 1.4: Intramuscular Electrodes [12]

Intramuscular electrodes consist of stainless steel fine solid, sharp point insulated wire. A needle placed in the skeletal muscle makes contact with the nerve, reaches the point where the measurement is to be made and picks up the electrical signal by the exposed tip. It is a well-recognized technique for clinical purposes under the proper supervision of a doctor.

Body-Surface biopotential electrodes are used to record the signal from the surface of the body. These are metal plated electrodes having the metallic conductor which came in contact with skin with a thin layer of Electrolyte gel for recording the signal. German silver gold, silver and platinum are the commonly used metals for EMG recording. These electrodes are quickly

placed with a sticker on the skin. No supervision of clinical expert or doctor is required to acquire the signal from the muscles. These days, electromyogram are prefer to use to pick up surface electromyography signal. sEMG signal has a vast variety of applications in numerous field such as physiology, ergonomics, prolonged force production and controlling the prosthetic device for rehabilitation.

Figure 1.5: Surface electrode with EMG cable [12].

In myoelectric prosthesis, the electrode is accommodated in the socket of myoelectric arm. The acquired biomedical signal from the muscles activation is then analyzed with different signal processing techniques explained in next section.

1.4 SEMG Signal Analysis

The analysis of the sEMG signal includes the information recorded from different sensors mounted on various locations of the muscles, feature extraction, using features to control the system, diagnosis of malfunction and evaluation which meets the functional requirement for quality control. In the processing technique, the major problem faced with the acquired signal is the noise. The probability density function of the noise can be like that of white noise, uniform noise or additive Gaussian noise. Therefore, first step is to remove the noise and to subject the de-noised system to further signal processing [13]. Different filtering methods such as adaptive impulse correlated filter, signal input adaptive filter, Adaptive filters [10] [11], Weiner filter, Infinite impulse response or finite response filter and Kalman Filter have been used for de-noising the signal. De Luca described the four types of noise such as: motion artifact, inherent instability, ambient noise and thermal noise in electronic components. First three types of noise can be reduced with the help of different filters as described above but the fourth noise ranges in the sEMG frequency band and is, therefore, difficult to remove by the

conventional filter [11] [12]. The advanced sEMG detection and analysis techniques [8] [9] [16] (Wavelet Transform, Wavelet packet transform, higher order statistical methods) are used to overcome the various limitations in the traditional signal processing. The previous methods were based on the time domain features because of their low computation complexity. From the time and frequency domain features, different authors reported that the time domain yields better performance than the frequency domain [Chapter 2]. Even in isotonic and isometric contraction, these time domain features provide more satisfactory recognition performance besides being faster than the other features. In the frequency domain, Fast Fourier Transform technique has failed to provide the exact location of frequency components [13]. Therefore, Short Time Fourier Transform technique got the attention of has come into study. However, the main issue of time-frequency resolution was overcome by the wavelet transform. Wavelets are a powerful statistical tool used most for the de-noising of biosignals, to compress and to smoothen the data signal [13]. It becomes a logical choice of denoising method in this work. The various wavelet families such as Daubechies, Haar, Symlet, Coiflets, biorthogonal, Meyer, Morlet and Mexican Hat are used to obtain the valuable component from the wavelet by eliminating the unwanted noise and interference. The inverse discrete wavelet transform process is applied to reconstruct the signal without noise [16] [17]. The features extracted from the optimal wavelet transform are used to classify different movements of the shoulder by using different classifiers. Number of classifiers have implemented by using various algorithms for classification of the signal in the previous study.Choosing the best classifier according to the application from a significant number of the classifiers is the main challenge of this study.

The extracted features are used to classify the signal. The classifiers are evaluated on the test data after getting programmed on the training data. There are many classification methods which include Artificial Neural Network (ANN), Support Vector Machine(SVM), Linear Discriminant Analysis (LDA), K-Nearest Neighbor (KNN), Hidden Markov Models (HMM), Fuzzy Logic (FL), Genetic Algorithm (GA), Naïve Bayes Algorithm (NBA), AdaBoost learning, Random Forest (RF) *etc*. for different applications [22] [23] [24]. Significant efforts have been reported in chapter 5 to choose the best classifier from the list of large number of classifiers. The input variable is in the form of different features extracted from the wavelet transformed signal or the time domain features from the raw signal to classify the group to which incoming data most likely belongs. In the traditional validation methods, the classes of the instances were known and, therefore, the performance of the classifier was optimistic.

However, in the current study, the different methods have been considered for the classification process like hold out, cross validation, K-fold and leave-one-out validation techniques. An efficient classifier should be able to predict the actual class of a previously unseen data sample in case of myoelectric prosthesis. Therefore, the study of optimal classifiers for the classification of the shoulder movement becomes a part of this work. The results in this thesis (Chapter 5) indicate that the proposed method of classification has an excellent capability of grouping the different shoulder movements for a transhumeral amputee having no muscles-activity in triceps and biceps muscles. Also, the proposed method can be used for the analysis of the extensive data set for the shoulder disarticulation in future.

1.5 Motivation and Research Gaps

The sEMG signal finds its applications in controlling the prosthetic devices for different levels of amputation. In the cited literature (Chapter 2), the extensive work was on upper and lower limb amputation. The upper limb data was acquired from the triceps and biceps muscles from the non-amputee. The available literature mainly focuses on the detection of the EMG signal and its accuracy after processing and is mostly from the non-amputee. However, a very limited literature is available on the upper-limb prosthetic design that collects the data from the amputee's muscles activation due to different movements of the arm. It is evident from the literature cited in next chapter [Chapter 2] that the researchers have largely ignored the real time sEMG signal for the transhumeral amputee persons with nearly zero muscles activation below the shoulder and it is difficult to acquire the signal from triceps and biceps muscle for making the sEMG based prosthetic device for such amputees. It was also observed that the myoelectric arm was not considered to derive the independent control signals for elbow and hand motions. This has served as a motivation in the present research work to process the real time sEMG signal, especially for a transhumeral amputee. The main emphasis is given to the study of the sEMG signal at different muscles location of the shoulder for various movements of the shoulder.

In recent years, predicting the upper limb motion of the human has involved growing research to improve the prosthetic device performance. Recording the signal from the forearm muscles cannot provide the natural movement for higher level amputation. The whole-body coordination is impossible to drive the limb naturally by using only forearm muscles. So, it is tough to make the prosthetic device for high-level amputation. Daily life motion presents a

relationship between the shoulder, elbow and hand structure when doing the upper limb activities like throwing and catching a ball or grasping the objects on the table. Therefore, the primary aim of this study was to investigate the shoulder muscles-activity with different motions of the shoulder. Most of the researchers did not compare the muscles of amputees and non-amputees in the above-elbow conditions. There is a broad range of steady-state changes in muscle activity between an amputee and non-amputee persons. One should have the knowledge about this difference signal before making a device for prosthetic users.

The amplitude level is directly proportional to the force exerted by subjects to move the shoulder. As the muscle contraction increases, more motor units become active and the firing rate of these units also increases. The combined effect of these processes in higher levels of contraction produces so many motor unit action potentials that they cannot be distinguished individually in the signal, which is then called the interference pattern [3]. The higher level of muscles activation by the amputee or non-amputee subjects leads to the injection of additional peaks in the detected output. As these extra observed peaks misguide the prediction of the movement of the shoulder, these need to be extracted and removed from the detected output.

The wavelet transform is a powerful statistical tool mostly used in denoising process. The different features can be obtained from the decomposition coefficient of the wavelet transform. While denoising the bio signal, the system should be able to detect the best wavelet function from the various wavelet families. The optimal wavelet function is dependent upon the application. Therefore, before extracting the features from the wavelet reconstructed coefficients, the use of the optimal wavelet function from the large wavelet family should be clear.

Machine learning algorithm is a subfield of computer programming. The prediction accuracy can improve by using these algorithms for the classification process. Many algorithms used the data mining process can be applied efficiently in sEMG classification. The classifier efficiency is also dependent on the way to extract the features from the raw signal and classify these features by using the best classifier to improve the performance of the upper limb prosthesis device.

1.6 Objectives

In the present research work, the primary emphasis is given to the classification of the various movements of the shoulder performed by amputee. It was observed that the placement of sEMG electrodes on active muscles near the shoulder region could give proper information of the movement made. The main objectives of the thesis were:

1. Use of algorithm for EMG signal analysis to control the myoelectric arm.
2. To identify the location of electrodes position for above shoulder amputees.
3. Analysis of EMG signal based on different movements of the arm under normal condition.
4. To operate the prosthesis, using the myoelectric signals from muscles which act in synergy with hand function as a control signal.
5. Simulation and verification of result using soft computing technique for above shoulder.

1.7 Methodology Used to Achieve Objectives:

The main motive of the thesis was to classify the sEMG signal from the shoulder muscles so that a prosthetic device could be designed for the upper limb prosthetic user and the device can be controlled by using the different shoulder movement of the amputee. The following steps and block diagram (Figure 1.7) depict the objectives mentioned above in Section 1.6.

In biomedical signal processing, extensive efforts have been made to develop new algorithms and different detection techniques to reduce the unwanted noise signal from the acquired sEMG signal. Therefore, it is significant to study the various existing algorithms and to choose the best algorithm for the analysis of the shoulder sEMG signal. Traditional methods have a lot of limitations for processing the original signal. With the advancement in the technology, different signal processing tools and various mathematical models have attracted attention. In the past, signal analysis techniques of time domain analysis, frequency domain analysis and time-frequency analysis have been carried out. The wavelet analysis, Fourier analysis, and higher order statistics are the new methods for analysing the sEMG signal. Artificial intelligent approaches like artificial neural network, genetic algorithm, fuzzy logic, hybrid and swarm intelligent algorithms are mostly used for characterization of EMG signal. Several machine learning algorithms have been explored to develop the efficient and accurate prosthetic model.

This technique would lead to improving the upper limb prosthetic system that is currently used for the amputees and this study has achieved the ***first objective***.

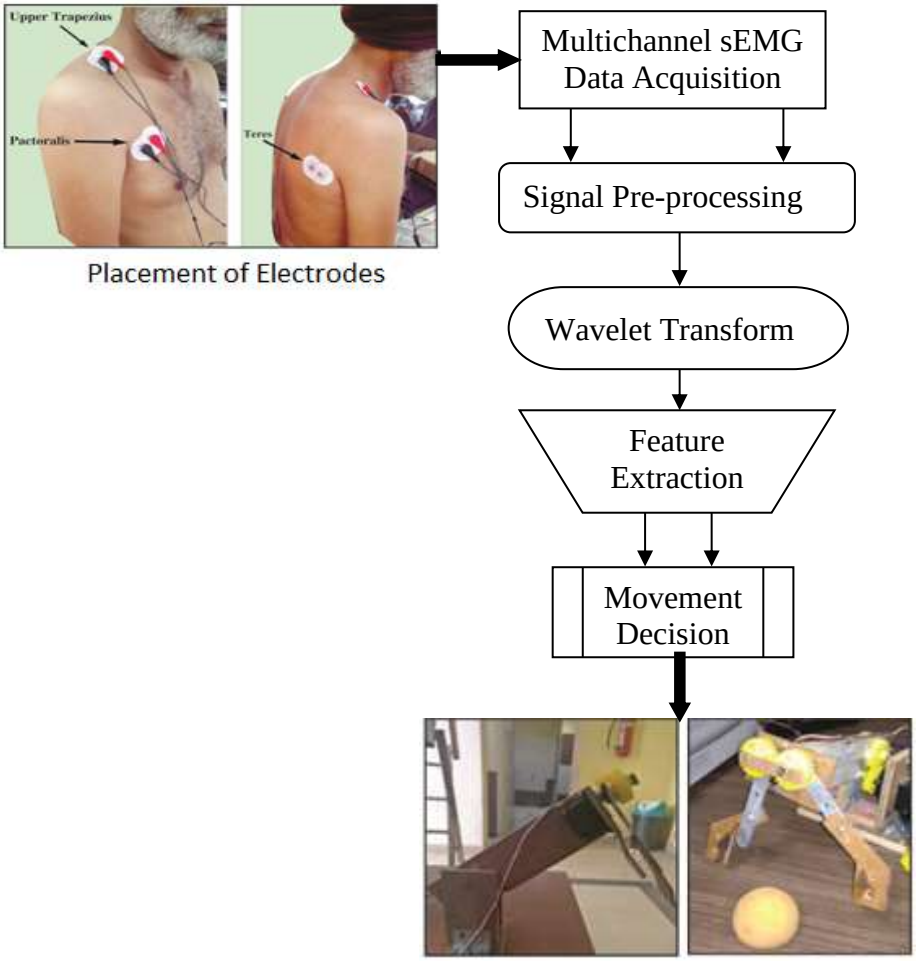

Figure 1.6: Methdoldogy of the system.

The placement of electrodes is a crucial task for data interpretation and movement modeling. The anatomy of the shoulder muscles provided the knowledge about different locations of the shoulder muscles to place the electrodes. The two types of muscles are the trapezius muscle and the deep muscles below the superficial muscles (deltoid, teres minor, teres major, pectorial minor and pectorial major) which can be used in the shoulder muscles activation process. In this work, four different muscles of shoulder were utilized to acquire the sEMG signal. The SENIAM (Surface Electromyography for the Non-Invasive Assessment of Muscles) recommendation [25] helped to guide the position of the shoulder muscles. The data was acquired from the six-upper limb right-hand amputee persons who had lost their arm due to some accident and had no activation of muscles below the shoulder. The detailed of this part

of methodology covered the ***second objective***, and the complete work is described in third chapter.

The four motions of the shoulder considered in this investigation. Different subjects were made a request to make the distinctive four activities with the right arm from the rest position to elevation, protraction and retraction and the left arm elevation to accomplish the fourth movement (**third objective)**. These four motions are utilized for the two degrees of freedom of hand open/close and elbow up/down development. Rest activity relax back the muscles in its natural state. It helps to demarcate the different movement or help to distinguish one activity from other activity. The amputee participants performed all the movements with their residual limb, and non-amputee participants performed this by stabilizing the arm motion. After recording of the information from various muscles, the acquired data was sent for pre-processing stage which contains different filtering processes to minimize the noise signal. A novel approach was adopted to adaptively adjust the threshold to filter the undesirable peaks in the pre-processing phase of the surface electromyography (sEMG) signal (Chapter 4).

The ultimate goal of this work was to operate the prosthesis using the myoelectric signal from the diverse shoulder muscles. The feature vector contained large number of features that cannot be utilized to operate the prosthesis straightaway. Therefore, the maximum amplitude value of the feature vector was considered to represent the sEMG signal which acts in synergy with hand function (***objective 4***). However, the amplitude level of the signal changed with the person's activity and it is not likely to operate well when performed practically for different amputee persons.

After pre-processing the signal, features vector was extracted from the reconstructed coefficients of the wavelet transform. The proposed data transformation technique was applied that converts the wavelet transformed data to a new data set called the features of the sEMG data set (Chapter 4). These features were applied to the machine learning algorithm. Machine learning is a relatively new technique which is quite reliable to identify and classify different arm and hand motions from the triceps and biceps muscles of trans-humeral amputee. Different machine learning algorithms like artificial neural network, support vector machine, genetic algorithm, K- nearest neighbour, fuzzy logic, hybrid, swarm intelligent algorithm and random forest were tested as to classify the EMG signal. Five different classifiers were compared to

determine the best classifier for the classification of different shoulder movements (Chapter 5). The output of the classifier was validated with hardware prototype to control the rotation of two motors corresponding to four movements of hand and elbow (***objective 5***).

1.8 Organization of the Thesis

Chapter 1 that we are already covering, introduced the need for the prosthetic arm devices, research gaps, motivation of doing present research and biomedical signal processing techniques used for making the prosthetic arm. The objectives, methodology to achieve the objectives and the structure of thesis are also elaborated in this chapter. Chapter 2 briefly discusses various methods and algorithms used in literature to analyze the sEMG signal for amputation. It provides a background review of the EMG system, its acquisition, feature extraction and classification. Chapter 3 elaborates the physiological description of generation and detection of sEMG signals. It starts with an overview of human anatomy to identify groups of active muscles on the shoulder during any particular movement of the shoulder. This movement is used to correlate the body structure with properties of the sEMG signals along with analysing tools/methods. The chapter provides the details of implementation of three channel sEMG acquisition system. Mention has also been made about the details of tasks performed by different subjects. In Chapter 4, the interpretation of surface electromyogram signal from shoulder muscles with four independent movements of the shoulder for both amputee and non-amputee persons is carried out. It also presents the proposed adaptive threshold method for peak detection to evaluate the features obtained from wavelet analysis. Machine learning algorithms were implemented to classify different shoulder movements of amputee subjects. Comparison is made among different algorithms to achieve the best algorithm to improve the class separability. A prototype, described in Chapter 5, was developed to demonstrate independent rotation movements of two motors representing hand and elbow. Chapter 6 provides the summary of the thesis and discusses the future work that could be taken up to extend the results of this effort.

Chapter 2
Literature Survey

2.1 Overview

In recent years, there is a steep rise in the anthropomorphic artificial limb quality improvement for physically upper limb amputees. One common method that makes and controls the prosthesis uses electromyography (EMG) signal generated by muscles-activity. It has allowed to increase the degree of freedom in arm and hand motions, especially for upper limb amputees. Several types of research have been carried out, but there still exists a gap between the natural state condition of human motion and the prosthesis emulating human hand and arm. Therefore, a lot of the effort has gone into the acquisition and analysis of the EMG signal. The improvement in the analysis of the EMG signal help to improve the prosthetics design. This chapter explores the comprehensive literature review of the research studies made in this direction. The review starts with the origin of the EMG signal described in Section 2.2 followed by different techniques (pre-processing, features extraction and classification) used for the analysis of the signal to improve the performance of the upper limb prosthesis device.

2.2 Origin of Electromyography (EMG) Signal

EMG is the electrophysiological phenomenon related to the electrical activity emanating from the muscles whenever muscles undergo contraction and relaxation. The investigation of muscles was first carried out by Leonardo da Vinci with the bulk of muscles in 1452-1519. Da Vinci was a painter who became popular due to his two famous paintings - Mona Lisa and the Last Supper and was the student of science, represented part of muscles in his sketches to a large extent, moreover, did the practical work on anatomy and collaborated with the physician-anatomist Marc Antonio Della Torre. Vinci filled numbers of books on invention and theory with painting, mechanism and human anatomy. In 1514-1574, Versalius, who did a remarkable work on the connection between muscles under the direction of Jacques Dubois and Jean Fernel in Paris, published seven books on the human body and also studied the advanced theory of Galen. Galen described the agonist and antagonist function in the skeletal system with the progression in the respiratory and nervous system [26] and carried out his anatomical dissection on pigs. After that with the increase in support, Vesalius published a book *"De Humani Corporis Fabrica"* in 1543 and transformed anatomy into a serious science [27].

In 1564-1642, Galileo, the professor of Mathematics who taught the standard astronomy to medical students, made a series of telescopes with lenses that produced four times better magnification for anatomy purposes and were better than the Dutch instruments [28]. Leeuvenhoet invented a new telescope by using his own lens and observed the composed structure of nerves with thin tubes. These vessels consist of the hollow tubes having some fluid in them. Then, Fonatanna (1730-1805) found the relationship between the hollow tube and nerves with magnified sharp needle and discovered that nerves were composed of many cylinders [29]. In 1781, Galvani investigated different experiments on frogs and discovered the electrical conduction in animal nerves [30].

Matteucci and Du Bios Reymond gave the breakthrough about the electric current associated with muscles contraction, and recording of this current was the starting point of the EMG (1806-1875). Du Bois-Reymond (1818-1889) got inspired by the Matteucci publications and repeated all the experiments on frog [30]. Reymond discovered the Galvanometer in 1849 and placed one end of the electrode on the cut end of the muscle and another end on the entire surface. When there was no contraction from the frog, the current disappeared from the galvanometer, named as the resting potential, but with the contraction, the needle deflected from the original position and he called that condition as the active condition of muscles. Finally, Reymond provided the primary representation of the EMG signal of the frog [30]. Einthoven Willens discovered the electrocardiography (ECG) then both Einthoven and Raymond utilized a large number of electrodes to acquire the EMG and ECG signal. In one of the sketches, Einthoven recorded the sum of the current with electrodes by holding the metallic bar in the left hand and a jar filled with water in right hand. The current passed from the right to left hand and recorded a signal that provided the difference in the muscles-activity between both hands. Raymond is famous as the father of the experimental electrophysiology who has given the idea of living tissues and the dynamic behavior of the muscles [27].

In 1907, Piper Rhythm demonstrated that the healthy person's EMG signal is orginated near or in the hand region of motor cortex during the contraction of the extensor muscles of the forearm at a frequency of 35-60Hz [31]. Coherence between the cortex activity and piper activity was seen more during voluntary activity of muscles. However, in a weaker contraction, the EMG lies in the lower frequency band. Thus the piper contraction was dependent on the degree of exerted force [31]. In 1922, Hill *et al.,* recorded the rhythmic sound without EMG activity and reported that this sound was produced with the difference in the grade of muscles

and this rhythm is less in the Parkinson's disease [32], [33], [6]. Brown *et al.*, also reported that the Piper rhythm was driven by the contralateral motor cortex. Western Electric Company made the cathode ray oscilloscope tube but refused to sell that tube to Gasser. In 1923, Erlanger and Gasser jointly developed a new oscilloscope device and used this to find the velocity of conduction in nerves [34]. Erlanger and Gasser, remembered for the exploration of the electrical activity of nerve action potential, jointly got the Nobel Prize in Physiology and Medicine.

In 1929, Adrian and Bronllys designed another needle electrode and used the action potential of deep muscles [35]. In 1960, Basmajian considered as the father of kinesiological EMG, provided the biofeedback system and worked towards rehabilitation. Basmajian published the report that the needle electrode generated pain and artifacts,therefore, not suitable for kinesiological EMG and also developed the sEMG electrodes to acquire data from the surface of the skin. Hardyck [36] and Booker [37] used the sEMG method for the treatment of disorders and retained this for the patients of various disorders. Cram and Steger [38] invented a handheld sensing device to improve the scanning of muscles. Steven presented the database of 104 subjects involving 15 muscles in sitting and standing postures and reported that the differentiation of muscles is dependent upon the degree of symmetry and posture. Afterwards, Donaldson studied the symmetry and asymmetry movements for patients and healthy persons and concluded that 20% asymmetry is acceptable [35], [27]. In this thesis, the data is acquired from the shoulder muscles with surface electrode. 'Surface Electromyography for the Non-Invasive Assessment of Muscles' Standards [25] were used to place the electrode on the shoulder muscles.

2.3 EMG Signal Pre-processing

2.3.1 Filtering

Various techniques has been used for pre-processing of the signal before features extraction, Data acquired has been divided into different segments and then filtered to get the noise free EMG signal. Segment length of EMG signal affects the classification of the acquired signal. The accuracy of the classifier degrades with less than 128 ms segment length. Therefore, Phinyomark *et al.*, [39] reported that the duration of the segment should be in between 125-500 ms to increase the accuracy of the signal. This vast segment length can be used in real time application for upper limb signal analysis. Englehart *et al.*, [40] suggested that the response

time value is also affected by real time constraint. Therefore, it should be less than 300 ms for better output results. The main aim of the pre-processing stage is to reduce the noise signal from the raw EMG signal with the band-pass filter with 20 - 500 Hz range for removal of different artifacts. Yeom *et al.,* [41]**,** [42] used the adaptive filtering concept to filter out the ECG signal from the EMG signal and applied a Butterworth sixth order low pass filter with frequency range 5 - 500 Hz [43]**.** In this thesis work, the frequency range was chosen as 20 - 500 Hz [18], [19] to reduce the motion artifacts with a notch filter that removed the 50 Hz power supply noise interference.

2.3.2 Thresholding

sEMG signal is a widely used approach to study biomechanical aspects of human muscles. The amplitude and frequency of the sEMG signal changes due to the electrical activity of muscles fiber during contraction, which is known as the muscle onset signal. Determination of the onset and offset muscles-activity is clinically useful to investigate the difference between amputee and non-amputee muscle activation [45]. EMG burst with unique muscle activation helps the researchers to identify the duration of offset and onset muscles-activity in different clinical conditions. The literature available mainly focussed on the detection of the EMG signal and its accuracy after processing the muscles activated signal. Gotman and Roy have used several spikes detection methods [46], [47]. In [48], Kaiser *et al.,* proposed a nonlinear energy operator method to find out the energy of the signal. This method has used for amplifying the spikes activity in which the output became proportional to the amplitude and frequency of the signal. For detecting the spikes in EEG signal, a smoother nonlinear energy operator with Barelett window was used to eliminate the spikes. Afterwards, a time-frequency based distribution of the signal was introduced that helps to reduce the effect of noises on the useful part of the signal [48].

Several new methods, such as the automatic threshold method [48], wavelet template matching [49], statistical criterion [50], the amplitude thresholding method (AMT) [51], Teager–Energy Operator (TEO) [47], [51] and the visual inspection (VI) [51] methods are most commonly used in peak detection technique. Out of all these methods, TEO algorithm is gaining much popularity for energy separation in the speech analysis [52]. This approach does not require any prior knowledge of the shape of the signal and also it improves the signal-to-noise ratio [53], [26]. Maragos *et al.,* [54] used the time and frequency analysis for peak signal detection and the other authors [55], [56] used the time–frequency analysis using TEO [47]. In [57], the

author used the Teager–Kaiser Energy operator to assess surface electromyography activity from the hip and trunk muscles during pediatric gait in children with and without cerebral palsy. Solnik *et al.*, used the peak counting method for a real-time muscles monitoring system [57]. It is evident from the referred literature [49-52] that the researchers have largely ignored the real-time sEMG signal for the upper limb amputees. This has served as a motivation for the author of this thesis to process the real-time sEMG signal for the transhumeral amputee person from shoulder muscles. No study has effectively provided signal accuracy with TEO for sEMG signals for the upper-limbs amputee. In the current research work analysis of a real-time sEMG signal from the shoulder muscles of an upper-limb amputee is being reported for the first time using the TEO method. Other literature used the different data sets and also not defined the different conditions under which the data sets has acquired. Therefore, in this work the author thought to take the original data set from amputee and non- amputee persons. Other researchers have used different data sets and also did not define the conditions under which the data sets were acquired. In this work, the author thought to take the original data set from amputee and non-amputee persons. So, sEMG signal analysis in this work cannot be compared with other literature results that have used different data in different conditions. The sentence has accordingly been modified as “So, sEMG signal analysis in this work cannot be compared with other literature results that have used different sEMG signals in different conditions. On comparing the results with AMT method, TEO method is more accurate and efficient. Finally, different sEMG signals from various movements were analyzed and the results confirms the expectation that TEO with a specific range of threshold level improves the signal quality.

2.4 EMG Feature Extraction

Feature extraction is a technique to extract the actual information hidden in the raw signal and convert it into the reduced set of features called the feature vector. It performs a critical role to achieve the performance in the classification technique [58]. EMG features extraction are divided into three categories - Time-domain features (TDF), Frequency-domain features (FDF) and Time- frequency domain features (TFDF) [59], [60].

2.4.1 Time Domain Features

In raw EMG signal amplitude changes with time and time domain features are extracted directly from the time series without the use of transformation method. The amplitude of the signal depends upon the muscles contraction by the person. Previous studies have focussed on

the time domain features because of the low computation complexity. In 1993, [61] proposed five different time domain features which were mean absolute value, zero crossing, slope sign changes, waveform length and mean absolute value slope. Then the signal was classified by artificial neural network and the author of this paper reported 95% classification accuracy with ±25% feature noise. Zardoshti-Kermani *et al.*, evaluated seven features and changes in the level of RMS amplitude were considered to check the reduction in the noise to control the myoelectric upper extremity [62]. Ahsan *et al.*, extracted the time domain and time-frequency domain features vectors to detect the hand motions using the artificial neural network [63]. Mean absolute value, variance and standard deviation, root mean square value, zero crossing, waveform length, Willison amplitude have been used in the study to make feature vectors. Ahsan *et al.*, introduced the new characteristics of a histogram and classified the features extracted from the signal with the KNN classifier. The work was extended by adding and selecting two or more features from different feature extraction methods and utilized for the classification process. Phinomark *et al.*, [64], [65] provided sixteen features from the three domains. They reported after testing with white Gaussian noise that the variations in the energy in different acquired EMG signals were the most used attributes especially for the opening and closing of the hand. Wan *et al.*, [66] evaluated a number of time domain features and selected the three features (Maximum amplitude, standard deviation, and root mean square value) from the biceps bracii, based on the statistical analysis by calculating the percentage of error. The author reported that the standard deviation provided better performance level than the Maximum amplitude and root mean square value. In one of the papers, the authors used the root mean square value as the input to the classifier and reported it to be the best parameter that provides the quantitate measure for the electrode selection [67], [44].

Table 2.1: Time Domain Features cited with references

Features	References
Wavefrom Length	[65]-[67]
Willison amplitude	[65],[60]
Entropy	[68],[69]
Zero Crossing	[65],[67]
log detector, Simple square integral, Cepstral Coeffcients	[65]
Skewness and kurtosis	[70]-[72]
Slope sign change	[65], [66],[60]
Standard Deviation and Variance	[63], [66],[67], [60]

Phinyomark *et al.,* proposed fifty features in both time and frequency domain [39]. Other than the above-cited references, the researchers used much more different time domain features illustrated in Table 2.1. A number of trials were recorded with the recording system and signal was analysed on the forearm and the upper arm muscles with eight different rotations of hand involving eight upper limb movements. The paper [33] concluded that the time domain features are better than the frequency domain in a number of aspects.

2.4.2 Frequency Domain Features

Frequency domain features are mostly employed in muscles fatigue [68]. Merletti utilized the mean frequency and power spectral density [69] to characterize the muscles contraction. Phinomark *et al.,* has extracted the features from the modified mean and median frequency of amplitude spectrum to track the progression of fatigue over time [65]. The information regarding the neural and the muscular changes induced by a stroke was assessed by using the mean power frequency of EMG signal [70]. It was observed that the average power frequency in paretic has less in value than the contralateral muscles. Then, the authors combined both time domain and frequency domain features and reported that the time domain features have low efficiency for pattern characterization [71]. In [72] Phinomark *et al.,* compared the twenty seven time domain features and eleven frequency domain features and reported that the time domain features yield better performance. Even in isotonic and isometric contraction, these time domain features provided more satisfactory reorganization performance. These features have low time consumption and are, therefore, faster than the other features. In [73], Tsai *et al.,* claimed that the time domain features performance were not satisfactory in EMG signal classification. The other frequency domain techniques including Fourier and Short-Time Fourier Transform (STFT) techniques, have been utilized for feature extraction. The Fourier transform technique may not be an efficient method to analyze the signal especially in fatigue [28] because variations get introduced in the spectral components due to change in muscle force, length and contraction of the muscle with time [74], [75]. It needs the signal to be stationary but the sEMG signal is non-stationary. Therefore, wavelet transform method was used to analyze the signal [74]. Alexandre [76] compared the FFT and wavelet transform for the electromyography indices of fatigue during cycling exercise. In this paper, the second objective was to compare the mean value of the median frequency obtained by the both mentioned techniques and reported that the wavelet transform is a better technique than the FFT.

2.4.3 Time-frequency domain

An ensemble of time-frequency domain features were proposed to improve the classification efficiency of the signal. In the short time Fourier transform (STFT), the window size must be determined to map the sEMG signal into the frequency components. Blanc *et al.,* used the STFT spectrogram to compare the muscles-activity of amputee and non-amputee subjects by using the time domain features [27].

Wavelet Transform (WT) is an alternative to other time-frequency representations. It has gained much attention in the biomedical signal processing in the time-frequency domain and is not affected by cross talks, yields a multi-resolution depiction and is relevant to the multicomponent signals. It has an excellent property of localization in both time and frequency, characterization, simplicity and can be divided into CWT and DW [63]. Haar introduced the first wavelet in 1909, and then the Gabour function was proposed by Denis Gabour in 1946 [62]. George Zweig discovered the continuous wavelet transform in 1975. In 1982, Grossmann and Morlet tried to observe the signal with the shorter wavelength signal with high frequency instead of equal duration pulses. Then in 1988, the ideas were formulated into a different mathematical tool by Daubechies who introduced the orthogonal wavelet transform. Stéphane Mallat with Daubechies collectively gave the filter implementation in the discrete wavelet transform. Afterwards, the author presented the iterative algorithm for the signal recovery by DWT technique [63]. The new approach of multi-wavelet bases with the traditional bases using the filter bank properties came in the study.

Merletti *et al.,* [15] and Narayan *et al.,* [64] have employed the DWT technique with the motive to obtain the signal representation for denoising or signal transmission and to decompose the signal into orthogonal time series. Wang [65] compared the time, frequency and time – frequency domain features by using one of the deltoid and trapezius shoulder muscles. Body posture influences the muscles activation with different movements. The subjects were involved in screwing and unscrewing the cap at the various positions on the table. The feature vector contained the root mean square value for time domain, mean frequency and mean power frequency in frequency domain and Daubechies wavelet function (db) in the wavelet family. By analysing these parameters, it was observed that the time-frequency domain has higher sensitivity to a change in the position. Englehart *et al.,* [35] presented that the one or two channel data for the features extraction technique is less efficient than the four channel data. In this research, the features extraction technique with wavelet transform and were used and then

the features dimensions was reduced with the Principal Component Analysis (PCA) technique. A frame work of non-stationary system identification was proposed to identify the time varying properties of the system [66]. Time-frequency domain features have high dimensionality and also high resolution [67]. Therefore, the dimensionality reduction concept came into this study to encounter the complexity of the features. Dimensions were reduced to determine the combination of the original features so that it can improve the error rate in classification by features projection method, also called a supervised method of reduction by using the Euclidean distance for the class separability. In features selection, PCA method has been utilized to determine the best subset of feature set also called as unsupervised dimensionality reduction method. The authors of [68] also investigated the performance of time-frequency domain features with a time domain features and calculated the classification error and concluded that the wavelet transform yields better results than the time domain features.

Kumar [69] provided a new approach to find the difference between the fatigued and non-fatigued muscle. He concluded that by appropriate choice of the wavelet transform and decomposition level, it is possible to identify the fatigue muscles by sym 5 and sym 6 wavelets with decomposition level of 8 or 9. Marcelo Bigliassi *et al.* [70] also worked on the muscles fatigue in one Km cycling trial on the Vastus Medialis, Vastus lateral and rectus femoris muscle in the thigh and presented that the WT is the most reliable and useful technique for the non-stationary signal. M.S Hussian *et al.,* [71] effectively presented the wavelet denoising method for pre-processing the EMG signal and reported that the db2 performed best among the wavelets for denoising purposes. Further, the new proposed method using the wavelet transform and statistics provided efficient processing [72], [73].

Denoising the signal is a very useful process in the wavelet analysis, it is a pre-processing stage of the wavelet techniques. The author of the paper [74] described the types of noise as ambient noise, motion artifacts, heating in electronic components and power line interference. Among these different noises, the first three noises do not fall in the energy band of the signal, but the power line interference noise has the frequency components at 50Hz or 60 Hz. These noise components are random in nature and fall in the frequency range of sEMG signal. The first three noise can be reduced by using the use of band pass filter. However, the last noise is inherent noise [75], [39] that causes difficulty to eliminate from the system by the conventional filter. Therefore, the adaptive filtering can be used to reduce the noise mentioned above but causes the complexity in the system. A wavelet transform is tool that reduces this random noise

signal from the non-stationary signal and help to resolve the noise problem. The denoising stage of the wavelet got huge success for recognition of limb movement [72], [76], [77], [78].

In the wavelet transform, the results are dependent on the choice of the mother wavelet and the decomposition level for the recognition system. Kim *et al.*, obtained the resolution components from the EMG signal by extracting the two features such as mean absolute value and root mean square from the reconstructed signal after denoising the signal with the wavelet [79]. The first and the second level coefficients were used to get the class separability in the feature space. Daubechies family with the fourth level of decomposition was the best family chosen by the author of the paper. Literature of the time frequency domain features utilized with different wavelet function with decomposition level is represented in Table 2.2.

Table 2.2: Literature of Time –Frequency domain features

Wavelet function	Decomposition level	Threshold selection rule	Threshold scaling method	Thresholding function	References
db5	5	-	-	HAD,SOF	[80]
sym5	3	Universal, SURE, Hybrid	-	HAD,SOF	[81], [82]
db2	6	Universal, SURE, Hybrid	-	HAD,SOF	[83]
sym8	4	LVMU	-	HAD,SOF, WAV	[84]
sym8	4	Hybrid	-	SOF	[82]
Daubechies (db) symlets, coiflet	6	Hybrid Byes Shrink		SOF	[76]
db2, db6, db8, dmey	4	-	-	HAD	[71]
db2, db4, db5	4	Universal		HAD	[72]
db6, db8, sym4					
symlets (sym2)	5	Minimax		SOF	[85]
Daubechies, symlets, coiflet, Discrete, Biorthogonal, Meyer	1 to 7	Proposed five universal method	Global	SOF,ADP	[86]

SURE : Stein's Unbiased Risk Estimate thresholding rule method

HAR : Hard function of threshold method SOF : Soft function of threshold method

ADP : Adaptive Denoising function WAV : Weighted averaging function

In 2000, Moshou *et al.*, [80] proposed the sEMG signal analysis with the wavelet transform with the main aim to separate the muscles-activity signal acquired from different movements of the shoulder. Wavelet based algorithm requires various parameters such as the wavelet basis function selected from the various wavelet families with large no of decomposition levels.

Therefore, the selection of particular decomposition level according to the application is the second requirement of the algorithm.

Three techniques such as threshold selection rule, threshold scaling and thresholding function are defined to choose the threshold level. The different authors of the papers who have used different decomposition levels and wavelet functions with the denoising technique to reduce the noise in the signal.

2.5 EMG Classification

In recent years, the main efforts was towards classification of the myoelectric surface pattern. The features extraction is crucial to the reliable classification after feeding the extracted signal into the classifiers. It helps to improve the accuracy of the myoelectric signal pattern classification by distinguishing the categories of the feature vector, therefore, classification has become the essential tool for the rehabilitation. To control the prosthetic limb, the classification of the signal is the main challenge of the study. Several techniques have been deployed to classify the signal such as linear discriminant analysis, fuzzy logic, artificial neural network, Hidden Markov Model, Support Vector Machine, k-nearest neighbor and many more.

Dorcas *et al.* provided the controller that was capable of controlling the single articulation such as hand, elbow or wrist. The controlling of the instrument was by the amplitude level of the EMG signal and the rate of change of signal [77]. The mentioned system was very successful, but it did not provide sufficient information to control more than one device [59]. Hudgins *et al.*, [61] considered the contents of the onset contraction of the muscles by using the bipolar electrode on the triceps and biceps muscle. A system was developed with time domain features to control the four upper limb motions from the selected muscles and provided the motion classification with the artificial neural network and reported about 10% error rate. By using these features, Englehart *et al.*, made the prosthesis with the microcontroller especially for the amputee persons [59], [78]. Afterward, the mentioned work was compared by Kevin Englehart with the short-time Fourier transform (STFT), the wavelet transform (WT), and the wavelet packet transforms (WPT) by using the data set of the same muscles and movement as described in the above citation. For the dimensionality reduction, author of the cited paper [53] used the PCA technique and reported significant improvement with an average error of 9.25% using linear discriminant analysis. The different advanced methods, including Fourier transform, Short-Time Fourier Transform, Wavelet Transform, Wigner-Ville Distribution and higher

order statistics have been used to analyze and classify the signal. Altimari *et al.,* [79] compared the STFT and CWT and suggested that both methods were efficient to analyse the muscles fatigue. However, results of variance were lower in CWT than STFT which indicated more variability of using the STFT for signal analysis [76]. The accuracy parameter of the STFT was also less than the WT. Canal *et al.*, [76] also showed that the WT provided excellent performance in the classification process and, therefore, can be utilized in clinical and research area.

The main concept of classification is to develop the prosthetic devices to classify the more complex hand motion. WT is a successful pattern reorganization method for this task [69], [81]. For different hand motions, Alkan *et al.*, [82] used the four upper arm movement and took the 256 points from biceps and triceps muscles. In this paper, the mean average value was utilized to classify the signal by using Support Vector Machine and Discriminant Analysis with cross-validation technique. The results described that the SVM is better than the discriminant method with 1.5% more efficacy. Engelhart *et al.,* used the four channel system for classifying the six hand motion. It is a wavelet based feature set method with PCA for dimensionality reduction [40] and also reported that the four channel system provided better efficiency than the one or two channel system. In [83] the acquired signal from the residual muscles was filtered out to calculate the mean and the variance values. Further, the supervised multi-layer neural network classifier was applied to classify the different patterns and reported improved efficiency.

For improving the classification the selection of relevant features from the full feature vector, extracted from the wavelet transform as decomposition coefficients was carried out [80],. Number of feature vectors were reduced the [85], [86] by Principle Component Analysis (PCA) or by selecting the more appropriate time domain or time-frequency domain features [87]. Sebastian *et al.,* [88] provided the self-correcting reorganization system for upper limb prosthesis control with multiple degrees of freedom and robustness. Geng *et al.,* [89] collected the data from five trans-radial amputees with different five movements of the arm. The data set subjected to the test set yielded an average classification error of 10.8% for amputated subjects. Most of the cited feature extraction methods focussed on the improvement of classification accuracy. With various combinations of advanced techniques, almost all the literature worth mentioning on this problem achieved greater than 90% accuracy. Even then the use of the myoelectric control is still a great challenge. In this thesis, five classifiers' (three

were the statistics classifier and two were the data mining classifier) performance was compared to find out the best classifier for classification of shoulder movements.

Support Vector Machine (SVM) was originally purposed by the Vapnik in 1992 [90]. It is a kernel based approach involving regression and classification. The main approach in SVM classifier is to decide the kernel function. Yoshikawan *et al.,* [91] used four electrodes on the patient forearm and distinguished seven hand movements by using the SVM technique with an input vector of integrated EMG and cepstrum coefficient and resulted in the classification rate variation from 87% to 92%. *Oskoei et al.,* [92] compared the SVM with Linear Discrimination Analysis (LDA) and multi-layered perceptron neural network to classify the upper limb motion. It modified some of the parameters slightly and achieved 95% efficiency of SVM that was the highest from the other used classifiers. Rekhi *et al.,* [93] extracted the EMG features through the wavelet packet transform and used singular value of decomposition to reduce the dimensionality. Results reported that the multi-SVM classifier provided 96% accuracy for six different types of hand motions.

In [94], the authors compared four different features extraction methods - Root Mean Square, Detrended Fluctuation Analysis (DFA), Weight Peaks (WP), and Muscular Model (MM) for below shoulder muscles. The two classifiers, Neural Networks (NN) and SVM, classified eight upper limb motions based on these attributes and reported that the highest accuracy rate (97.7%) was produced by the WP feature. Leon *et al.,* [95] recognized nine different motions related to four degrees of motions of the forearm. Ten subjects' muscle data were given to the SVM, ANN and LDA classifiers. From these classifiers, SVM achieved the best performance with 99.57% efficiency. Different authors compared SVM with KNN and reported that the SVM provided more efficiency than the KNN classifier. Phinyomark *et al.,* [39] acquired the signal from non-amputee male subjects using the Nexus -10 recording device with three channel system. Different fifty time domain and frequency domain features were aquired for the feature vector for eleven upper limb motion classification. Linear discriminant analysis was used to compare different features. The obtained results recommended that the sample entropy provided highest accuracy (93.37%) followed by approximation entropy (84.68%).

Kilby *et al.,* [96] acquired the data from the biceps brachii muscles under sustained contraction. The author compared five different families (Daubechies, symlet, coiflet, bi-orthogonal and haar) and recommended the first three families for the EMG signal analysis. Another group

Hariharan *et al.,* used four wavelet families (Daubechies, symlet, coiflet, bi-orthogonal) to classify five types of hand motions and recommended coiflet and bi-orthogonal family for sEMG analysis. With the implementation of the classifiers, general regression neural network and probability of neural network, author of this paper reported higher accuracy by the combination of General regression neural network with the coiflet wavelet family. sEMG signal was applied on the three classifiers such as quadratic discriminant analysis, Linear discriminate analysis and KNN [97]. The feature vector was a combination of different features such as Willison amplitude, root mean square value, sample entropy, myopulse percentage rate and difference absolute standard deviation value. Results reported that the combination of the above said features except Willison amplitude provided 98.56% accuracy. These recognition techniques were used for controlling the hardware. In [98], Jonghwa *et al.*, made the EMG-based gesture signal interface using the KNN and Naive Bayes (combination) classifier with different feature vector matrix of mean, maximum and minimum value, variance and root mean square value. The interface provided 94% efficacy to control the car by the gesture.

Machine learning algorithms such as Decision Tree and Random Forest algorithm have a significant role in the investigation of EMG signal. Not much work has been done on classification by using these classifiers. In one paper [99], the author have compared the Naïve Bayes with the decision tree algorithm and mentioned classifier efficiency of 81% and 78% respectively for neuromuscular disorders detection. These machine learning algorithms are mostly used in the data mining methods. This is an important area with direct application to prosthetic devices. Alison *et al.,* [100] used the real time EMG classification method to classify the six forearm muscles by using the energy synergies in the muscles. Leave one out validation method was used that provided an overall accuracy of 79±6:6%. Ercan *et al.*, in 2015 [101], used a different decision tree algorithm with DWT for neuromuscular diagnosis. The author used the multi-scale Principle Component Analysis for denoising purposes, DWT for the feature extraction and the decision tree algorithm for the classification. The results showed that among regression tree, C4.5 and Random forest, the random forest was the best classifier with 96.67% efficiency. Narayan *et al.*, [21] used the same method for classification of the elbow movement and proved 97.9 % efficiency of decision tree classifier. They reported that that the classifier efficiency is dependent on the way to achieve the features from the raw signal and classify these features by using the best classifier from a number of classifiers. Amnah *et al.,* [102] used the wavelet packet decomposition for feature set extraction from the muscles contraction. Then classified the signal by different ensemble tree Random Forest, rotation

forest and multi boost method. The best efficiency achieved was 92% by the random forest with K- fold technique using different performance metric parameters. They declared that this method has got the application in control and rehabilitation. Duane *et al.,* [15] identified the hand motion combination of the discrete wavelet transform and wavelet neural network. Six healthy subjects and one amputee subject with wrist disarticulation were part of the study and utilized three channel system and the feature vector of the discrete wavelet transform coefficients. Wavelet neural network was used to classify the six hand motions and provided an excellent result with 94.64% efficacy. Manuel *et al.,* [103] presented a comparison of 179 classifiers from different 17 families and used 121 data set from the repository and derived the result that Random Forest is the best classifier with the maximum efficiency of 94%. Detection of the upper limb motion using the classification method has attracted growing research. Soma ,*et al.* [104] specified that the whole body coordination is impossible to drive the limb naturally by using only forearm muscles. It is tough to make the prosthetic device for high-level amputation. Most of the daily life activities need a coordination of shoulder-hand complex. Through the analysis of the experimental data [105], and it is possible to distinguish the hand and arm motions from the shoulder motion. Then [106] recognized the three different grips and five directions of the arm with five channels of EMG and four channels of accelerometer by using the neural network method.

The sEMG signal finds applications in controlling the prosthetic devices for different levels of amputation. In the cited literature, extensive work was observed on upper and lower limb amputation. The upper limb data was acquired from the triceps and biceps muscles from the non-amputee. The researchers have largely ignored the real time sEMG signal for the transhumeral amputee persons who have zero muscle activation below the shoulder and it is difficult to acquire the signal from triceps and biceps muscle for making the sEMG based prosthetic device for such amputees. It was also observed that the myoelectric arm was not considered to derive the independent control signals for elbow and hand motions. A very limited literature is available on the upper-limb prosthetic design that collects the data from the amputee's muscles activation due to different movements of the arm. This has served as a motivation in the present research work to process the real time sEMG signal, especially for a transhumeral amputee. Daily life motions present a relationship between the shoulder, elbow and hand structure for almost every upper limb activity like throwing and catching a ball or grasping the objects on the table. Therefore, the main emphasis is given to the study of the

sEMG signal at different muscles location of the shoulder for various movements of the shoulder.

Summary

This chapter provides a background review of the EMG system, its acquisition, feature extraction and classification. Time domain, frequency domain, time- frequency domain features and different classifications method have been recommended. Continuous efforts are needed to make sophisticated and reliable classification so that the system become more accurate for medical applications and development of the prosthetic devices for amputee persons becomes easier.

Chapter 3
Physiology, Methodology and sEMG Signal Acquisition System

3.1 Overview

The human skeletal system forms the internal framework of the body. It includes all the bones, cartilages, and ligaments. Bones support the weight and movement of the body. It also protects internal organs of body. Cartilage provides flexible strength and ligaments prevent excessive movements of the joint. Muscles of the body provide movement of the skeleton and help to balance the body in any position. When muscles contract, they pull on the bones and provide the movement of the body in a controlled manner. During the contraction of muscles, generated electrical current is represented by the neuro- muscular activity also called the myoelectric activity. *Myo* is the Greek word which means muscles and *electric* pertains to electricity; "*electrical activity produced by a contracting muscle"* [11]. In 1942, Herbert Jasper, Montreal Neurological Institute at McGill University constructed the first electromyogram and used the needle electrodes to perform the groundbreaking work. Human muscles can be categorized into a number of muscles groups including those of head and neck, muscles of trunk and muscles upper limb and lower limb muscles. sEMG signal is a biosignal which implies acquiring of electrical signal produced by the electrical activity of skeletal muscles from the surface of body. sEMG is a stochastic signal controlled by the nervous system [84]. The signal influenced by the anatomical and physiological behaviour of the muscles, peripheral nervous system schemes as well as the detection and processing characteristics of instrumentation utilized for acquiring the signal [28], [35]. With a specific end goal to get appropriate parameters to control the prosthesis, the information ought to be legitimately acquired and then processed [107].

The main goal of this chapter is to study the behavioral characteristics of upper limb amputee. This chapter elaborates the physiological description of shoulder muscles (Section 3.2), followed by an outline of sEMG signal generation and human anatomy to identify groups of dynamic muscles of shoulder during its specific movement (Section 3.6) and also provide the details of the different tasks performed by subjects. Four muscles were selected that help to perform the motion of hand and elbow by the amputee. It additionally specifies the detail of the two and three channel sEMG procurement framework to collect the raw sEMG signal by electrodes and store the data for analysis purposes (Section 3.7).

3.2 Anatomy of the Shoulder Girdle

The shoulder is an elegant piece of human body. It provides the largest range of motion to the body. The shoulder girdle is a complex system *i,e.*, composed of bones, joints, ligaments, muscles, nerves, tendons, blood vessels and bursae. Human body shoulder consists of three bones named as Humerus, Scapula and Clavicle also called upper arm bone, shoulder blade and collarbone, respectively. Among these bones, longest one is the humerus that is connected to shoulder through humeral head [108]. The upper limb consists of the upper arm, forearm and hand and is attached to the axial skeleton by the shoulder girdle (Figure 3.1). The shoulder girdle consists of clavicle and scapula. Clavicle provides a mobile attachment of the upper extremity to the trunk. It is a bony structure that connecting the link between the scapula and the sternum. Scapula is a major bony component with triangle shape structure situated on the posterolatera.

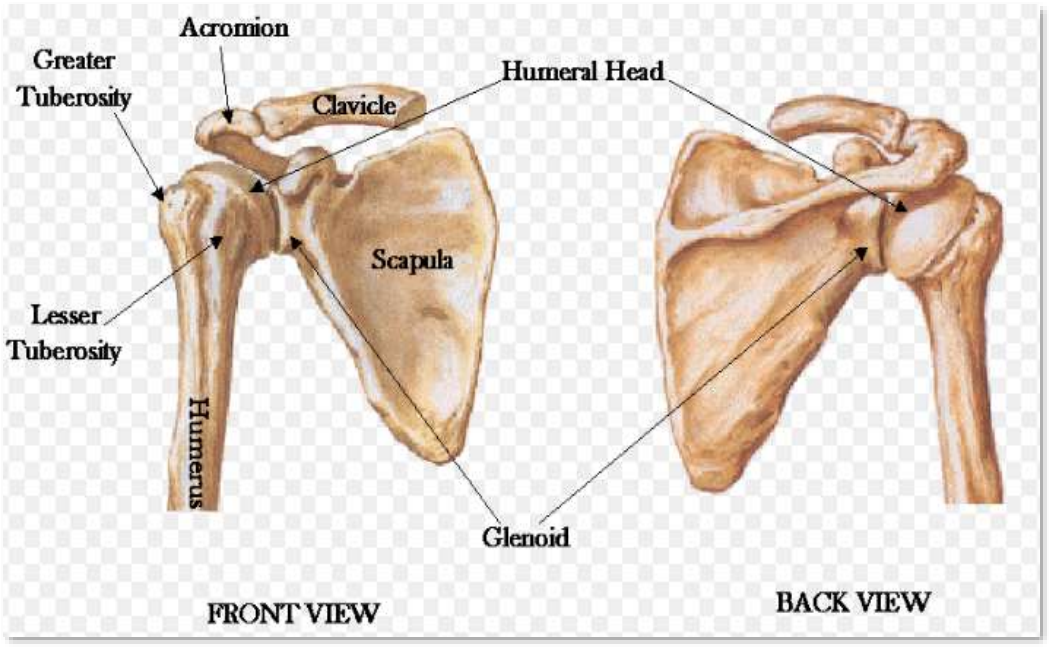

Figure 3.1: Shoulder joint Anatomy[109]

Figure 3.1 shows the overview of the front and back side anatomy of the shoulder joint of human body. The joint of scapula at the humerus is called as the glenohumeral joint and clavicle frames a joint with the thorax at the sternum named as the sternoclavicular joint. The points of clavicle articulates with the acromion forming the acromioclavicular joint [110] [108]. The shape of the glenohumeral joint gives the motion to the shoulder making it the most versatile of the considerable number of joints in the human body. The humerus is the main bone of the upper arm and joins with the bones of lower arm.

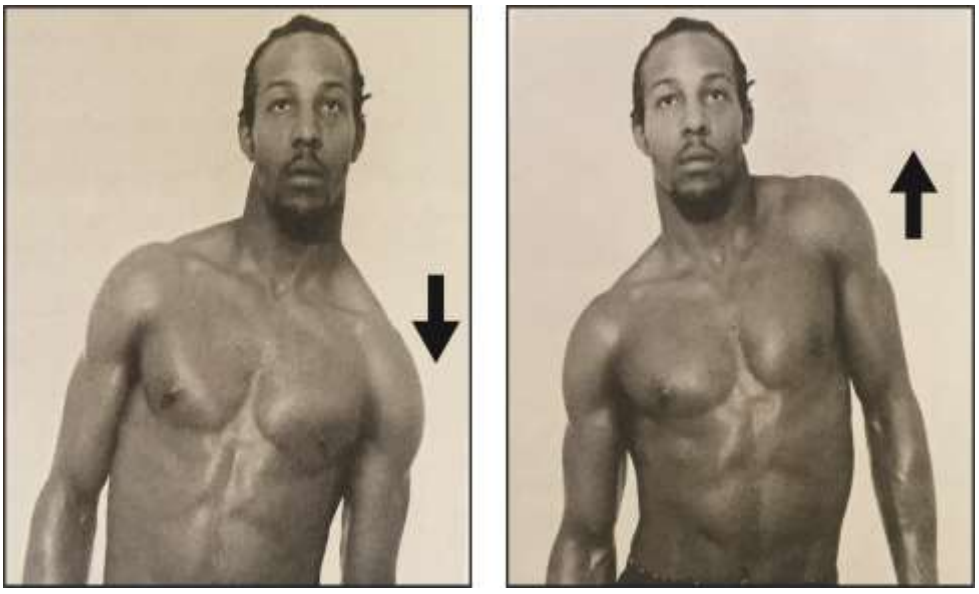

Figure 3.2: Scapular movements during elevation and depression of shoulder [111]

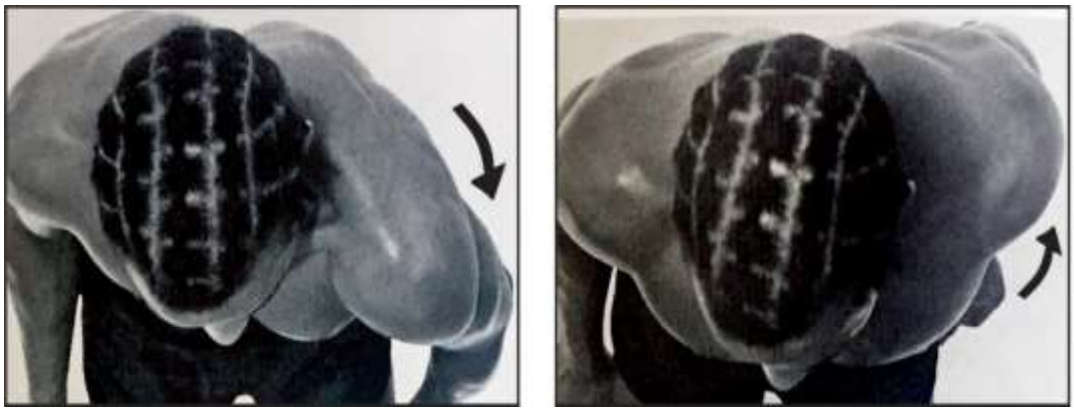

Figure 3.3: Flexion (abduction) and extension (adduction) of scapula [111]

The shoulder girdle provides a mobile attachment of the upper extremity to the trunk. Bony articulation with the trunk occurs only using the clavicle. Motions that occur about the shoulder include motion between the glenohumeral joint and between the scapula and the trunk, sometimes referred to as the scapulothoracic joint [111] [112]. The scapula moves in four directions: elevation (Figure 3.2) in the cephalad direction; depression, in the caudad direction (Figure 3.2); flexion (abduction) away from the midline (Figure 3.3) and extension (adduction) towards the midline. Combinations of these basic motions will produce clockwise and counter clockwise rotations of the scapula in such movements as reaching above the head.

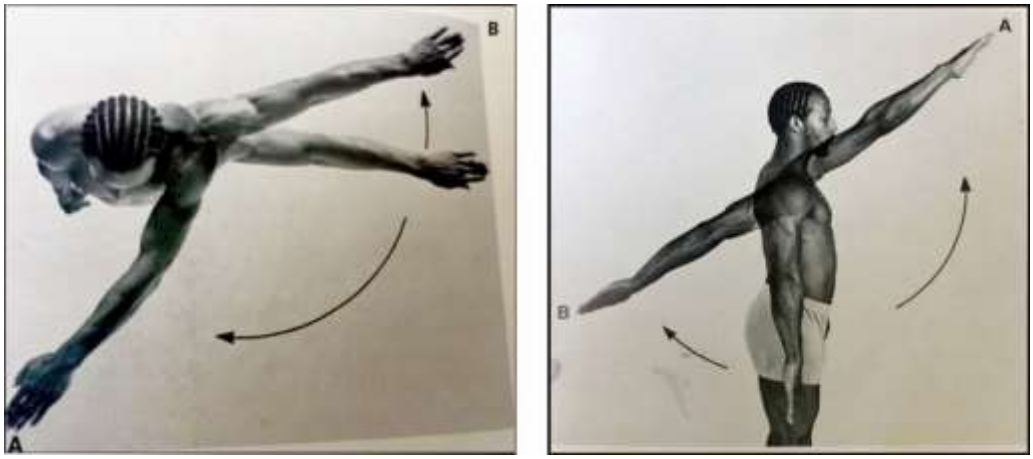

Figure 3.4: Flexion (A) and extension (B) of shoulder in horizontal and in vertical plane [111]

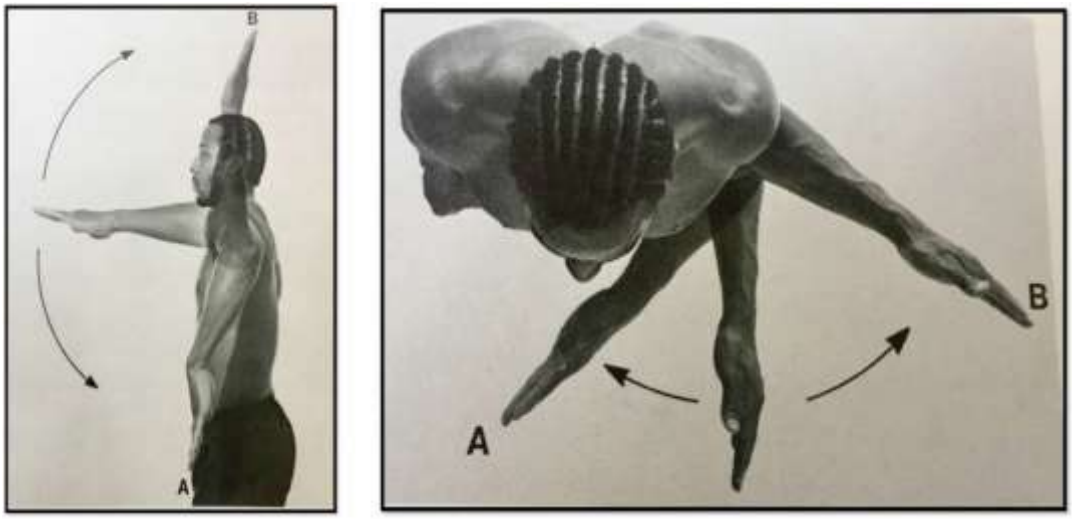

Figure 3.5: Internal (A) and External (B) rotation of the humerus with the arm vertical and horizontal direction [111]

Motion at the glenohumeral joint consists of flexion, extension, abduction (away from the trunk), and adduction (towards the trunk) shows in Figure 3.4. The humerus, which can also rotate in the glenohumeral joint. With the elbow flexed at 90^{o}, and these movements can also be carried out with the arm vertical [111]. Motion at the glenohumeral joint, excluding rotational motions, occur in concert with motions of the scapula on the trunk and through the arm at the side, Internal, external rotation moves the hand away from the trunk shows in Figure 3.5. acromioclavicular and sternoclavicular joints. Usually, the first 30^{o} of motion occurs between the humerus and scapula, but from that point on for every 30^{o} of shoulder motion, 20^{o} occurs at the glenohumeral joint and 10^{o} between the scapula and the thorax.

3.3 Shoulder Muscles

Major muscles are involved in the movement and support of joints. Figure 3.6 shows two anatomical groups of upper limb muscles i.e., shoulder group and elbow group. The shoulder group is considered because the current research work is focussed on the amputee who has no activity or very less activity of muscles under the shoulder and the electrical signal from the shoulder muscles was not sufficient to measure [113]. This very low value or zero value of signal cannot be used to derive the prosthesis for amputee person. Main group of the muscles of shoulder are called Rotator cuff muscles (infraspinatus, supraspinatus, subscapular and teres minor) [112]

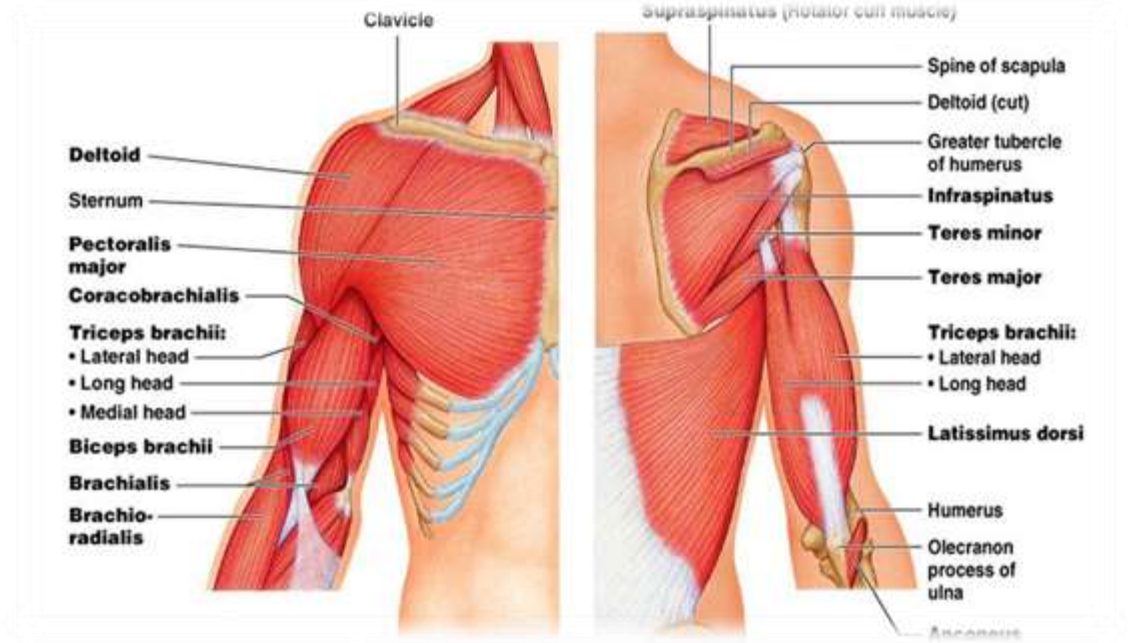

Figure 3.6: Anterior and posterior view of shoulder muscles of human body [109]

These muscles provide the support for the glenohumeral joint by linking the scapula to the humerus and play the major role for internal and external rotation of the upper arm. Muscles around the rotator cuff shoulder joint work with supraspinatus to abduct the arm.

Interiorly, the Pectoralis major and minor work together to flex and adduct the scapula and humerus. Elevation of the scapula is performed chiefly by the upper fibres of the trapezius and the levator scapulae muscles. Depression of the scapula occurs by the action of the lower fibres of the trapezius and gravity. Figure 3.10 shows the trapezius is assisted in depression by the latissimusdorsi and pectoralis major, acting through the glenohumeral joint. Adduction, or

backward movement of the scapula, preformed by the rhomboids and the levator scapulae, again with some assistance from the trapezius [111]. Abduction of the scapula is performed by the serratus anterior assisted by the pectoralis minor. The serratus anterior also steadies the scapula and holds it close to the chest wall. Paralysis of this muscle causes winging of the scapula when one attempts to push a heavy object with arms outstretched. In movements about the glenohumeral joints, the supraspinatus, infraspinatus, teres minor, and subscapularis make up a group referred to as muscles of the rotator cuff. They are mainly responsible for stability of the head of the humerus in the glenoid fossa. These muscles are not usually considered prime movers of the shoulder joint; they serve instead as agonists assisting the larger muscles. Abduction of the shoulder joint is accomplished mainly by the deltoid muscle assisted by the biceps and the rotator cuff.

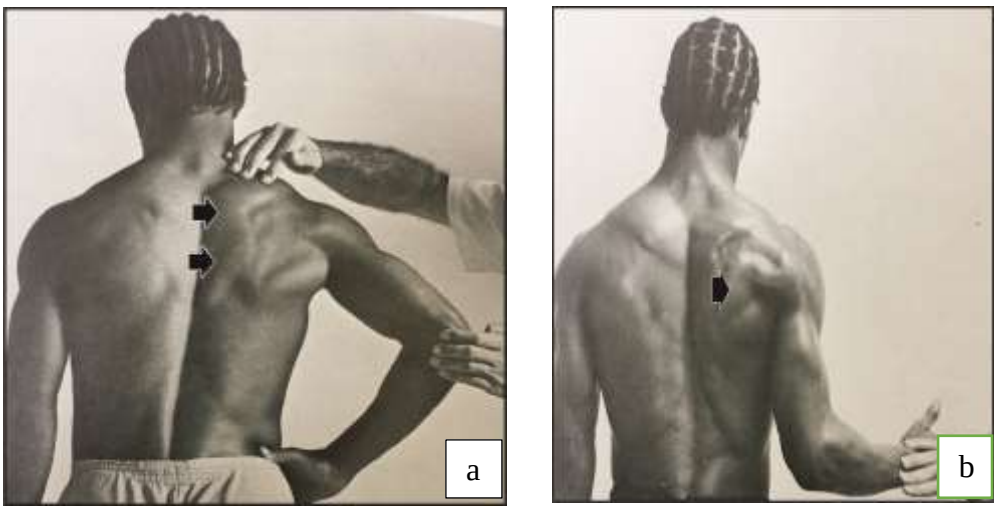

Figure 3.7: Trapezius (a) and rhomboids (b) muscles activation [111]

Subject elevates its scapula against resistance. Trapezius can be seen in Figure 3.7 (a) indicated by an arrow. The scapula is extended against resistance. The Rhomboids can be palpated deep to trapezius 3.7(b). Extension of the shoulder occurs by contraction of the latissimus dorsi, with some help from the posterior fibres of the deltoid muscle. Flexion of the glenohumeral joint is by the anterior fibres of the deltoid with some assistance by two muscles attached to the coracoids process, the biceps and the coracobrachialis. Adduction of the arm occurs with contraction of the pectoralis major, working synergistically with the latissimusdorsi. Medial rotation of the humerus occurs by contractions of the prctoralis major and latissimusdorsi assisted by the teres major which is also an adductor of the humerus.

Figure 3.8: Deltoid muscles activation [111]

Lateral rotation of the humerus is brought about chiefly by muscles of the rotator cuff, the infraspinatus, and the teres minor. The subject elevates the arm against resistance. The deltoid can be seen and palpated in Figure 3.8. It indicates the muscles of the pectoralis region are all supplied by branches from the nerves of the brachial plesus, fifth cervical through first thoracic. The pectoral muscles are supplied by the lateral pectoral nerve form the latest cord and by the medial pectoral nerve, which, in turn, is derived from the medial cord. This physical movement involves the activation of the muscles forces.

Electrodes are used to measure the electrical signal generated from the muscles with the muscular force called the electromyography (EMG) and the waveform referred as the electromyogram. Some studies have been carried out which show the relationship between the force and EMG signal [113]. Most of the researchers declared the linear relationship between the force and EMG but others claim that this relationship is not linear [Gregor et al., 2002]. With the theoretical analysis, De Luca have concluded in one of his paper [114] that the amplitude of the signal increased with the square root of the force generated. Sometimes in the experiment, the area of connected electrodes is not sufficient to detect the generated signal. Even the signal from the electrode includes the cross-talk variations due to the involvement of synergistic muscles in force generation. The location of electrodes should be proper to improve EMG force relationship on the muscles that are responsible for force production. The noise associated with the EMG signal while traveling through different tissue were observed in the range of 0.01–10 mV, 10–2,000 Hz.

3.4 Methodology to Acquire sEMG Signal

sEMG signals or the myoelectric activity of the muscles were acquired from the amputee and non- amputee participants. The signals were collected from the non-amputee and amputee persons who have upper limb amputation and have no activity on the below shoulder stump after amputation. Figure 3.12 shows the methodology to acquire the sEMG signal and the description of detail is in the following sections.

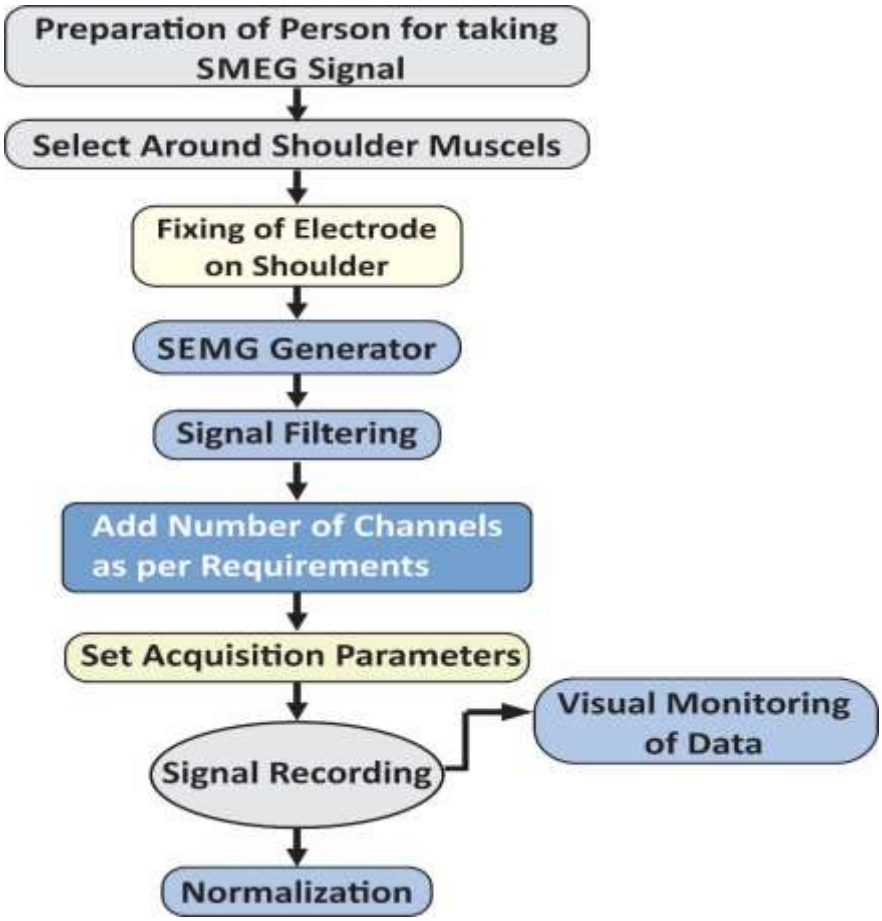

Figure 3.9: Methodology to acquire sEMG signal

3.5 Participating Subjects

In all sixteen subjects in two groups participated in the current research work.

First Group: Ten non-amputees male with 19-35 years age, 45-100 kg weight.

Second Group: Six right-hand amputees 28-50 years age, 70-110 kg weight, time since amputation 10-20 years. Table 3.1 and 3.2 shows the participating male subjects having no muscular disorder history. Prior to conducting the experiment, procedure of experiments was described to all the participants verbally. All the subjects gave the signed consent letter. The

local Ethical Committee has approved the measurements procedure of the sEMG signal from the human beings.

Table 3.1: Demographic details of non-amputee body male participants.

Subject ID	Age (Years)	Weight (Kg)
sEMG A001	19	63
sEMG A002	29	71
sEMG A003	30	73
sEMG A004	23	67
sEMG A005	22	61
sEMG A006	27	69
sEMG A007	32	80
sEMG A008	35	85
sEMG A009	26	50
sEMG A010	25	55

Table 3.2: Demographic details of amputee body male participants

Subject ID	Age (Years)	Weight (Kg)	Years Since Amputation
sEMG A001	40	80	10
sEMG A002	36	85	12
sEMG A003	30	75	15
sEMG A004	48	105	10
sEMG A005	49	78	18
sEMG A006	39	90	16

3.6 Location of Electrode on Shoulder Muscles

In human body, the bioelectric conductivity is because of the ions as charge carriers. Picking up this bioelectric signal and transducing this ionic current due to charge carriers into electric current by transducing function is done by electrode. Many different types of electrodes have been used for acquiring the signal. The types are broadly divide into *intramuscular electrode* and *Body-Surface Bio-potential Electrodes* (Chapter 1). Before recording the signal, the placement of electrode is a very typical task; placement of electrode should be in between a motor points and the tender insertion. Because at the tendon of muscles, fiber becomes thinner, thereby reducing the amplitude of the acquired signal and causing the crosstalk problem [115].

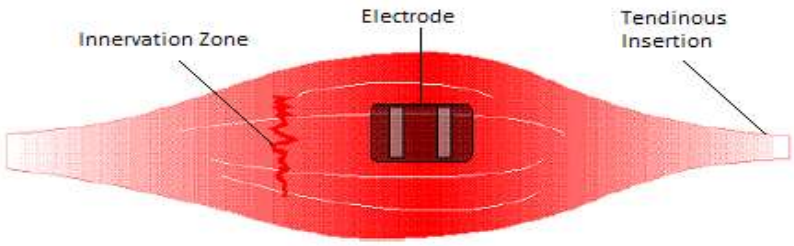

Figure 3.10: Schematic representation of the preferred electrode location [115]

The placed electrode should be remoted from the motor point because this point usually has the greatest natural density and in this region, the action potential travels along the muscles fiber causing the high-frequency component in the resulting EMG signal. The both positive and negative phases of the action potential add and subtract with some phase difference.

The experimental sEMG signal was procured from the shoulder muscles by the best possible position of pre-gelled electrodes on the identified muscles. Here, SENIAM project (Surface Electro-myography for the Non-Invasive Assessment of Muscles) standards for sensor placement procedures and signal processing methods for sEMG acquirement were used. Skin surface were clean and dry to avoid artifacts before the placement of Ag/AgCl electrodes on the body surface [25]. The used tear faced electrode (Chapter 1) have robust form adhesive for more challenging applications. The electrode foam was wat to provide quicksignal retention with strong quality of signal. The electrodes were placed at the desired locations after the skin dried up. The separation kept between the two electrodes on single location should be less than 20 mm. In this research, distance maintained between two electrodes was 15 mm and the reference electrode was located on the other arm. With the bipolar electrode, the optimal position of the electrode is parallel to the muscles fiber to maximize the probability of proper signal acquisition [116].

3.6.1 Two channel electrode placement

In this method, two distinct muscle groups were used to control the terminal device. The system acquired the data from the two set of electrodes. Two channel combinations were selected to study the different values of muscles-activity according to the specified exercises. Several muscles contribute the movement around the shoulder. Before the placement of the electrode,

oil or dust was removed from the skin surface with an alcohol swab. The dual electrodes were placed at the desired locations for maximum coverage of the signal after the skin dried up

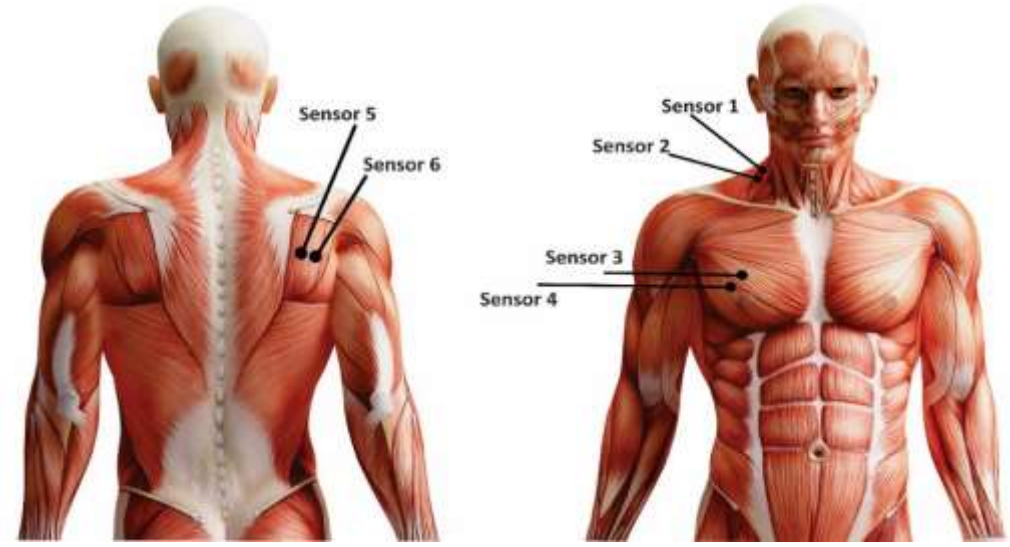

Figure 3.11: Two channel electrode placement around the shoulder muscles

In Figure 3.11 Sensor 1 and 2 indicate the location of electrode on the scalene muscle. Pectoralis and Infraspinatus muscles electrode location are indicated by the sensors 3, 4 and sensors 5, 6, respectively. Afterward, subjects were asked to perform four sets of action of the shoulder as resting, elevation, adduction and abduction described in Table 3.3. Control subjects were asked to do the exercise from the neutral position.

Table 3.3: Description of muscles activation with shoulder movement

Shoulder movements	**Description**	**Muscles involved**
Resting	The subject relaxed his shoulder without any activation of muscles	None
Elevation	Lifted his shoulder towards the ear gently and then slowly relaxed down at resting position.	Scalene
Horizontal Adduction	Rolled them forwards, squeeze the shoulder blades at the chest	Pectoralis major (Pect)
Horizontal Abduction	Rolled them backwards, squeezed the shoulder blades at the back	Infraspanatus (Infra)

The amputee participants were asked to perform the same with their missing arm. Bipolar electrodes were placed on the shoulder muscle of subjects of both groups and the sEMG signal was recorded by the NeXus-10 Mark II hardware. The sEMG system had a gain factor of 19.5 and CMRR $\geq$ 100 dB. The sampling rate of sEMG signal was kept 1024 samples/second for

each channel and the resolution was 12.2 nV/bit. With two channels, the combination of two muscles (SP, IP, IS) was taken for collecting the signal.

3.6.2 Four channel electrodes placement

sEMG signal was acquired from the four muscles Teres Major, Trapezius and Pectoralis Major muscle around the right side shoulder and the fourth sensor was on Trapezius muscle on left side through non-invasive electrode. For electrode placement bipolar configuration four independent channel pair and one reference channel (placed left side of wrist /arm) were utilized. Figure 3.12 shows the autonomous channel for different muscles. The sEMG data were collected from the distinctive positions of shoulder muscles point combinations with teres major muscle (sensor 5, 6) trapezius right side (sensor 1, 2), trapezius left side (sensor 7,8) and pectoralis major (sensor 3, 4).

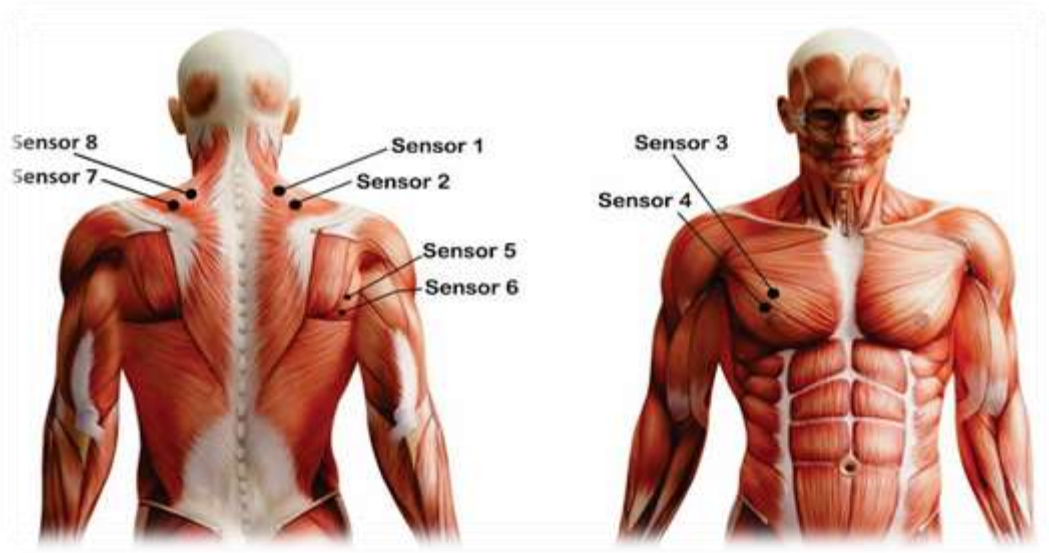

Figure 3.12: Four channel electrode placement around the shoulder muscles

Figure 3.13 shows the presentation of different movement of shoulder indicated by the sketch from the internet source. Resting stage when there is no movement of shoulder. In *elevation*, protraction and retraction the different muscles are activated as per the force exerted by the individuals. It clarifies about the action performed by the amputees and non- amputee persons after placing the electrode on the above-mentioned shoulder muscles. Similarly, for *protraction* motion, the right shoulder was moved from the rest position to rolling the shoulder forward thus squeezing the shoulder blades at the chest. The shoulder moves in a backward motion, squeezing the shoulder blades at the back for *retraction* movements. The amputee participants

performed all the movements with their residual limb and non-amputee participants performed this by stabilizing the arm. Four channels system was used for the above stated three muscles location. All the subjects were trained to perform shoulder movements in three different directions from right side of shoulder and elevation from the left side to acquire. Each movement of muscle was performed for about 5 seconds and in each trial, the participant performed various movement of shoulder four times. To reduce the effect of tiredness, the participants were allowed about five-minute relaxation break between two consecutive movements.

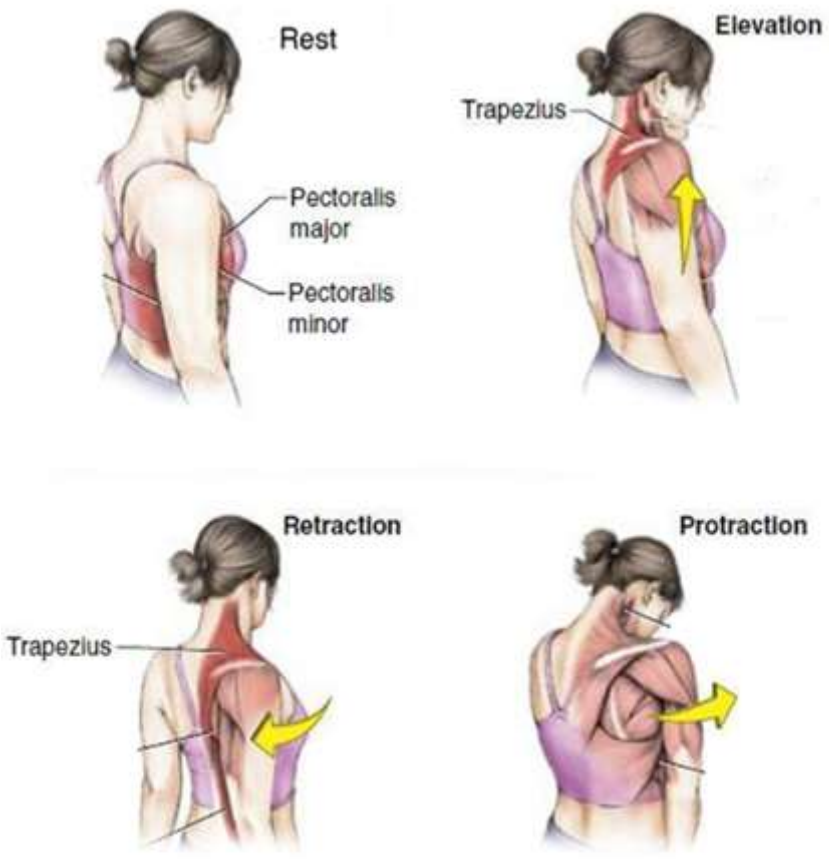

Figure 3.13: Different movements of shoulder carried out by the participants [117]

3.7 Data Acquisition

For acquiring sEMG signal, NeXus-10 Mark II version V20 (of Mind media International B.V and TMS International BV, The Netherlands) multi-channel physiological monitoring and feedback platform system was used. It is intended to acquire high quality bio-electrical and other physiological signals. The NeXus-10 Mark II encoder contains precision electronics for signal and data acquisition, data storage, transmission and help to recover the entire signal. The

Nexus-10 system transfers sEMG signals from human body to a computer for processing and analysis. It is intended for use with the BioTrace+ application software for data analysis and presentation. In the sEMG system, the DC amplifier is used with very low input noise and high input impedance. The notch filters are used to suppress the 50 Hz main power interference. The sEMG system had a gain factor of 19.5 and CMRR ≥ 100 dB. The maximum sample rate of the nexus is 8192 sample/sec, analog to digital output is 24 bit and the resolution is 12.2 nV/bit. A data acquisition session consists of initialization, configuration, execution and termination.

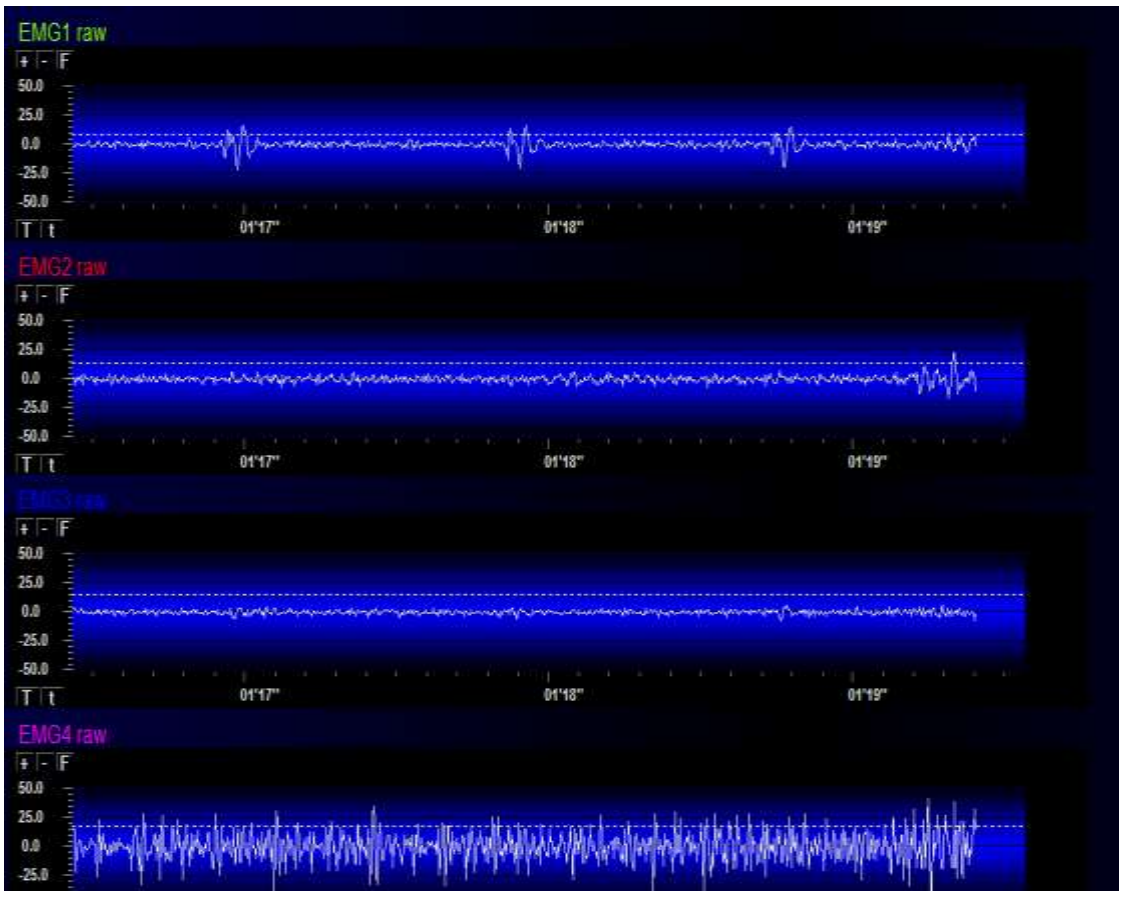

Figure 3.14: Screenshot of four channel sEMG signal acquired with the Nexus

Softs scope is a graphical user interface configuring the Nexus hardware with the Biotrace Software and perform live data analysis. It displayed and analysed the data using interface. Data of the 16 subjects was acquired using NeXus-10 Mark II physiological monitoring and feedback platform. Three channel sEMG system was used to analyse the changed estimations of muscle activity [2]. The four-channel system was used to acquire data for two degree of freedom. The raw sEMG sample rate was chosen as 2048 samples per second. Each sample has 24-bit resolution. The signal was filtered by the four order IIR band-pass Butterworth filter with frequency range between 20 – 500 Hz. The three channels placed on the three muscles

i.e., Pectoralis Majors, Trapezius and Teres Major are denoted as EMG1, EMG2, EMG 3 and EMG 4 (Figure 3.17). The acquired raw signal amplitude changes with respect to the movement of the shoulder. The raw signal obtained is useless if it cannot be quantified. Therefore, various methods like artificial intelligent, time series and time frequency domain analysis, Wigner-Ville Distribution (WVD) and genetic algorithm has been applied to achieve the accurate information from the sEMG signal [2], [118], [84]. Chapter 2 provides the explanation of the analysis methods used. In this thesis, the acquired signal was first pre-processed and then analysed the signal with the wavelet transform technique. Before using the wavelet transform, the optimal transform selection according to the acquired signal is the main difficult task. The next chapter shows the methods to pre-process the signal and the analysis of the signal through wavelet transform method.

Summary

The sEMG acquisition system has been designed to acquire signals from muscle on the shoulder. For this, an overview of the human shoulder muscles anatomy was carried out. The sEMG data were collected from the distinctive positions of shoulder muscles point combinations viz. teres major muscle, trapezius and pectoralis major with protraction, retraction and elevation movement of the shoulder.

Chapter 4
Surface Electromyography Signal Analysis

4.1 Overview

Surface electromyography (sEMG) determines the level of muscle activity through the activity of myofibrils [119]. It is a non-invasive tool to provide the information regarding the muscles fatigue and also indicates the velocity of the action potential through the excitable membrane. sEMG signal has highly complex time and frequency characteristics. During the acquisition of the signal, several variations like amplitude and frequency get introduced due to the noise in the acquired signal which misguides the prediction of motion of the shoulder. These artifacts need to be minimized before the analysis of the signal. The analysis of sEMG signal is usually performed in the frequency domain through the Fast Fourier Transform (FFT) and Short Time Fourier Transform (STFT). However, the FFT method is not suitable for the signal of non-stationary nature; it needs the stationary signal. In our work, the signal is a non-stationary sEMG signal and, therefore, we need to explore different techniques that provide results both in static and dynamic exercises. To overcome this problem, STFT and wavelet transform (WT) are proposed for the analysis of the signal. This chapter deals with the theoretical study and experimental results of the methods used in sEMG signal processing namely STFT and WT. The chapter is divided into three sections:

Section1: *Adaptive threshold method for peak detection of surface electromyography signal from shoulder muscles.*

This method aims at adjusting the threshold adaptively so as to filter the unwanted peaks in the pre-processing stage of the surface electromyography (sEMG) signal.

Section 2: *sEMG signal variations in amputee and non-amputee subjects*

To make a prosthetic device for an amputee person, sEMG signal has been found to be very useful and also easily acquirable from the skin surface. Different parameters are defined and estimated to characterize the limb movements. Most of the interpretation have done on the healthy persons and a very little work has been done on amputees who have lost their arms. Therefore, the main aim of current work is to investigate the shoulder movements of amputees and non-amputees and compared these movements. For improving the accuracy of the signal, these results are to be verified with time-frequency representations. The signal analysis using

the STFT (Short time Fourier transform) spectrogram was the main part of this section and it is described in detail.

Section 3: *Selection of optimal mother wavelet transform for shoulder muscles*

It is based on the optimal selection of the mother wavelet transform. The wavelet transform is one of the most powerful tools in biomedical signal processing. It is a time frequency analysis method especially useful for the non-stationary signals. Before using the wavelet, the unwanted signal appearing due to the extra force exerted by the individual was reduced. These peaks were removed by the proposed method will explain in the next section of this chapter. Afterward, selection of the optimal mother wavelet family function with and without the addition of noise signal in the original signal is described.

4.2 Adaptive Threshold Method for Peak Detection of Surface Electromyogram Signal from shoulder muscles

Determination of the onset and offset of muscle activity is clinically useful to investigate the difference between amputees and non-amputee muscle activation [45]. Onset detection of muscles is a challenging because of the stochastic nature of the EMG signal. There are many different approaches to EMG data-processing and analysis described in many research papers and dissertations [120], [84]. Numerous methods, including wavelet transform [121], [122], [84] artificial neural networks [123], K-means clustering [124], statistical criterion [50] and adaptive filtering [58] have been proposed for the analysis of the signal, peak detection and their deletion [123], [53], [125], [57]. However, the performance of these methods is based upon a priori knowledge of the signal. Owing to the random nature of EMG, the methods mentioned above failed to provide the exact nature of the extracted signal. Therefore, several new methods, such as the automatic threshold method [25], wavelet template matching [49], statistical criterion [50], Amplitude thresholding method (AMT) [126], Teager–Energy Operator (TEO) [47], visual inspection (VI) [51] method, are most commonly used for peak detection. Out of all these methods, TEO algorithm is gaining much popularity for energy separation in speech analysis [52]. This method does not require any prior knowledge of the shape of the signal and also improves the signal-to-noise ratio [26]. Maragos *et al.,* [54] used the time- frequency analysis for the peak signal detection and one of the authors [56], [55] used the time–frequency analysis using TEO [47]. In [128], the author used the Teager–Kaiser Energy operator to assess the surface electromyography activity from the hip and trunk muscles during paediatric gait in children with and without cerebral palsy. Dayan *et al.,* used the peaks

counting methods for real-time muscle monitoring system [58]. EMG burst with unique muscle activation helps us to identify the duration of the offset and the onset of the muscle activity in different clinical conditions that will be covered in the next section [48].

It is evident from the literature cited above that the researchers have largely ignored the real-time sEMG signal for the upper limb amputees. This has served as a motivation for the author to process the real-time sEMG signals for the transhumeral amputee persons. However, no study has effectively provided accuracy with TEO for sEMG signals for the upper-limb amputee.

4.2.1 Adaptive Threshold Detection

TEO is a nonlinear energy-tracking signal operator in a number of applications, namely signal processing, image processing and colour image processing [42], [128], [49]. It is based on using both amplitude and the frequency analysis simultaneously.

For continuous time, the TEO is defined as

$$\psi[x(t)] = [x(t)]^2 - x(t)x''(t) \quad (4.1)$$

where $x''(t)$ is the second-order derivative of x(t). The discrete-time TEO is defined as

$$\psi[x(n)] = x^2(n) - x(n+a)x(n-a) \quad (4.2)$$

where x(n) is the input signal and a is an arbitrary integer ($a \geq 1$). TEO is quite sensitive to detect the changes in muscle activity due to different movements. It is given by the local mean value denoted by β.

$$\beta = (x[n-a] + x[n] + x[n+a]/3 \quad (4.3)$$

The original TEO as shown in Equation (4.4) is the combination of β values and frequency content. The variations in the β-value and frequency increase simultaneously and emphasizes the peaks [53].

$$\psi[x(n)] = (local\ mean)[2x(n) - x(n-a) - x(n+a)] \quad (4.4)$$

Let the signal x (n) be the combination of the two signals $x_1(n)$ and $x_2(n)$. The non-correlation of these signals is represented by the expectation operator E $\{\cdot\}$

$$E\{\psi[x(n)\} = E\{\psi[x_1(n)]\} + E\{\psi[x_2(n)]\} \quad (4.5)$$

The presence of the spike is indicated by the equation:

$$E\{\psi[x(n)]\} = ks_1(p)rs_1(p,p) + ks_2(p)rs_2(p,p) \quad (4.6)$$

where $rs_1(n)$ and $rs_2(n)$ give the auto correlation function of the wanted and unwanted peaks respectively. The ks_1 and ks_2 are the ratio of energy of high frequency to the total signal energy. Equation 4.6 first term becomes zero, when only noise signal is present. A hypothesis was

tested in the detection theory. For the wanted peaks signal, the null hypothesis (H_0) and for unwanted peaks combination alternate hypothesis (H_1) are considered. The $E\{\psi[.]\}$ is a test statistic. If $E\{\psi[\cdot]\}$ > Threshold, then unwanted the peak signal is present and the null hypothesis is rejected. The main purpose of this study is to set the adaptive threshold level for sEMG signal.

The mean (μ) and standard deviation (σ) have been computed for each signal and then the threshold level is approximated as:

$$T = \mu + m\sigma, \tag{4.7}$$

where T is the adaptive threshold detection factor; The multiplier factor gives the level of threshold depending on the probability of the false alarm denoted by the factor 'm'. sEMG is a non-stationary process. Therefore, the $E\{\psi[\cdot]\}$ can be replaced by the frequency domain hamming windowing function W(n) with the window length 5, defined as

$$\psi_n([x(n)]) = \sum_{n=0}^{Wl-1} W(n)\, \psi[x(n-a) \tag{4.8}$$

The value of μ_s can be determined by

$$\mu s = (Rxx(0) - Rxx(2)) \sum_{n=0}^{Wl-1} W(n) \tag{4.9}$$

where Rxx(k) is the auto correlation function of x(n) at the lag k [6,24]. The expected value of $\psi_n([x(n)])$ can be calculated by

$$\psi_n([x(n)]) = \sum_{n=0}^{Wl-1} W(n)\ E\{\psi[x(n-a)]\} \tag{4.10}$$

with

$$E\{\psi[x(n)]\} = E\{x2(n)\} - E\{x(n+1)x(n-1)\} \tag{4.11}$$

$$E\{\psi[x(n-a)]\} = (Rxx(0) - Rxx(2) \tag{4.12}$$

where x(n) is assumed as the wide-sensed stationary process and the estimation of Rxx(k) can be made by variance estimation given by

$$Rxx(k) = 0.25\,[var\{x + x_k\} - var\{x - x_k\}] \tag{4.13}$$

The variance of $\psi_n([x(n)])$ is given by

$$\sigma^2 = var\{\psi_n([x(n)])\} \tag{4.14}$$

$$= E\{\mu_n^2([x(n)])\} - E^2\{\psi_n([x(n)])\} \tag{4.15}$$

$$= E\{\mu_n^2([x(n)])\} - \mu_s^2 \tag{4.16}$$

The sEMG recordings are the mixture of noise and signals; thus, it becomes difficult to remove the noise from the data completely. Therefore, the value of μ and σ help us to provide an adaptive threshold value and to estimate the separation between the noise and signal.

4.2.2 Results and Discussion

Human body as a whole is electrically neutral, but even in the resting state, nerve cell membranes are polarized and produce a signal called the resting stage of muscles, as shown in Figure 4.1. It shows the normal muscle activity is the resting phase of the muscles when there is no motion of the individual. The amplitude more than 120µV demonstrates the extra force exerted by the individual to move the shoulder. The resting and active condition of the muscle signals of the trapezius, teres and pectoralis muscles at different amplitude levels for approximately 360 data samples. The data set shows that the activation of trapezius muscle (above 100 micro volt) is more as shown by the orange color in figure 4.1. The amplitude of the infraspinatus muscles seems to be 120 µV but actually, the peak amplitude was 90 µV. The higher value of amplitude was due to the transient force.

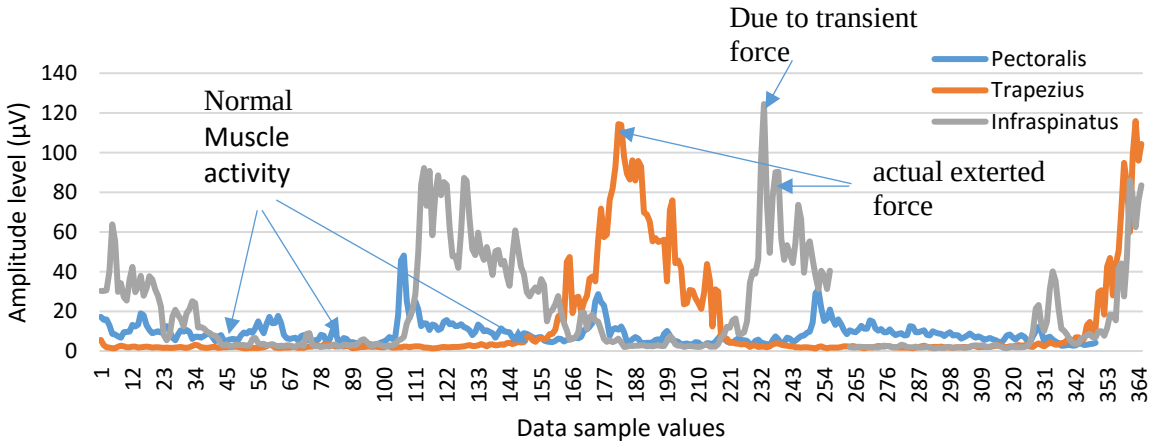

Figure 4.1: sEMG signal with different muscle activity

With the movement of the shoulder, muscles get activated and generate the electrical signals with different amplitude levels. This amplitude level is directly proportional to the force exerted by the subjects to move the shoulder. As the force exerted, motor units become more active and the firing rates of these units also increase accordingly. In general, effect of contraction forces is manifested by firing of several motor units. Due to which many action potential are generated simultaneously which cannot be distinguished individually in the signal [127]. The transient force exerted on the muscles by the amputee or non-amputee subjects leads to the injection of additional peaks in the detected output, which is shown in Figure 4.1. As these extra observed peaks misguide the prediction of the movement of the shoulder, these need to be extracted and removed from the detected output.

For the peak detection, the main aim is to determine a proper threshold value for the accurate EMG signal analysis [128]. For this purpose, AMT and TEO operations were applied after the filtration using the Butterworth band pass filter. In AMT method, the input signal was first inverted and then threshold value T was set to mσ, where m is the multiplier factor and σ is the standard deviation of the signal. On the other hand, the adaptive threshold detection factor in the TEO method was evaluated from Equation (4.7) and the values of μ and σ were calculated using Equations (4.9) - (4.14). The multiplier factor 'm' was varied arbitrarily from 1 to 10 with a step of 0.5, which would further generate different threshold levels corresponding to each value of m. The test statistics were employed to reject the noise and extra detected peaks of the sEMG signal with the selected operator (TEO). In addition to this, the probability of the error was also calculated for the signal to evaluate the value of m required for thresholding using the TEO. It eventually leads to an efficient and accurate identification of sEMG signal with a minimum probability of false alarm. Figure 4.2 shows the relation between probability of false alarm and multiplier values. The curve clearly indicates that the chosen multiplier value greater than 2 for thresholding provides efficient and accurate identification of the sEMG signal. It means probability of false alarm is zero with the multiplier value 2.

Multiplier value used in the TEO is determined by the difference of the two metrics (TPR and FPR). The relation between the difference and the multiplier range is shown in Figure 4.3.

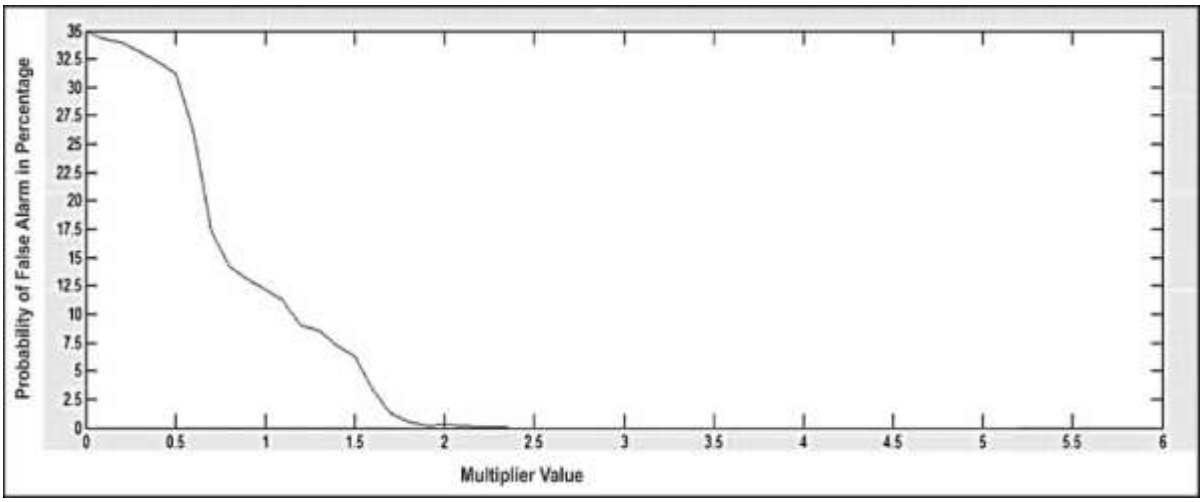

Figure 4.2: Variation of false alarm probability with the value of multiplier when using the TEO method.

It observed from the Figure that the optimal range of the multiplier required for an accurate identification of the sEMG signal used in this study is 2.5 - 4, which was similar to the value chosen by the probability of error method and has been selected in our analysis.

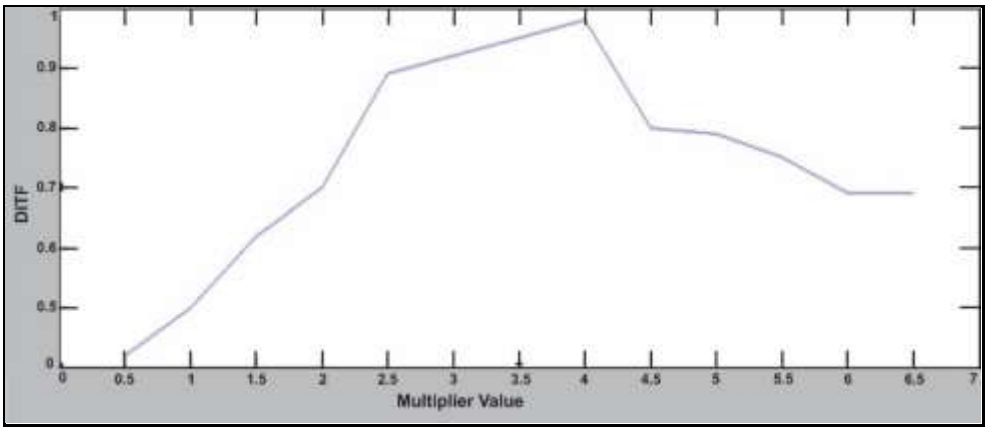

Figure 4.3: DITF values versus multiplier values

The comparison of TEO and AMT methods with the multiplier values was done using two metrics: True-positive rate (TPR) is called sensitivity and False-positive rate (FPR) referred as 1 - specificity. Term TPR is the ratio between the numbers of extra peaks correctly detected to the total number of peaks while FPR is the ratio of the number of false detections to the total number of detections.

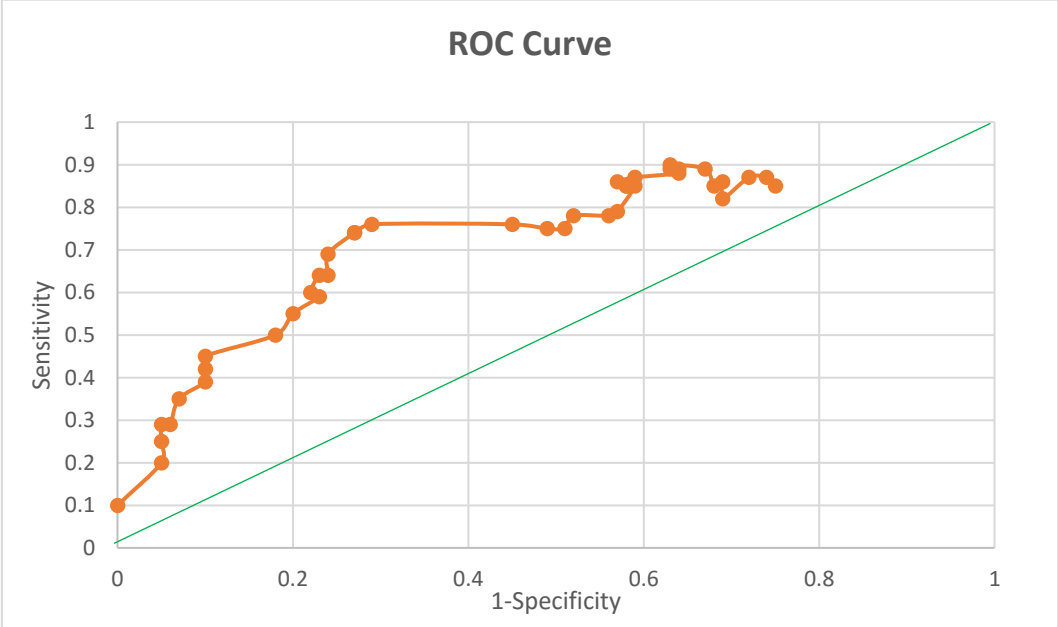

Figure 4.4: ROC curve of AMT operator

The comparative result between sensitivity (TPR) and 1 – specificity (FPR) were evaluated by the receiver operating curve (ROC), as shown in Figures 4.4.

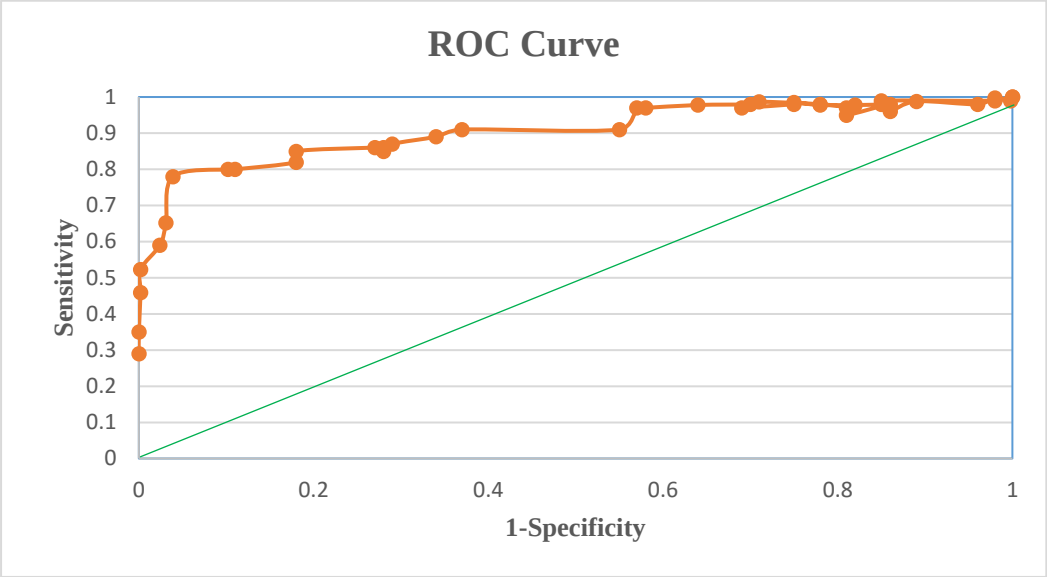

Figure 4.5: ROC curve of TEO operator

Accuracy is derived from Sensitivity and Specificity as Accuracy = (Sensitivity+ Specificity) /2. From Figure 4.6, it is clear that the TEO gives more accuracy than the AMT method. The consolidated graphical view for the different value of m indicates the accuracy difference between the AMT and TEO method. The multiplier range of 2- 4.5 gives maximum accuracy in TEO method , while m is 5 -6.5 for the AMT operator.

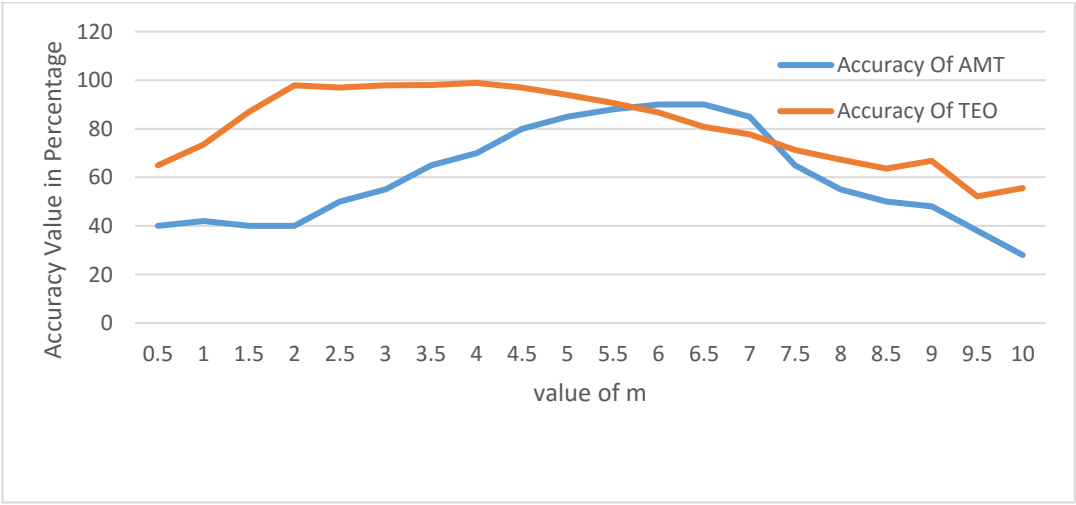

Figure 4.6: Accuracy curve for the data set used with the different value of muliplier factor for both TEO and AMT operator

The mean absolute error (MAE) is the next parameter to estimate the performance of both the operators. It is a quantity used to measure the nearest value of predicted value with the eventual outcomes and it is defined as

$$MAE = \left|\frac{p_i - y_i}{p_i}\right| \tag{4.17}$$

where p_i is the prediction and y_i is the true value.

VI method is based on the visual condition of the signal in which an expert person is assigned the task of identifying the peaks (unwanted and wanted). Operator manually analyses the signal to correctly identify the peaks. Owing to the fact that VI is a manual identification method, the sensitivity and specificity are of high value. Table 4.2 shows the MAE value processed for the two types of conditioning and comparison of these values with the VI method. Results indicates that the efficacy of the TEO method is better than the AMT method. Its value is nearer to the VI method with minimum value of mean square error. The above two comparisons justify that TEO outperforms the AMT operator. This method has been used to investigate the results with VI method. The error is 0.3 in AMT method as compared to TEO method with approx. zero error value. Figure 4.7 shows the signal with detected peaks using threshold technique, which clearly indicates the required signal extracted by ignoring the signal of the transient force exerted with the active muscles. The red-dotted line shown in Figure 4.7 indicates the selected peaks that were less than the threshold value and others above the level (peaks due to transient force) were rejected.

Table 4.1 Comparison of AMT and TEO method with the visual conditioning

Reference Signal	AMT	TEO	VI	Absolute Error between VI and AMT	Absolute Error in between VI and TEO
1	102	140	141	0.38235294	0.0071429
2	120	145	144	0.2	0.00689655
3	56	70	70	0.25	0
4	45	50	50	0.11111111	0
5	85	74	74	0.129411765	0
6	135	150	152	0.12592593	0.0133333
7	68	54	51	0.25	0.05555556
8	85	102	102	0.2	0
9	38	54	54	0.42105263	0
10	87	120	120	0.37931034	0

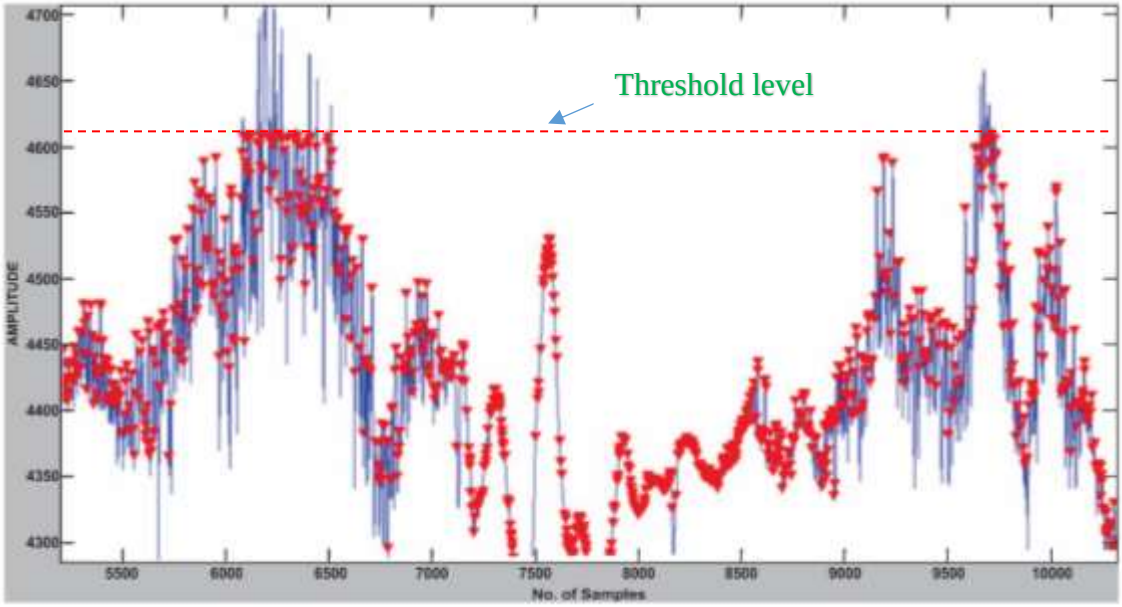

Figure 4.7: Location of actual detected peaks according to threshold level

The literature available mainly focuses on the detection of EMG signal by the visual detection and the threshold-based detection method [129], [128]. To the best of the author's knowledge, analysis of a real-time sEMG signal from the shoulder muscles of the upper - limb amputee is being reported for the first time using the TEO method. So, the sEMG signal analysis cannot be compared that with other literature results that had used different biological signals. But, if we broadly compare our results with the literature cited above, we saw that the TEO method is more accurate and efficient than the AMT method. The different sEMG signals from different movements were analysed and confirmed our expectation that TEO with a specific range of the threshold level improves the signal quality. Secondly, a majority of methods, such as template matching, amplitude measurement, statistical measurement and probability criterion [130], [53], [128] are based on threshold-level measurement using the varying amplitude of the signal. The method considered in the analysis is based on both amplitude and frequency of the sEMG signal. Recording and interpreting the signal from the shoulder muscle of an amputee is a challenging task. The placement of the electrode on shoulder must be accurate to avoid the crosstalk and the additional force exerted by the individual subject. These factors increased the variability and decrease the quality of the signal. TEO is an automatic technique that reduces the time required to analyse the signal.

Clinical scientist has investigated the muscles' activity in numerous fields. Therefore, a reliable and accurate method of the sEMG analysis is necessary to appropriately maintain the rigour of scientific research. To meet this goal, the TEO method with adaptive threshold has been a valid tool to detect the required onset muscle activity and ignore the undesirable signal. Muscles data were acquired from the muscles of the upper-limb amputee shoulder with different movement of shoulders. To validate the efficiency of the proposed method, the TEO method was compared with the automatic threshold method (AMT) using the VI method. The TEO method outperforms the AMT method and the mean-square error of TEO is almost zero when tested with the VI method. The relevance of this method to other clinical populace will establish its feasibility for recommendation on its use in the prosthetic design by extracting the accurate and effective sEMG signal.

After the pre-processing of the signal, the next part of this work was to analyse the sEMG signal for the characterization of the distinctive shoulder movement. But the first thing should be the clarity of the comparison between the amputee and non-amputee muscle activity so that a proper prosthetic device can be made for the amputees. This will be the next section of the study.

4.3 Surface EMG Signal Variations in Amputee and Non-Amputee Subjects

The sEMG signal is persistently changing over the time and can be depicted in terms of amplitude and frequency. sEMG signal performance is dependent on the physiological changes in the muscles. Time frequency methods give the effective representation for determining and enhancing the accuracy of signal [127], [131]. The sEMG signal investigation utilizing STFT demonstrated a greater inconsistency in the signal with the dynamic exercise [45]. In this section of the thesis, an examination of sEMG signals across a wide range of steady-state changes in the muscle activity of above-elbow amputees and non- amputee persons was carried out. Assurance of the onset and offsets muscle activity is clinically helpful to determine the distinction between muscle initiation of non-amputee and non-amputee body. One should have the knowledge about this difference signal before making a device for the shoulder prosthetic users.

4.3.1 Time-frequency analysis of sEMG signal

Time frequency analysis has assumed a central role in the area of signal processing. It is mostly used in the processing of non-stationary signal like radar, telecommunication and biomedical signal. The strategy of the fourier transform is not suitable for non-stationary signal because it provides the frequency content with finite time support. The frequency contents of the signal are represented by the frequency spectrum. With the muscle fatigue, the frequency of the signal changes with time, therefore these types of signals are analysed by the time-frequency techniques wherein the time perspective is equally important as the frequency content. Frequency spectrum shows all the frequencies present in time, but the time-frequency distribution shows that the different frequencies present at different range of time [79]. The time - frequency analysis applies the Fourier transform to an overlapping section of the entire signal.

4.3.2 Discrete fourier transform

Many images and signal processing algorithms are implemented by using the Discrete Fourier Transform (DFT) method. To compute the frequency content of a time series of the signal $x(n)$ the DTFT (Discrete Time Fourier Transform) is defined as:

$$X\left(e^{j\omega}\right) = \sum_{n=-\infty}^{\infty} x(n)e^{-j\omega n} \tag{4.18}$$

where *n* is a discrete-time instant. $X\left(e^{j\omega}\right)$ is also called spectrum and can be defined for all ω. It cannot be used practically because there are an infinite number of points in that range (Eq. 4.18). Therefore, to restrict it to the finite length and in that case the DTFT equation can be modified as:

$$X\left(e^{j\omega}\right) = \sum_{n=-\infty}^{N-1} x(n)e^{-j\omega n} \tag{4.19}$$

For the fixed N-point sequence, the equation can be improved in terms of sampling points of the signal

$$X(k) = \sum_{n=-\infty}^{N-1} x(n)e^{-j2\pi kn/N} \tag{4.20}$$

where *k* are the different frequency samples at $\omega = 2\pi k/N$, k = 0, 1, 2….. . . . , N − 1.

The sampled version of DTFT (at N discrete frequencies) is called the Discrete Fourier Transform (DFT). The difference between DTFT and DFT sinusoidal signal is indicated by the Figure 4.8.

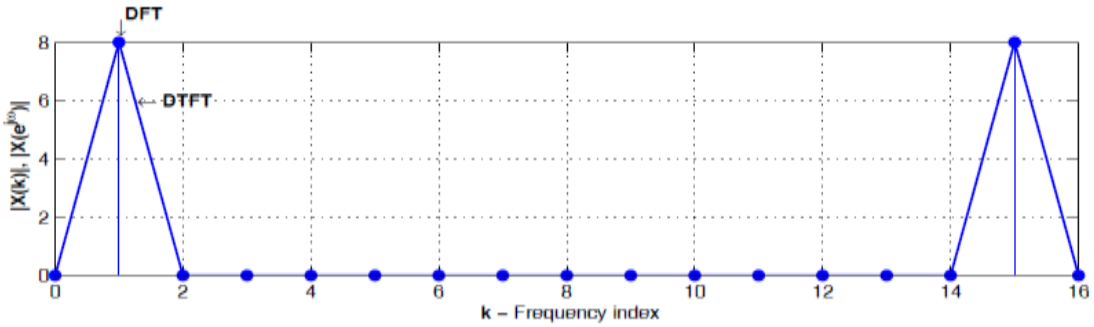

Figure 4.8: Comparison between the DTFT and DFT of a sinusoidal signal

4.3.3 Short-time fourier transform

It is the extended version of the Fourier Transform. In case of statistical signals, the STFT is used to analyze the frequency content of the signal when the frequency content varies with time. In STFT, non- stationary signal is divided into the different shorter segments assumed to be stationary and then the Fourier Transform is applied to each segment separately. The size of the segment depends on the window size. At each time, the different spectrum is obtained and the totality of these spectra is a time frequency distribution.

4.3.3.1 Continuous time STFT

Consider an analog signal x(t) . The Fourier Transform of this signal obtained by:

$$X(\omega) = F[x(t)] = \int_{-\infty}^{\infty} x(t)\, e^{-j\omega t}\, dt \qquad (4.21)$$

For STFT, consider that the fixed time is τ and the function to be transformed is multiplied by a window w(t) which shifts by τ as shown in Figure 4.9. For simplicity, consider the w (t) is symmetric.

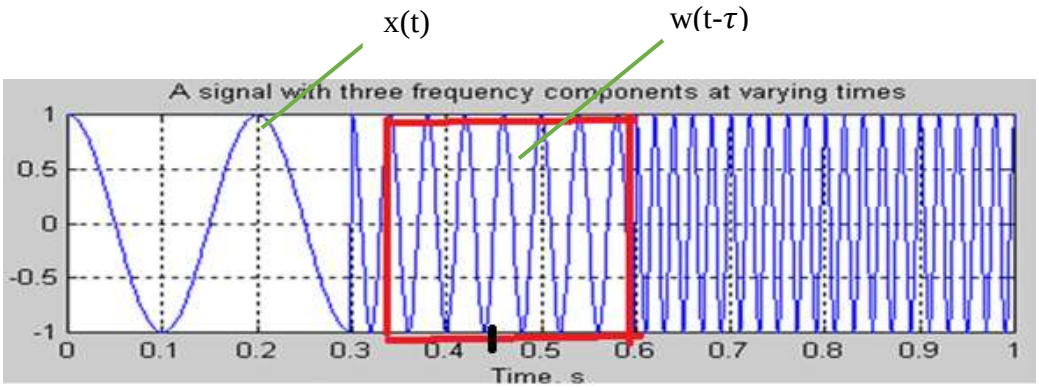

Figure 4.9: Signal with three different frequency components.

Consider the sampled signal x(t, τ)= x(t)*w(t- τ). This gives the part of the segment in the window. Then, STFT of this signal is represented by the following equation:

$X(w, \tau) = F[x(t) * w(t-\tau)] = \int_{-\infty}^{\infty} x(t)w(t-\tau)\, e^{-j\omega t}\, dt$ (4.22)

By sliding the window along the time axis, the Fourier transform of all the segments is taken for getting the resulting signal.

4.3.3.2 Discrete time STFT

The discrete time STFT is obtained by multiplying different time segments of the signal x[n] with the shifted sequence ω(k-n). Therefore, the expression is given as

$X(k, \omega) = \sum_{n=-\infty}^{\infty} x(n)\omega(k-n)e^{-j\omega n}$ (4.23)

where $\omega(n)$ is called the analysis window. The sequence $x(n)\omega(k-n)$ is a short time section or segment of x(n). The fourier transform of the short time segment gives the frequency function $X(k, \omega)$. To obtain the next portion or $X(k+1, \omega)$, we slide the analysis window to its new position from the previous one and do the same step as previously defined. The window in the STFT has a great impact on the analysis. Changing the analysis window changed all the analysis of STFT. The different window functions like Hamming, Rectangular and Blackman utilized for the analysis part. In this study, we have used the Hamming window with 256 point sample window for further analysis.

4.3.3.3 STFT Spectrogram

Spectrogram is the visual representation of spectrum of frequency with the normalized squared magnitude of the STFT coefficients. The energy in the spectrogram is equal to the energy in the time domain signal due to the Parsvel's energy conservation property.

Spectrogram (t,w)= $|STFT(t, w)|^2$ (4.24)

A shorter window length provides good time resolution, but frequency resolution is coarse. Therefore, it is difficult to get the exact components of the frequency of the signal. From this, only band of frequency can obtained. On the other hand, a long window length provides good frequency at the expense of losing some resolution in time, therefore it is difficult to get the knowledge about the occurrence of frequency. It is not possible to achieve good time and frequency simultaneously in STFT spectrogram. The spectrogram is represented by different colours which denote the frequency power level. Yellow band corresponds to the time period of the signal (Figure 4.10).

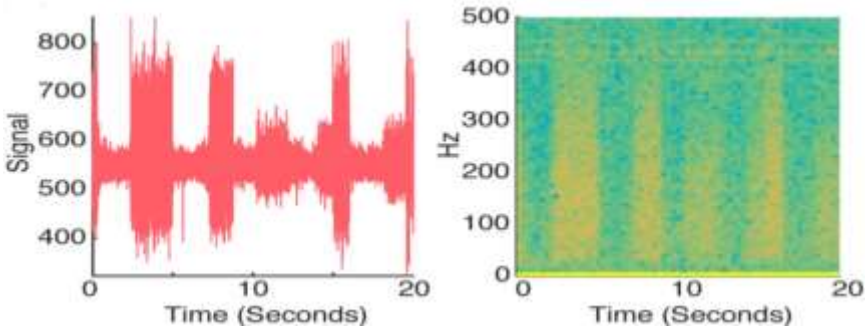

Figure 4.10: Data signal and its spectrogram

In this condition there is enough time resolution to be able to measure the duration of the signal. But frequency resolution is poor. Spreading of the yellow band indicates that some signal power has spread across the band of the frequency but it gives better results if there is a narrow band in frequency. The bright colour indicates the high value of the energy. The window size increases with some resolution loss in the time domain to obtain the frequency resolution. The spectrogram is not only used to detect the frequency but also to determine the order of frequency. In the result section, this STFT spectrogram has been utilized to compare the muscle activity of the amputee and non amputee persons.

4.3.4 Results and discussion

The main interest of this study has been to estimate the role of muscle activity in voluntary shoulder movement. A two channel experimental set up (Chapter 3) was utilized to analyze the effect of the three signals from shoulder muscles (Infraspinatus muscle at the backside of the shoulder (I), Scalene at the shoulder (S) and Pectoris major at the position on the chest (P) for different movements (elevation, adduction and abduction) from resting. The two channels and three muscles signals combined in terms of SP, PI and SI were used to verify the different results.

4.3.4.1 Magnitude level of the signal

The estimated value of sEMG signals from different muscles was characterized by different level of amplitude measured in the microvolt in both the subjects (amputee and non-amputee).

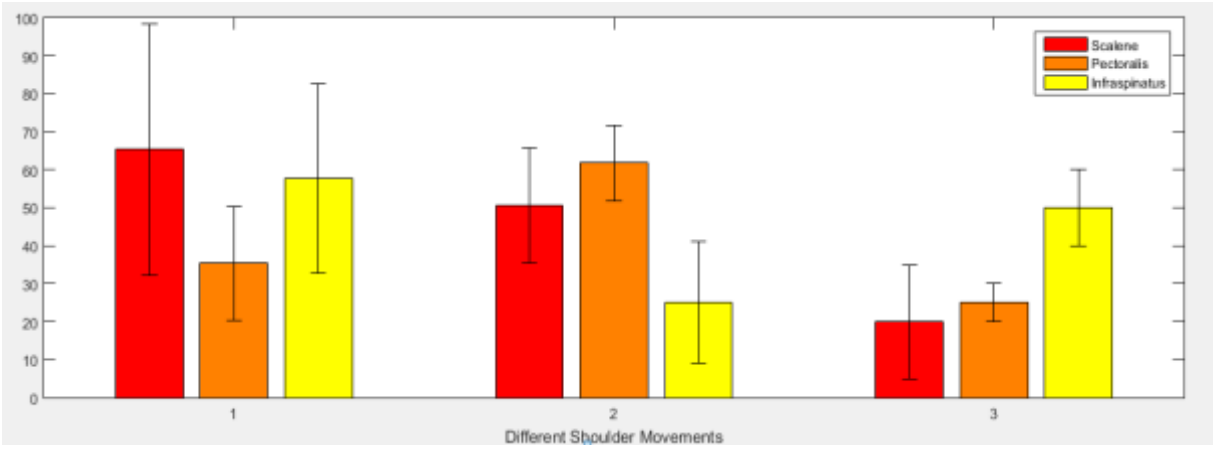

Figure 4.11: Muscles activity during different shoulder movements of non- amputee subjects

Different three muscles with three movements were utilized as mentioned above. Figure 4.11 indicates the muscle activity, with elevation, adduction and abduction shoulder movement. The y axis of the box plot shows the mean value of the different trialss from the non-amputee subjects and the line in the box represents the highest and lowest values in the data.

indicates the graphical view of the maximum value of the shoulder muscle activity of the non-amputee from different trials during the above defined three movements of the shoulder. The elevation movement of the shoulder produced the amplitude level of 100 μV that was more than the abduction and abduction movement of the shoulder. The scalene muscle was the most active muscle from all the chosen muscles during the elevation.

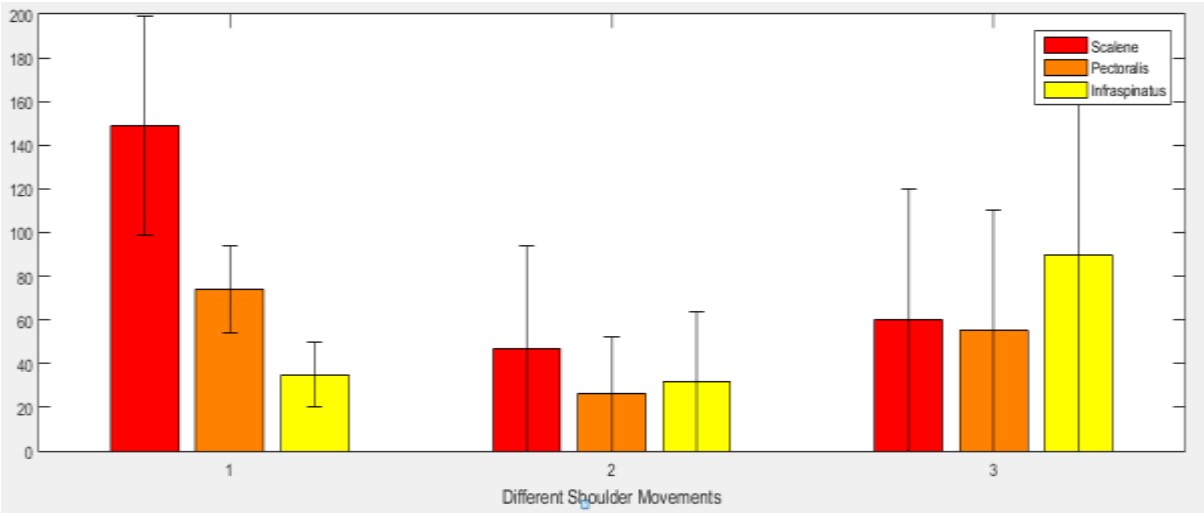

Figure 4.12: Muscles activity during different shoulder movements of amputee subjects.

Figure 4.12 shows muscle activity, with elevation, adduction and abduction shoulder movement. The y axis of the box plot shows the mean value of the different trials from the amputee subjects and the line in the box represents the highest and lowest values in the data. During the adduction motion, pectoralis (Pect) muscle was significantly more activated than the other muscles with the amplitude level of 80 μV. For the same movement, the activity of scalene muscles was less. In the abduction motion of the shoulder, the infraspinatus (Infra) muscle was the most activated one with 60 - 70 μV. From these results, it is observed that the muscles activation output value was totally dependent on the shoulder muscles. By changing the movement of the shoulder, the output were changed. This fact provided us independent signals for each shoulder motion. Above mentioned results were then compared with the amputee person muscles-activity. The amputee was made to do these defined movements with their intact limb. Figure 4.12 shows that the activation of scalene muscles of amputee person was of high value with more than 200 μV while for the non-amputee person, it was only 100 μV. Even in the amputee muscles, again the scalene muscles provided the maximum electrical signal value. In the abduction movement, the infra muscles have more value of the signal than the other muscles in the range of 80 – 120 μV. In the experiment, the adduction movement was not perfectly differentiated by the defined muscles because it always provided a small level of magnitude. Due to the statistical nature of the sEMG signal, the change in the amplitude with the time differed significantly for different subjects. This was the main challenge of this the shoulder muscles study. Table 4.3 shows the variation in amplitude value for different participating subjects.

Table 4.2: Amplitude variations of the sEMG signal of non-amputeeand amputee person

Muscles ⇨ Movements ⇩	**Non- Amputees (μV)**			**Amputees (μV)**		
	Scalene	**Pectoralis**	**Infraspinatus**	**Scalene**	**Pectoralis**	**Infraspinatus**
Elevation	65.32±33	35.4±15	57.7±25	149±50	74±20	35±15
Adduction	50.6±15	61.76±10	25±16	47±10	26±20	32±17
Abduction	20±15	25±5	50±10	60±35	55±15	90±30

From Table 4.3, it is clear that the activity level of scalene muscle, with the elevation movement of non-amputee and amputee person provided the amplitude value with 30-100 μV and 100-200 μV respectively. By the same time the protraction movement gave the results as 35-65 microvolt with the same activity. The signal were mixed if both muscles provided the output with the same variable. This was the main limitation of the use of the STFT on the sEMG data. Therefore, next approach was to use the STFT spectrogram and check the results visually. The graphical view in form of bar plot with the error value means mean ±standard deviation value were shown in figure 4.13.

4.3.4.2 STFT spectrogram analysis

In time-frequency representation of the sEMG signal, that is, STFT spectrogram, the sampling rate of the sEMG signal was set at 2,048 samples per second. The main challenge was to select the exact window size. Therefore, we have checked different window size resolution output (Figure 4.13) with the same data set to get the optimal window size..

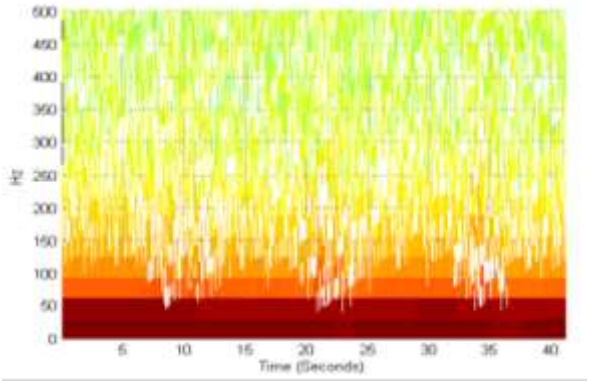

Figure (a) 64 samples window size

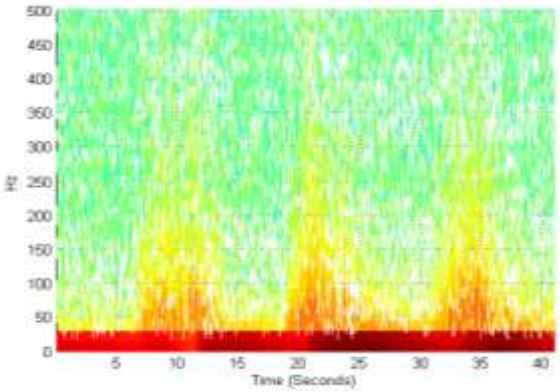

Figure (b) 128 sample window size

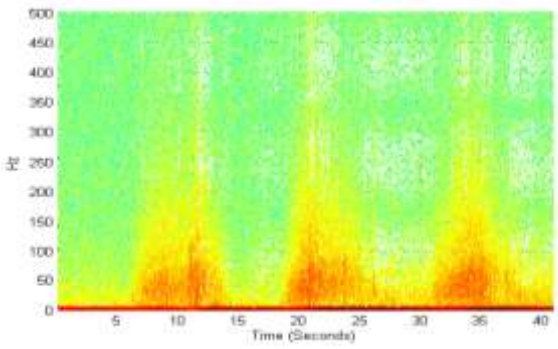

Figure (c) 256 sample window size

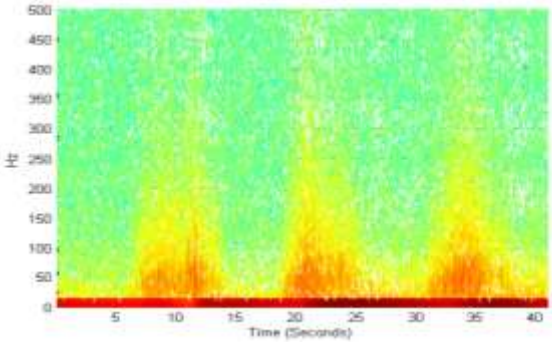

Figure (d) 512 sample window size.

Figure 4.13: Different spectrograms for 32 to 256 samples window size

The window size was increased from 64 to 512 samples to select the window which provided best resolution. In the spectrogram, action potential begins to appear when the muscles are smoothly contracted [132]. The EMG increases with the strength of the muscle contraction. The random group and non-periodic action appears when the muscles are fully contracted. The energy was not differentiable with window size 64. Indeed, even with 128 samples, the energy distribution of the signal is more spread out along the frequency axis and is more compact along the time axis resolution when the window length is wide. Therefore, the 256 window size was chosen for the EMG data resolution, by increasing the window size more than the 256 values, the energy distribution of the signal was some more blurred.

After fixing the optimal size of the window, we generated the spectrogram of different activities of the shoulder muscles. Spectrograms of Figure 4.14 and 4.15 show the activity of infra and pect muscles-activity with the movement of the arm for both amputee and non-amputee participants.

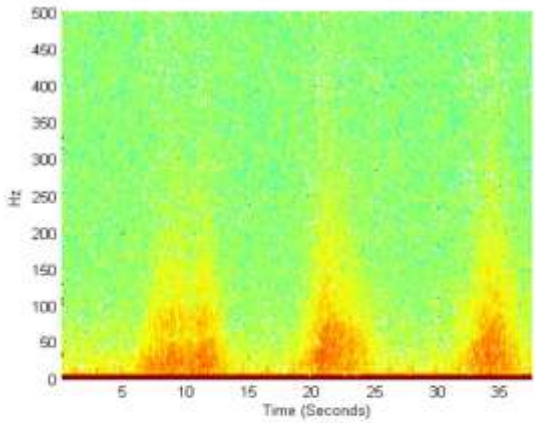

Figure (a) Infra muscles with elevation

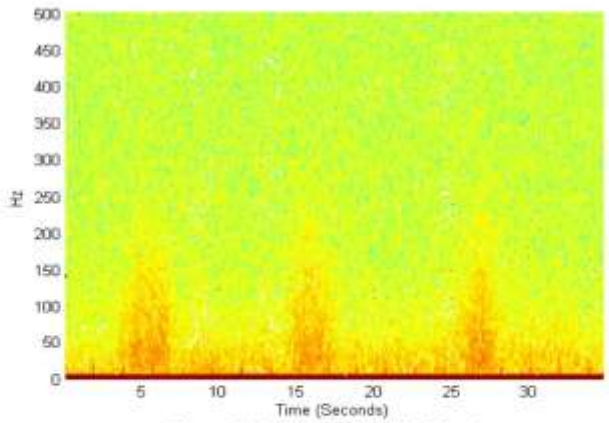

Figure (b) Infra muscle with abduction

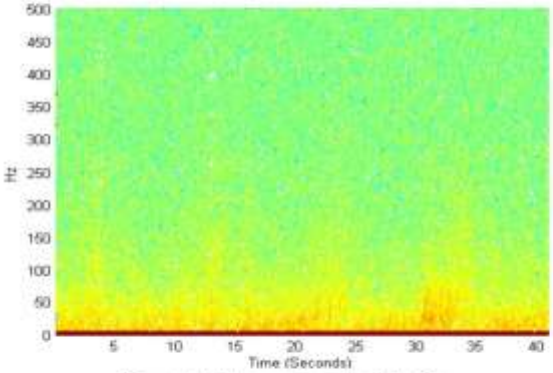

Figure (c) Infra muscle with adduction

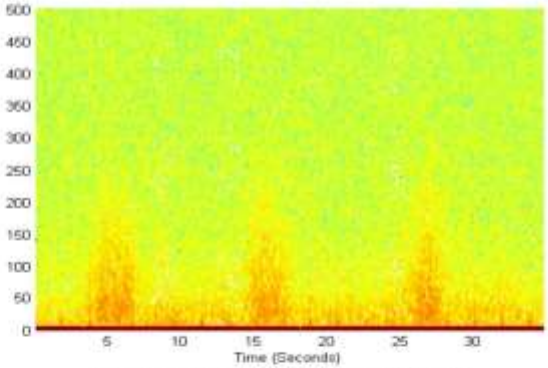

Figure (d) Pectoralis muscle with elevation

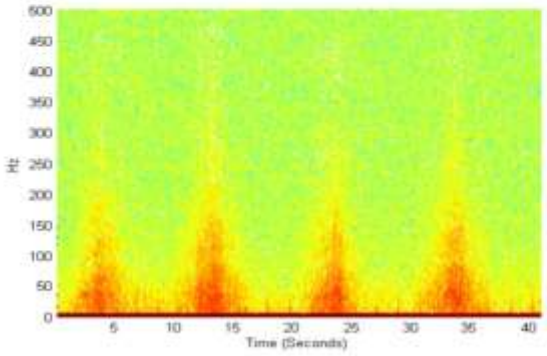

Figure (e) Pectoralis muscle with abduction

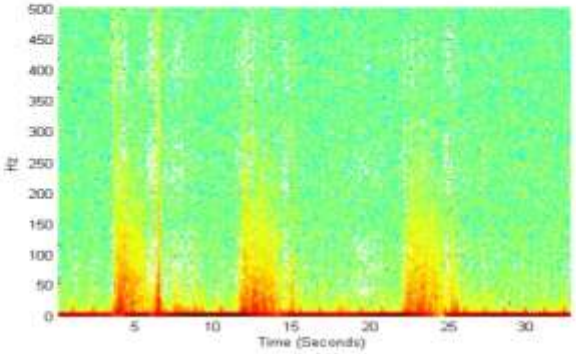

Figure (f) Pectoralis muscle with Adduction

Figure 4.14: Different muscle activation of infra and pect for amputee subjects

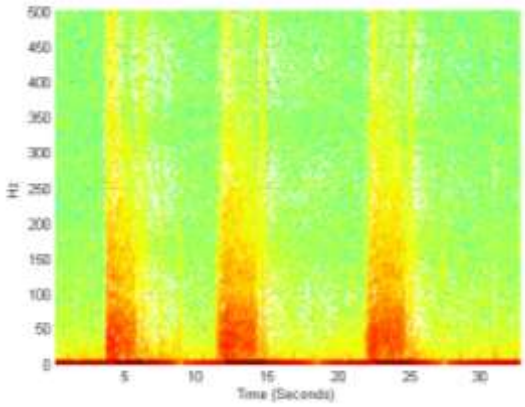

Figure (a) infra muscle with abduction

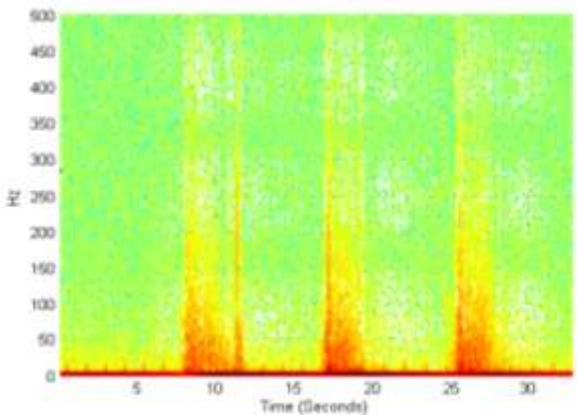

Figure (b) Infra muscles with elevation

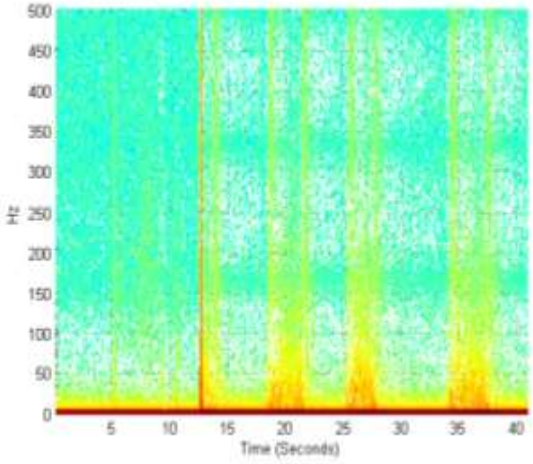

Figure (c) Infra muscle with adduction

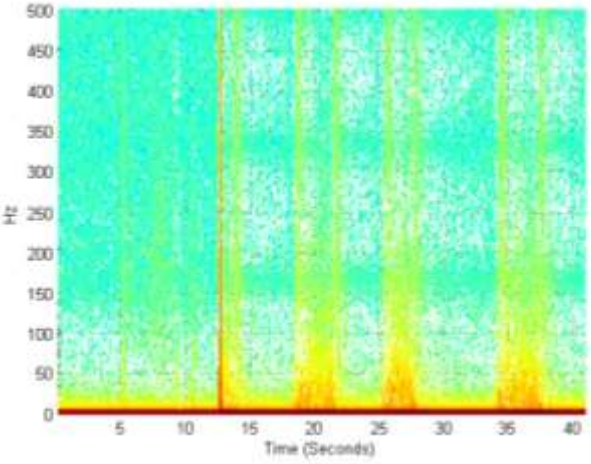

Figure(d) Pectoralis muscle with elevation

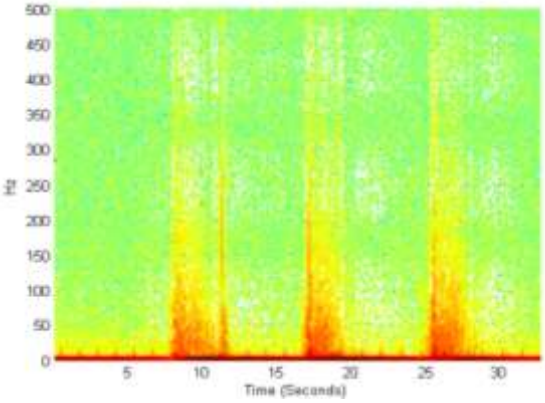

Figure (e) Pectoralis muscle with abduction

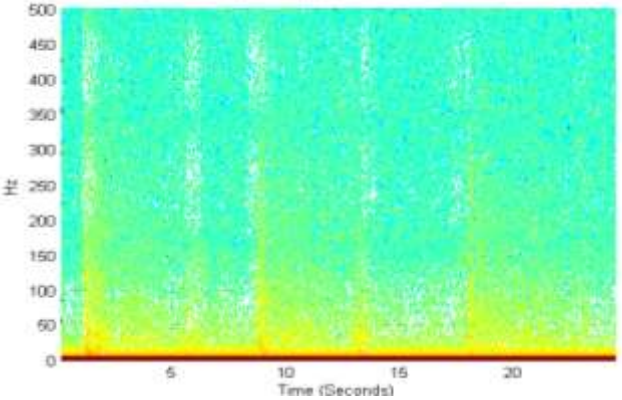

Figure (f) Pectoralis muscle with adduction

Figure 4.15: Different muscle activation of infra and pect for non-amputee subjects

A majority of the lower amplitudes and the darker colour show the change in amplitude with the contraction of the muscles in both amputee and the non-amputee data. On account of non-

amputation, the highest amplitude value of infra muscles with abduction was located at the time range of about five seconds with the frequency range about 10 - 90 Hz. In case of infra muscles for adduction movement, the values were up to 130 Hz in the same time range. The activity of the pectoralis muscles during the adduction movement of the shoulder is at higher frequency level. Therefore, this is the dominant muscle with this movement.

In case of amputation, the spectrogram signal produced more jagged response. Spectrogram showed an increase in the duration of action potential, and the muscle contraction is totally different. The Infraspinatus muscles gave the maximum activation in abduction motion with values up to 200 Hz in the frequency domain. But pectoralis did not give perfect response as the output shows. Age and amputation range were specified for both the control and the amputee group. The shoulder muscles of an amputated residual arm give different sEMG patterns when performing the same movement using a healthy arm. The MUAP (motor unit action potential) of muscular tissues with different shoulder actions were measured. The results proved the behaviour of three selected muscles around the shoulder and indicated that muscle activation has a larger value in amputees even if they had lost their arm 5–10 years ago. The overall EMG of the muscles in an amputee is higher than in a non-amputee. The amplitude of the measured signal from both types of subjects is a good parameter to activate the motion of a prosthetic arm for upper-extremity amputees.

The spectrogram shows that the three movements may be achieved with three different muscles independently. This study helps to distinguish different motion of the shoulder between the amputees and the control subjects. Implementation of these types of system gives the prosthetic user capability to perform different tasks with maximum efficiency in daily living. Using sEMG signal, it was observed that the muscles around the shoulder indicate more activity in amputee person than in a non-amputee person. STFT spectrogram gives the plot of maximum muscle contraction. By varying the STFT window size, choice of 64 sample window with 512 frequency bins provided the best resolution for the spectrogram plot.

With the movement of the shoulder, muscles get activated and generate the electrical signals with different amplitude levels. This amplitude level is directly proportional to the force exerted by subjects to move the shoulder. As the force contraction increases, more motor units become active and the firing rates of these units also increase. The combined effect of these processes in the higher forces of contraction produces so many motor unit action potentials that

they cannot be distinguished. To solve this problem, adaptive peak detection was used before the analysis of the sEMG signal. The next issue was that we had to compromise in choosing the size of window function for the STFT. A fixed window size for complete data set causes the resolution problem. When the window size is too large, the STFT becomes the normal FT. The choice of the window function is application dependent. The Fourier transform does not represent abrupt changes efficiently therefor data are not localized in time or in space. Therefore, there is a need of new class function that can accurately analysed the signal and images with abrupt changes localized in time and frequency. To resolve this problem we resorted to wavelet transform techniques to analyse the signal with adaptive resolution property. But because the uses of wavelet techniques there must be optimal selection of wavelet function from various wavelet families.

4.4 Selection of Optimal Mother Wavelet Transforms for Shoulder Muscles.

Wavelet analysis is a new development in the area of biomedical signal processing. As a part of wavelet analysis, selection of the mother wavelet is an important step to determine the effect of wavelet transform in decomposition, denoising and reconstruction of different coefficients. The selection of mother wavelet may be either empirical or by visual inspection of the signal or by previous experience and knowledge of the person. The selection of the decomposition level before the mother wavelet is the matter taken up in this section. The different decomposition levels and mother wavelet in the analysis of the signal were used [96], [133]. Zhang and Luo in 2006 [134] proposed the sym8 wavelet function with 4 decomposition levels with weighted averages rescaling method including soft and hard threshold functions for upper limb prosthesis control. Hussain *et al.,* in 2009 proposed db2, db6, db8, dmey, sym8, sym4 and sym 5 wavelet functions with decomposition level 4 and universal scaling with hard threshold function to determine the muscles contraction. For the feature selection from different hand functions, Phinyomark et al., [18], [135] summarized that the best performance can be obtained from db2 with level 2 and db7 with the decomposition level 4. But in [84], [136], [137] the researchers recommended for the wavelet functions as db2, db7, sym2, sym5, coif 4, bior5.5 and bior 2.2 with the decomposition level 4 for de-noising. It is clear that for the selection of the mother wavelet, characteristics of the signal and properties of wavelet transform should be carefully matched.

4.4.1 Wavelet transforms

The wavelet transform is the time scale analysis of the signal. The first wavelet was introduced by Haar in 1909. Then the Gabor function was introduced by the Denis Gabor in 1946. George Zweig discovered the continuous wavelet transform in 1975. In 1982, Grossmann and Morlet tried to observe the signal with the shorter wavelength signal with high frequency instead of equal duration pulses. Then in 1988, complete idea was formulated into the different mathematical tools by Daubechies who introduced the orthogonal wavelet transform. Then Stéphane Mallat with Daubechies jointly gave the filter implementation using discrete wavelet transform. Wavelet analysis allows to isolate and manipulate specific type of pattern hidden in the masses of data. These were designed for the non-stationary data like sEMG signal that were difficult to analyze in time domain. Wavelet has ability to examine the signal simultaneously in both time and frequency. It decomposes a signal into a set of basic functions called wavelets which means a small wave. Wavelet ψ has energy concentrated in time and is a function of zero average. These wavelets are obtained from the mother wavelet $\psi($ (). The daughter wavelet can be formed by dilations and shifting. It is a two-dimensional array value and is defined as:

$$\psi_{x,b}(t)= \left(\frac{1}{\sqrt{x}}\right) \psi\left(\frac{n-b}{x}\right) \quad (4.25)$$

where x and b are the scaling factor and translation (shifting) factor respectively. For the function to be wavelet, it should be time limited. Scaling refers to the stretching or shrinking of the signal in time. There is a centre frequency caused due to the constant of proportionality. The scale and frequency of the signal are reciprocal to the constant of proportionality. The stretched wavelet is corresponding to the lower frequency and the large scale factor whereas the shrunken wavelet is corresponding to the high frequency with the small scale factor. Shifting the wavelet along the length of the signal is called delaying the onset of the wavelet function. In other words, for high resolution in the signal, the mother wavelet contraction captures all the sudden changes appearing in the signal for time domain analysis. The wavelet transform is of two type viz. continuous wavelet transforms (CWT) and discrete wavelet transform (DWT)

4.4.1.1 Continuous wavelet transforms (CWT)

The continuous wavelet transforms (CWT) can resolve both time and frequency events. It provides better output than the STFT. It is defined as

$$CWT(b,x) = \psi(b,x) = \frac{1}{\sqrt{|x|}} \int x(t) b\left(\frac{t-b}{x}\right) dt \quad (4.26)$$

ψ is the analysing function called wavelet function. Scaling is stretching a function denoted by 'b' and the shifting or translation is denoted by $'x'$. These scaling and position parameters are continuously varied for getting the cwt *coefficients C (b, x).* ψ *(t)* is the mother wavelet which implies that it can generate other window functions. In CWT, the most common wavelet functions are Morlet wavelet and the Mexican hat. CWT may be a complex valued variable function or a real valued variable function of the scale and the position. This depends upon the nature of the wavelet function (real or complex).

4.4.1.2 Discrete wavelet transforms (DWT)

The discrete wavelet transforms has a critical role for processing the different human signals in biomedical engineering. It is obtained by the discretization of the CWT values and used in the time-frequency plane. It's computational time is less than continuous WT. It decomposes the signal into various sub-bands. At the high frequency signal, DWT exhibits good time resolution and at low frequency, it provides a good frequency resolution. Thus, low frequency components are more significant than the high frequency elements. It reduces the computation and provides the adequate and sufficient data of the original signal for analysis and synthesis.

$$DWT_{i,j}(f) = x_0^{-m/2} \int f(t)\psi(x_0^{-it} - jb_0)dt \quad (4.27)$$

The integer value i and j can be defined by the solution of a dilation equation or by an analytical expression. The value of x_0 and b_0 can be 2 and 1 respectively. The mother wavelet is obtained by dilated, translated and scaled version of the wavelet function and is defined as:

$$\psi_{x,b}(t) = \left(\frac{1}{\sqrt{x}}\right)\sum_r \psi\left(\frac{r-b}{x}\right)f(n),\ b>0 \quad (4.28)$$

DWT applies a series of the low pass filter (l) and high pass filter (h) on data for extracting the high and low frequency components of the signal respectively via a finite impulse response. In this study, DWT is used to extract the features from the signal. It is a multi-resolution technique used in real time, engineering applications employed to set of function called the scaling and wavelet function.

$$h(l) = (-1)^n l(1-x) \quad (4.29)$$

$$\phi(p) = \sum_n l(n)\sqrt{2}\phi(2x-n) \quad (4.30)$$

$$\phi(x) = \sum_n h(n)\sqrt{2}\phi(2x-n) \quad (4.31)$$

The quadrature mirror filter (QMF) output is

$$A = \sum_n l(n-2L)x(n) \quad (4.32)$$

$$D = \sum_n h(n-2L)x(n) \quad (4.33)$$

QMF has been used for splitting the signal in the frequency domain and to provide different sub-bands. The signal x (n) convolves with $l(n-2L)$ and $h(n-2L)$ which acts as high pass filter and low pass filter respectively and L is related to the mother wavelet function. The two components namely approximation component and detailed components are represented by cA and cD respectively. When these sub band signals are recombined then the original signal can again be reconstructed. The decomposition level along with the level can be obtained in the DWT technique by multi- level subsets. In this study, the raw data was decomposed by the DWT method. But before the decomposition, the level of decomposition and the optimal wavelet function should be selected according to the application.

4.4.2 Methodology used for optimum mother wavelet selection

The total time for one trial of single movement and then rest position is of approx. 4 second. Sampling rate is 2048 samples / second. The total samples for one trial were 4*2048 = 8192 samples. The total trials are 8, therefore the total no of samples for a single movement for a subject were 65,536. In this study, the total subjects were six and the four channel data set were used for the analysis purpose. Here, mother wavelet function methodology is described as shown in the Figure 4.16 and 4.18 described the denoising of the original signal is introduced while in other extra noise level is added to find out the best mother wavelet which leads to a better filtration performance respectively. The different steps in the methodology are follows. After acquiring the signal form, the multi-channel combination (Chapter 2 and Chapter 3), the next step was to find the optimum mother wavelet for denoising the acquired signal.

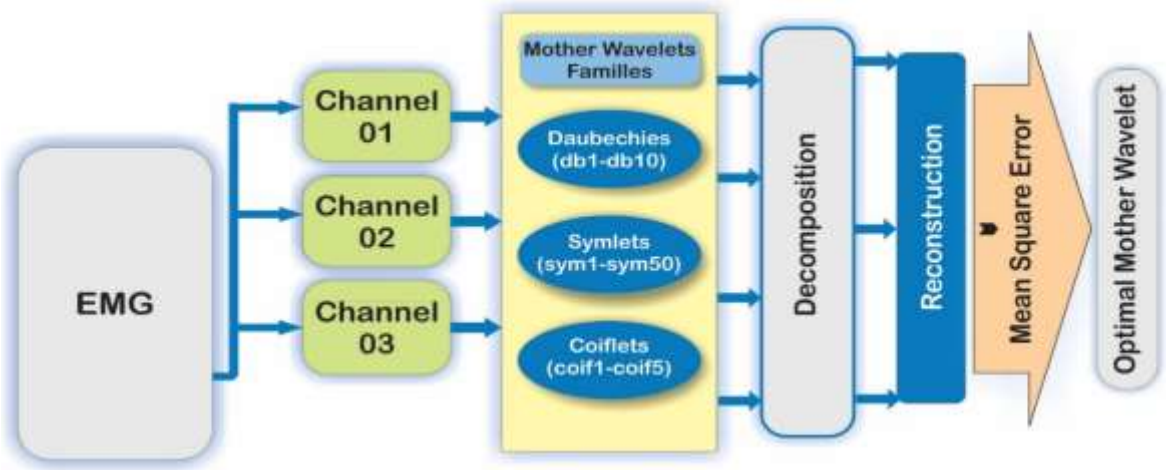

Figure 4.16: Methodology to find the optimal mother wavelet for shoulder muscles signal

4.4.2.1 Different mother wavelet

Mother wavelet transform, wavelet decomposition, threshold values and reconstruction of the signal are the signs of better performance in wavelet based signal investigation. Mother is chosen on the premise of the similarity with the shoulder sEMG signal. It additionally helps to retain the original signal and improves the frequency spectrum of a de-noised signal.
All the wavelet families used in this study are presented in the Table 4.2.

Table 4.3: List of used 21 wavelet function from four different wavelet family.

Wavelet Family	Wavelet subtypes
Daubechies (db)	db1,db2, db3,db4,db5,db6,db7,db8,db9,db10
Symlets (sym)	Sym1,sym2,sym3,sym4,sym5
Coiflet (coif)	Coif1,coif2,coif3,coif4,coif5
Discrete Meyer	dmey

The setup for the selection of the optimal mother wavelet is given in Figure 4.16. The main motive behind choosing the optimal mother wavelet from wavelet families was that the reconstructed signal should be free from the artifacts that contaminate the sEMG signal. In this study, different orthogonal families, including (db1-db10), Symlets (sym1–sym5) and Coiflets (coif1–coif5) were selected. The right wavelet family determines the proper analysis and reconstruction of the signal. The error between the reconstructed signal and original signal was calculated as the mean square error (MSE) value defined as

$$MSE = \frac{\sum_{i=1}^{N}(H_i - R_i)^2}{N} \tag{4.34}$$

where H_i and R_i represent the sEMG signal and the noised signal respectively. The less value of the MSE indicates the better performance of the wavelet method.

4.4.2.2 Wavelet decomposition

To analyze the sEMG signal, the initial step is the determination of ideal decomposition levels on the premise of the dominant frequency. The output signal is maximal if the input signal looks like the mother wavelet and energy will spread over a large number of coefficients. The variation of the decomposition level is from the first decomposition level to the last decomposition level depending on the factor 1 to $M = \log_2 N$ where N is the length of the samples in time domain. So, the decomposition levels are dependent on the dominant frequency of the signal. The original signal, denoted by s (n) was passed through the high pass and low

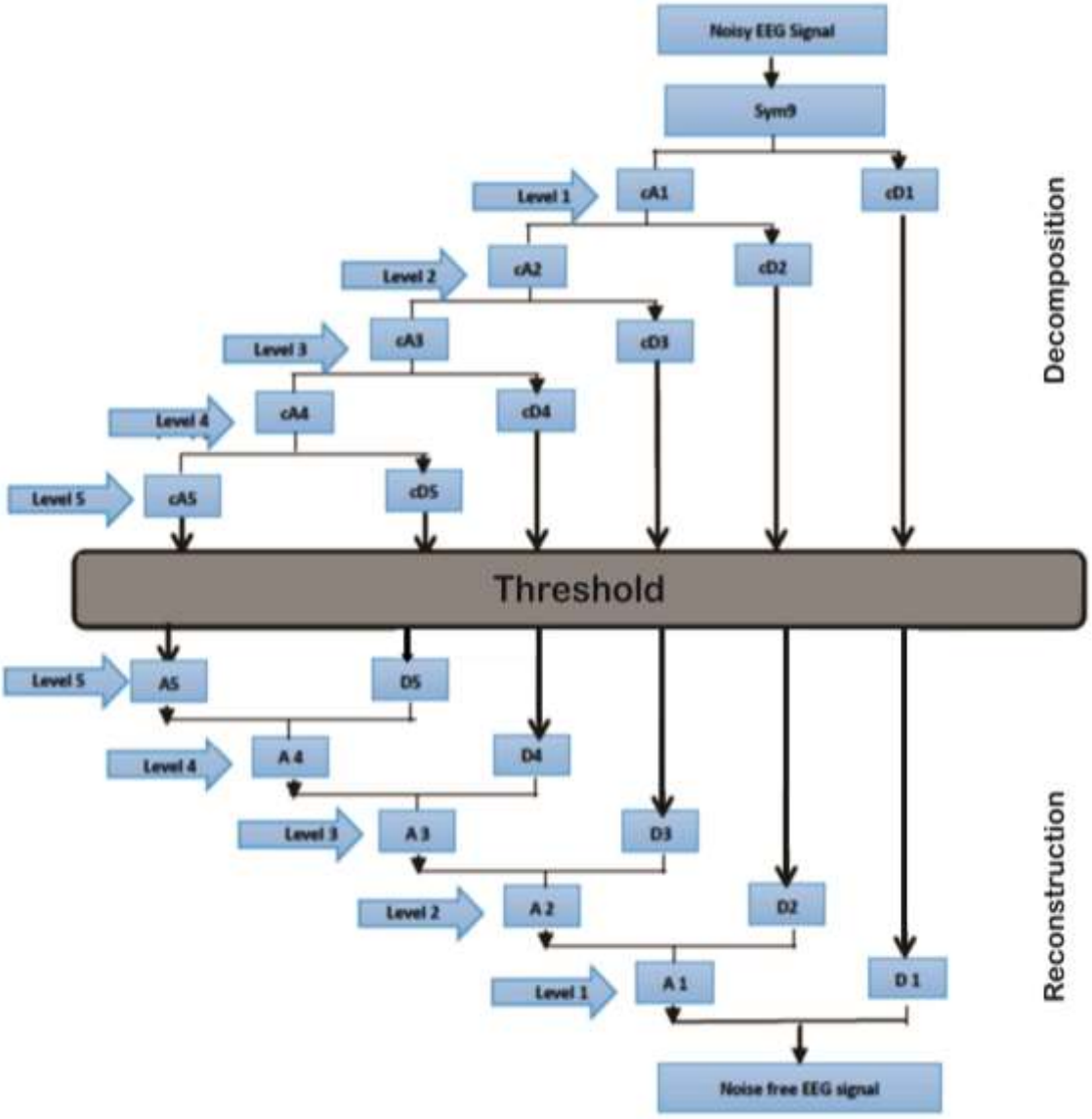

Figure 4.17: Wavelet decomposition tree with the sEMG signal [138]

pass filters. The high pass filter coefficients are called detailed coefficients denoted by D_{k+1} (n) whereas, the low pass filter coefficients are called approximate coefficients denoted by A_{k+1} (n). In this study, sampling frequency of the sEMG signal with shoulder muscles was 2048 Hz. Figure 4.17 shows the first level approximate coefficients (cA1) can obtain with the down sampling of the low pass filter and the first level decomposition coefficient (cD1) can with the same sampling of the high pass filter. In second level decomposition was on the cA part by same down sampling method and the second level decomposition coefficients can obtain. The process was repeated up to the desired level of decomposition shown in the Figure 4.17. It shows that the down sampling frequency produced the different decomposition (cD) and approximate coefficients (cA) for five different decomposition levels (1,2,3,4,5). After

thresholding, the signal moves through the reconstruction process as inverse of the decomposition process with the same level. The process generally goes on up to three or maximum four decomposition levels. Here, the sampling frequency of the sEMG signal with shoulder muscles was 2048 Hz. The decomposition levels were selected for different mother wavelet functions.

4.4.3 Wavelet Denoising

To get best wavelet denoising method, the additional noises are added and each time the noise decomposition level is varied from low to high noise decomposition level. Figure 4.18, shows the white Gaussian noise with 5dB SNR were added in the signal. This noise level has been removed from the signal by denoising the process before the reconstruction. The small value of MSE proved that the undesired part of the noise was removed and the useful information remained in the signal. To grab this outcome, the DWT procedure involved different steps: threshold selection rule, threshold rescaling and threshold function. In addition to this, the decomposition level and the wavelet function must be evaluated which is described in this section.

4.4.3.1 Thresholding techniques

The observed coefficients can themselves be considered as the noisy version of the wavelet coefficients and after decomposition, these coefficients can be denoised. So, the thresholding technique is applied to the detailed decomposition level coefficients. After the decomposition, the denoising technique is applied to the signal to remove the noise level from the original signal. This procedure removes the level of noise from the original signal. The output will be maximized if the input signal most resembles the mother wavelet. Since, the wavelet transform is linear therefor, it works for additive noise with equal power at all the frequency level as noise affects every single frequency component over the whole signal. Therefore, the thresholding method is used in the wavelet domain.

4.4.3.2 Threshold Selection Rule

The main part of the thresholding is to choose the threshold value. Phinyomark *et al.,* [85] and Donald *et al.,* [119] have utilized different universal threshold values and shown that the de-noising capability of this method is better than other thresholding methods like SURE, hybrid and minimax method.

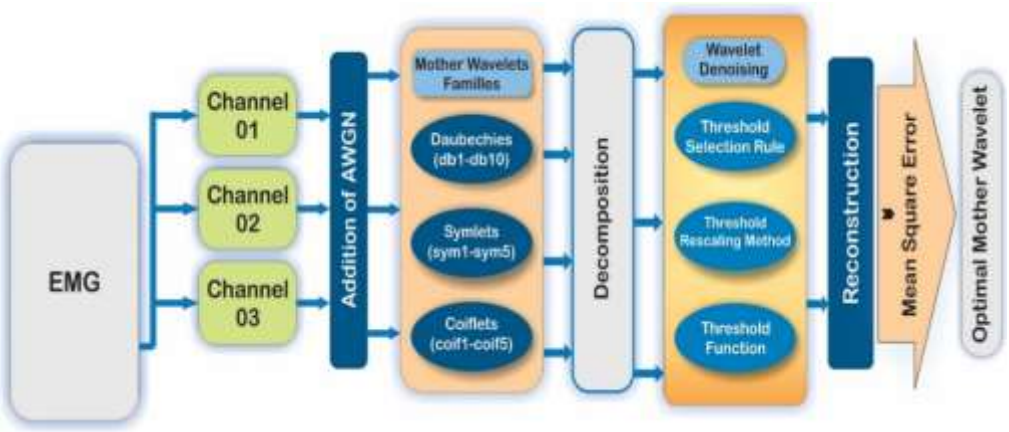

Figure 4.18: Methodology to find the optimal mother wavelet addition of additive white Gaussian noise

Universal method was proposed by the Donald and Johnstone which is defined by THR=$\sigma\sqrt{2\log(N)}$ where σ the standard deviation and N is the length of the samples. SURE is selected using the rule of Stein's Unbiased Estimate of Risk. Mixture of SURE and the threshold was provided by both. Minimizing the value of Risk gives the threshold. Afterwards, Stein proposed the minimax method and tested its performance by using the mean square error values. The different rescaling methods can be used for the smoothening of the threshold. The *wavelet threshold functions* are described and categorized as Hard and Soft functions. Any of the functions can be used for investigating. The smoother effects are provided with the soft threshold whereas better edge preservation is obtained in hard threshold.

4.4.3.3 Reconstruction process

To obtain the effective sEMG signal, the de-noised signal is reconstructed by using the inverse wavelet transform of the final decomposition level (cD1, cD2, cD3, cD4 and cA4). In the inverse process, the reconstructed approximate (A4) and detailed (D1, D2, D3 and D4) signal can be obtained by up-sampling the signal. The signal is passed through low pass and from the high pass filter and received signal is added for providing an output.

4.4.4 Results and discussion

The results were evaluated for optimal mother wavelet in the wavelet transform based on wavelet decomposition, de-noising the signal and reconstruction of the signal. Table 4.4 described the used four-wavelet family for three different muscle activations. Thereafter, these three-channel data was decomposed and reconstructed by the wavelet families. The combined sEMG data contained the activation of three muscles with three different movements. The three muscles having a different magnitude level with respect to the movement were individually

analysed by the wavelet. Mean square error (MSE) method was used to find the best mother wavelet in decomposition level,

4.4.4.1 Optimal wavelet selection for trapezius muscles

From the three-channel data set, the first data set of trapezius was analysed to find out the optimum mother wavelet by using the mean square error. The MSE was calculated from 24 wavelet functions presented in the graph (Figure 4.19) for all the decomposition levels of the trapezius muscles data set used in this study. The results from the decomposed trapezius data indicate that levels 1, 2 and more than 6 produced a very large value of MSE so they were neglected and therefore not shown in Figure 4.19. The decomposition levels 3,4,5,6 were chosen for Trapezius muscles data.

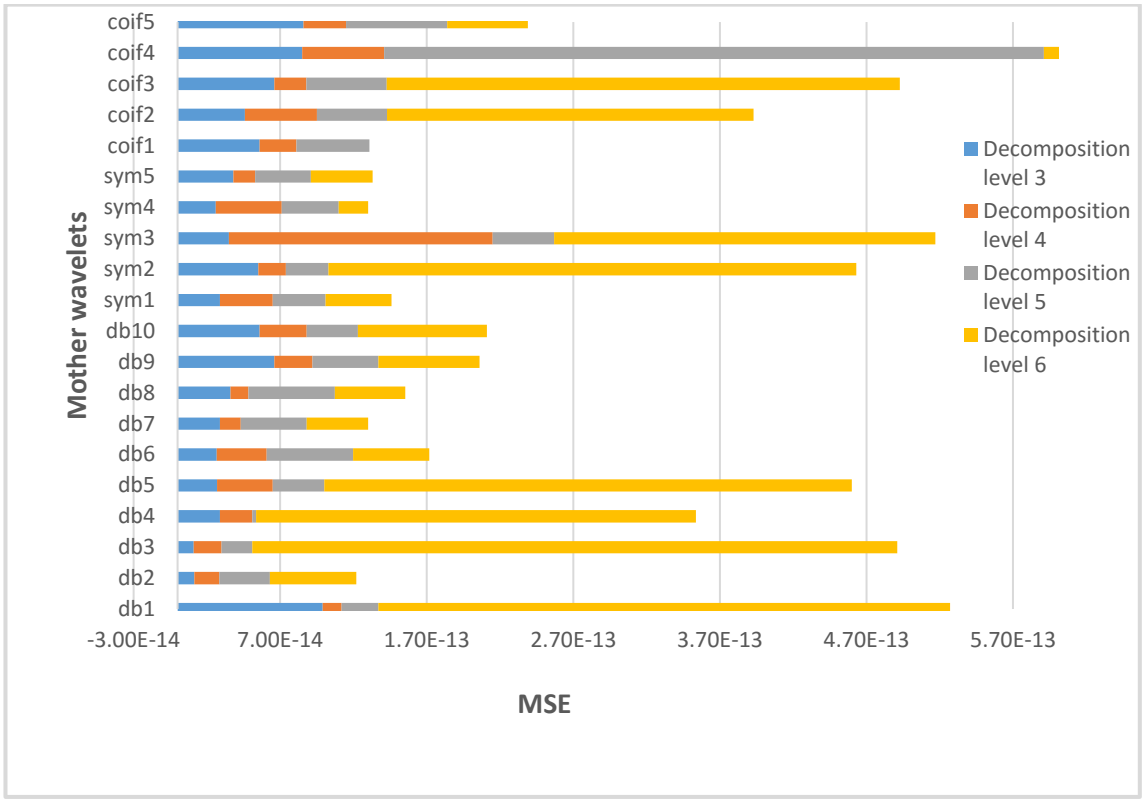

Figure 4.19: Performance of the db1-db10, Sym1-sym5 and coif1-coif5 mother wavelet families for trapezius muscle

A particular colour depicts the level of the error at the different decomposition level regarding the wavelet function (Figure 4.1. sEMG signal was decomposed with different decomposition coefficient levels and afterwards reconstructed by denoising the signal using a universal thresholding rule with the soft thresholding function. In case of mother wavelet db1, the orange colour indicates that the MSE value was minimum for the 4th decomposition level but it

increased with other chosen levels. In the case of db2 wavelet function the MSE was minimum with third decomposition level. On the average, MSE between the original signal and reconstructed signal is less when the signal was decomposed by level 3 or level 4. On the decomposition level 6, all wavelet families produced the large value of the MSE, so these were neglected for this particular data set. The most terrible wavelet function is Discrete Meyer (demey). Its MSE varied in the range of 7.2E-7 to 8E-7 that was very large value as compared to the other wavelet functions and, therefore, not considered in the next part of the study. The calculated value of MSE is very high in the case of the decomposition level 5 and 6 as compared to the level 3 and 4. Therefore, it can be concluded that the decomposition levels 3 and 4 are better than the other levels used in this study for the trapezius muscle sEMG signal. The next part in this case was to choose the mother wavelet on the basis of these decomposition levels (level 3 and level 4).

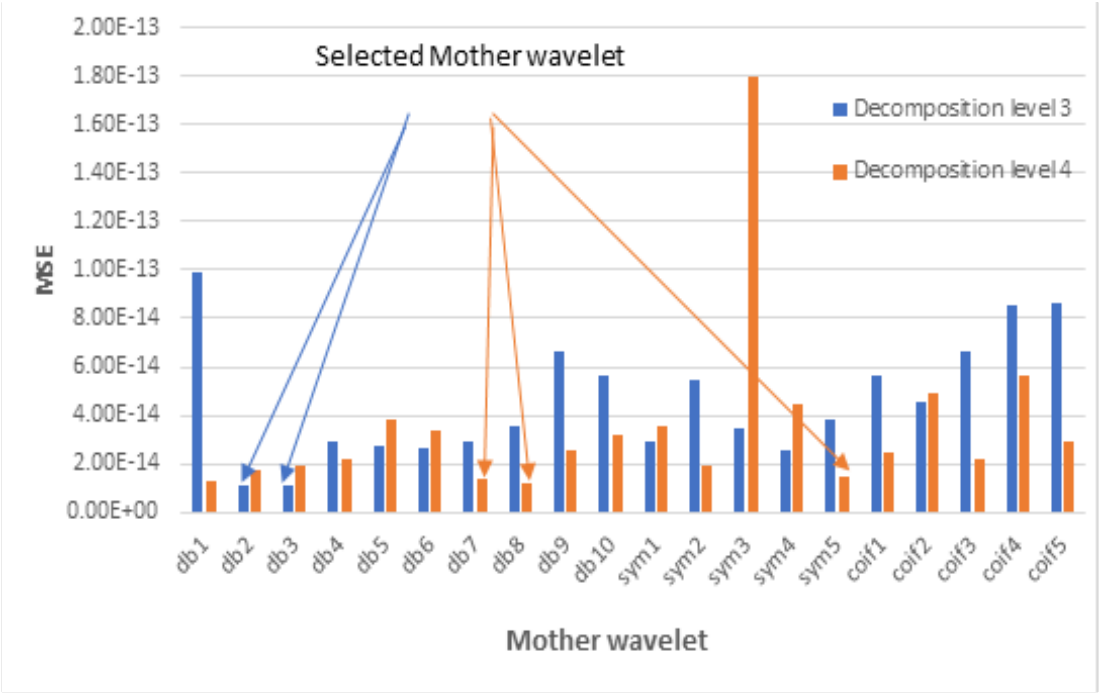

Figure 4.20: Optimal mother wavelet functions for trapezius muscle signal with different shoulder movements

Figure 4.20 shows that the MSE value of the db1-db10, sym 1-sym 5 and coif 1- coif 5 mother wavelet family with the decomposition level 3 and 4 to find the function with minimum MSE for trapezius muscle signal with different shoulder movements. The value was very less (1.14E-14 and 1.10E-14 for db2, db3 respectively) in the reconstructed signal decomposed by the db2 and db3 mother wavelet at decomposition level 3. The decomposition level 4 was best for the wavelet function db1, db7, db8 and sym5. The coif 3, sym 2 and db4 provided marginally better

performance than the rest mother functions with decomposition level 4. Discrete Meyer (demey) produced the worst performance which is not shown in Figure 4.20. A particular colour depicts the level of the error at the different decomposition level regarding the wavelet function sEMG signal was decomposed with different decomposition coefficient levels and afterwards reconstructed by denoising the signal using a universal thresholding rule with the soft thresholding function.

4.4.4.2 Optimal wavelet selection for teres muscles signal

The second channel data was examined by the wavelet family by choosing an optimal mother wavelet for the teres muscles signal. The wavelet universal thresholding rule with soft thresholding function was used. The 1 to 6 level decomposition was done for the sEMG teres signal for different wavelet families. Others levels led to an increased MSE value and were not considered. The calculated MSE value for the teres muscles around the shoulder with three upper limb movements to find out the optimal decomposition level from decomposition levels DL1 to DL6.

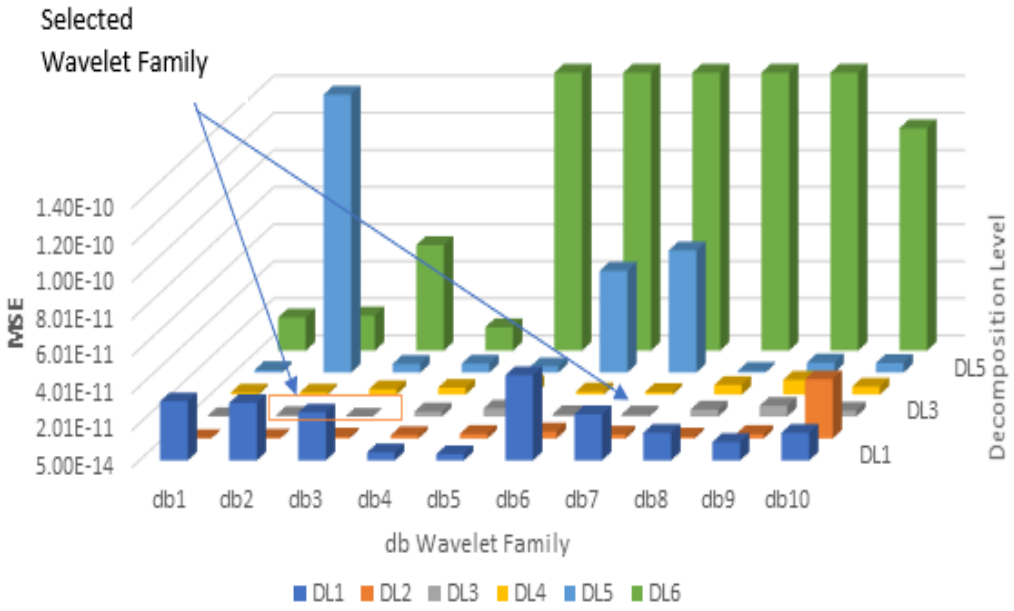

Figure 4.21: Performance of Daubechies wavelet family for teres

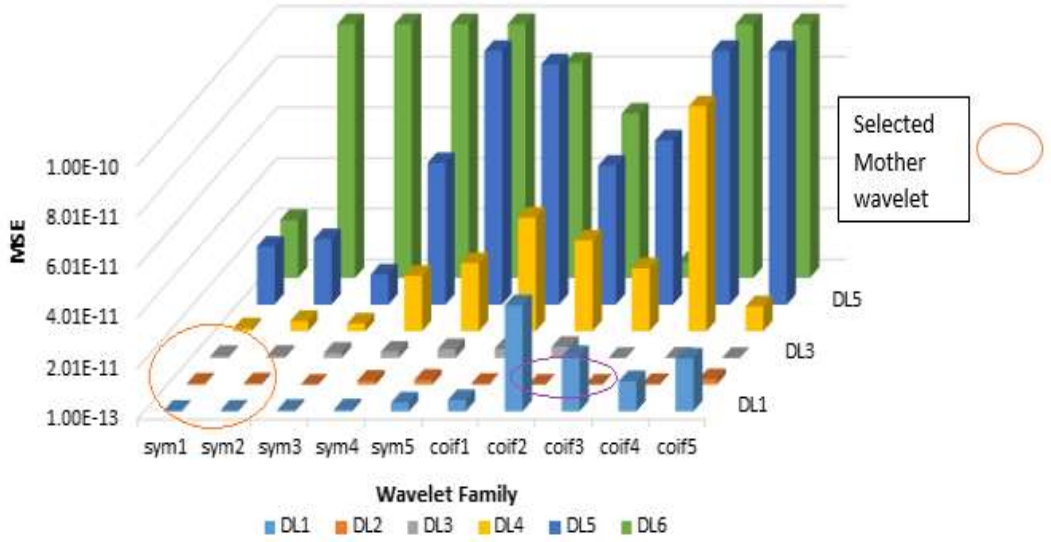

Figure 4.22: Performance of the sym and coif wavelet family function for teres muscle

.

The data resulting (Figure 4.21) from the wavelet analysis indicated that the DL2, DL4 and DL3 were the selected level with a minimum value of MSE for the db2 and db 3 wavelet family. In second case, Figure 4.22 shows the performance of the sym and coif family and resulted that the DL1 to DL3 were the optimal wavelet decomposition level for sym 1 to sym3 wavelet function. But in case of coif function DL1 was the optimal for coif 1 to coif 3 and DL3 was for the coif 3 to 5. Therefore, the optimal level for further study was DL1, DL2 and DL3 from these six level.

For further clarity on optimal wavelet family, the wavelet families were extended to the above chosen decomposition levels (Figure 4.23). With the second level decomposition, the coif 2 and coif 3 produced less error than the other wavelet families. Even the db2 has a very small error for the same decomposition level, but greater than coif 2. If one considers the third level of decomposition, then optimal wavelet functions were db2, coif 3 and coif 4 with a minimum value of MSE. Finally, it was concluded that for the teres muscle, the optimal wavelet families were coif 2 and coif 3 with decomposition level DL2 and with the decomposition level 3 db2, coif 3 and coif 4 performed better.

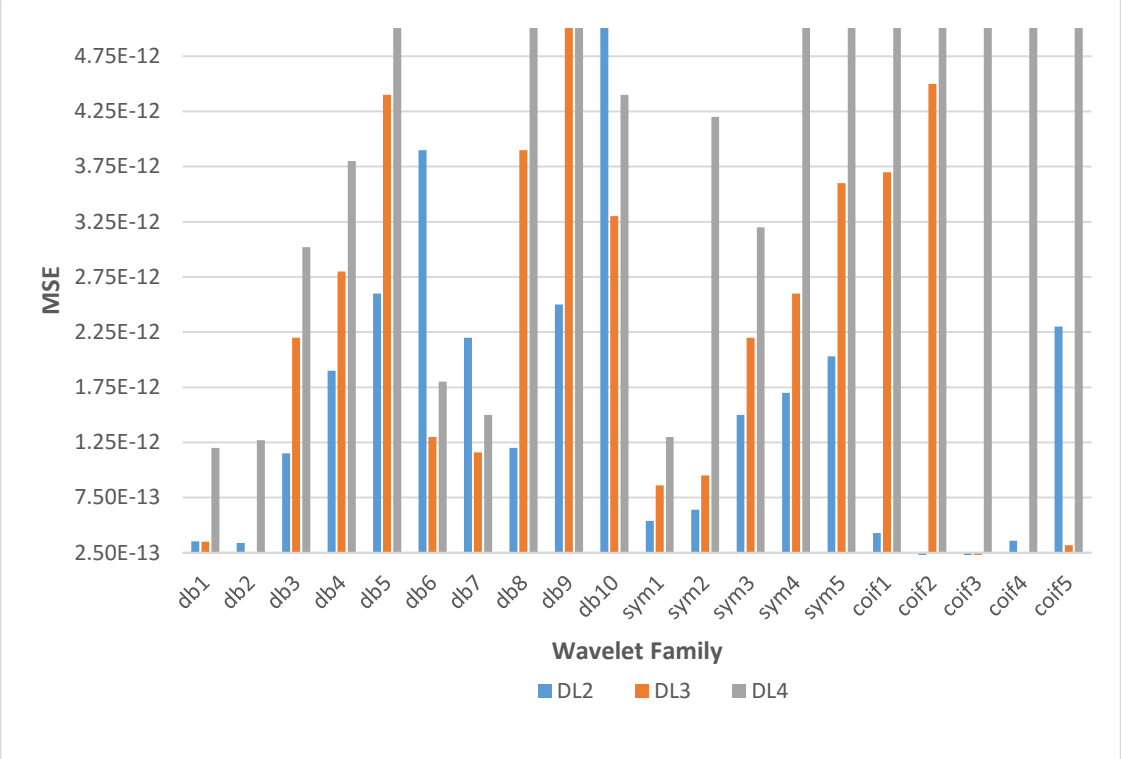

Figure 4.23: Optimal wavelet function selection for the teres muscle

4.4.4.3 Optimal wavelet selection of pectoralis muscles signal

Pectoralis muscles data was applied and decomposed with different number of levels for all the wavelet families. Figure 4.24 shows the calculated MSE value with the different wavelet family db1-db10 (0-10), sym1-sym5 (11-15), coif1–coif5 (16-20) with the DL1 to DL8 decomposition level.

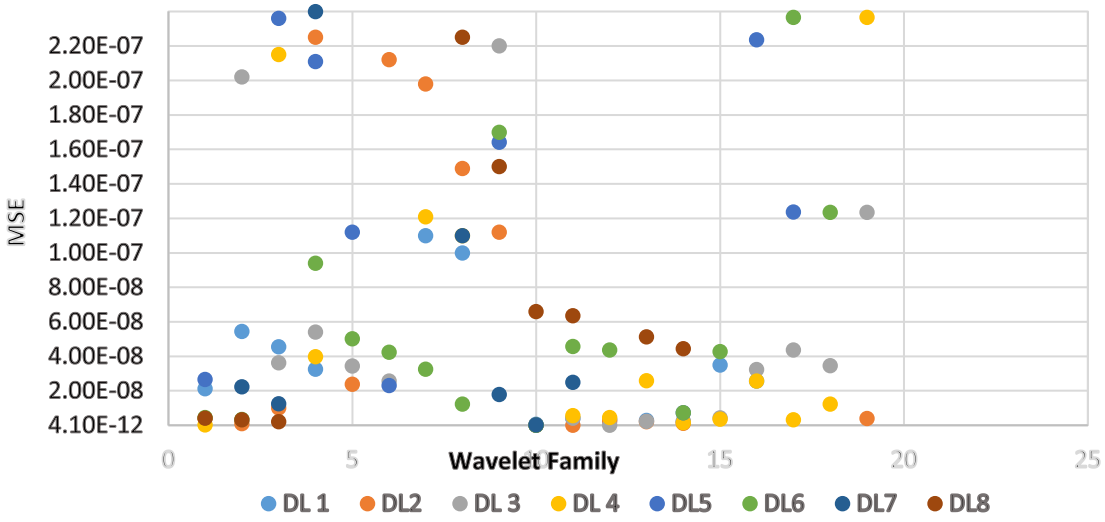

Figure 4.24: Optimal wavelet function selection for pectoralis muscles output

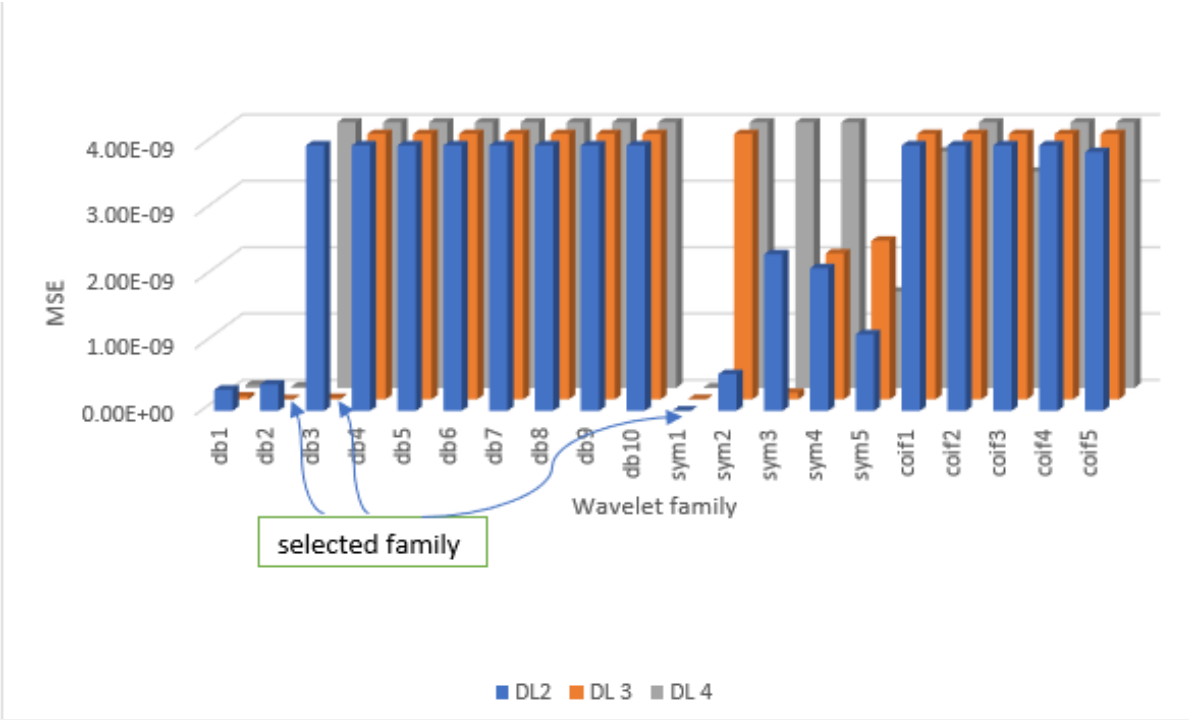

Figure 4.25 Selection of optimal wavelet function with decomposition level 2 -4.

It indicates that the decomposition level 1 to 4 produced a minimum mean square error less than 6.00E-08 in the distinctive wavelet family. From eight different decomposition level, DL3 produced minimum error in db and coif wavelet family but DL2 produced minimum error in sym wavelet family indicated by yellow and grey colour respectively. In some of sym and coif family function, DL2 also shows the minimum MSE value. Therefore, these three levels DL2, DL3 and DL4 were broadly concentrated again for all families shown in Figure 4.25. The dmey function had a large error value of 0.03 to 0.006. Therefore, this was not indicated on the graph shown in Figure 4.25. In which db1 and sym 1 wavelet functions were the optimal wavelet functions from the db, sym, coif produced very small error.

4.4.4.4 Wavelet denoising

The sEMG data that was recorded from the three muscles as explained in Chapter 3 to evaluate the ability of wavelet denoising algorithm. For this, 5 dB additive white Gaussian was added into the original signal before decomposition. After decomposition, the wavelet de-noising methods were introduced in the analysis part.The wavelet denoising process was applied to different shoulder muscle signals. Muscles data contained trapezius, teres and pectoralis muscles with three shoulder movements.

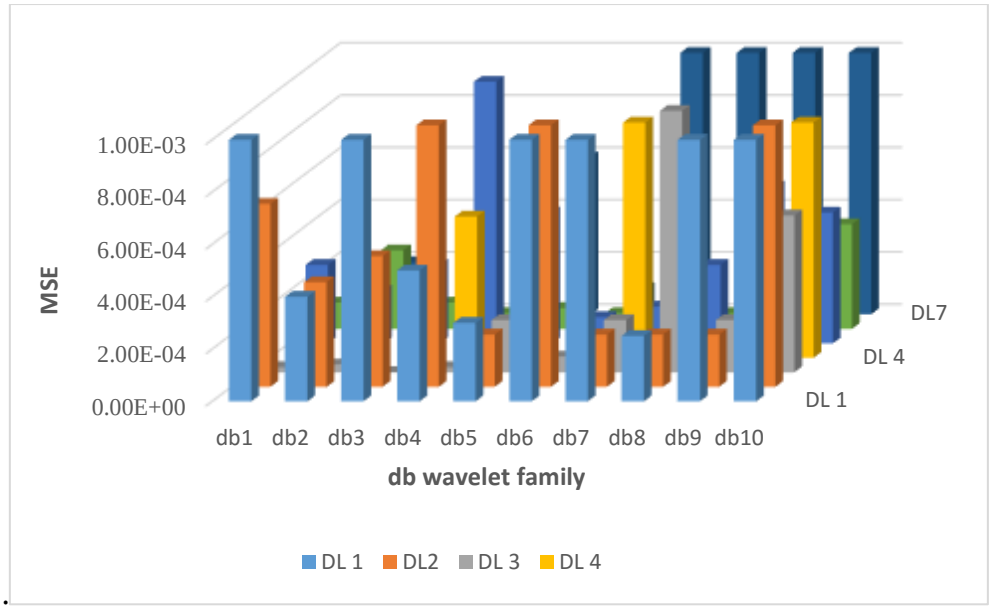

Figure 4.26 Performance of db family with DL1 to DL7 decomposition level for trapezius muscles

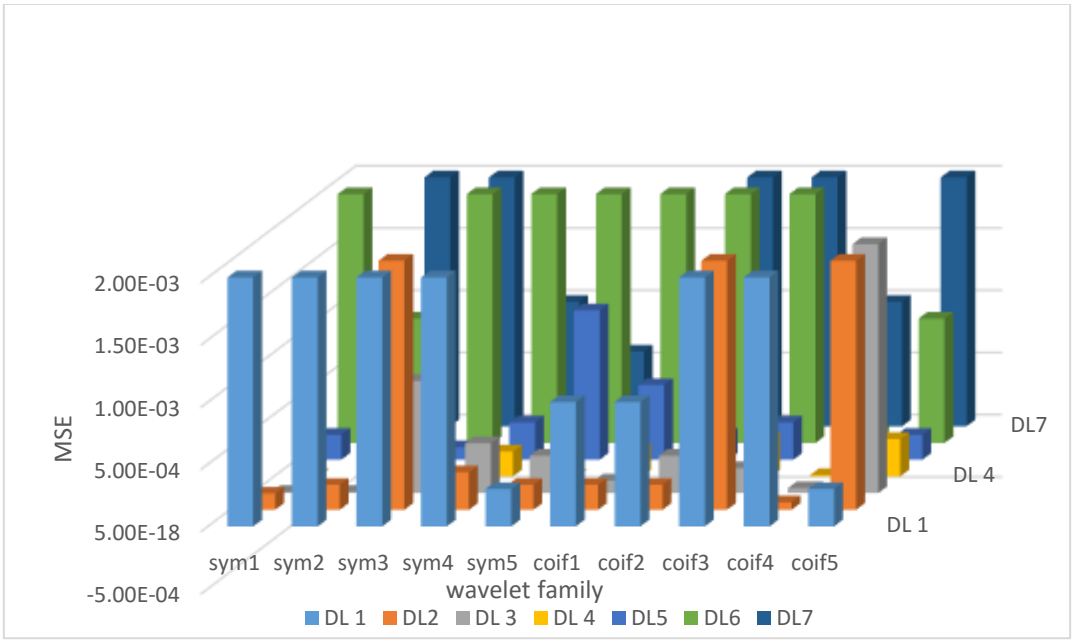

Figure 4.27: Optimal value of wavlet function in denoising for trapezius

From the db family the decomposition levels 3, 4 were the best levels because these produced the low value of MSE. But if we compare the original signal with the reconstructed denoised signal, then the sym1,4 with the decomposition levels 3, 4 and coif 3,4 with decomposition level 4 provided a better result with the low value of MSE of E-04 to E-05.

Firstly, the trapezius muscles signal was decomposed by different wavelet families. Figure 4.26 shows the calculated denoised MSE value of sym and coif mother wavelet families with different decomposition level DL1 to DL7 for the trapezius muscles around the shoulder, with

three upper limb movements to find out the optimal wavelet function with the optimal decomposition level.

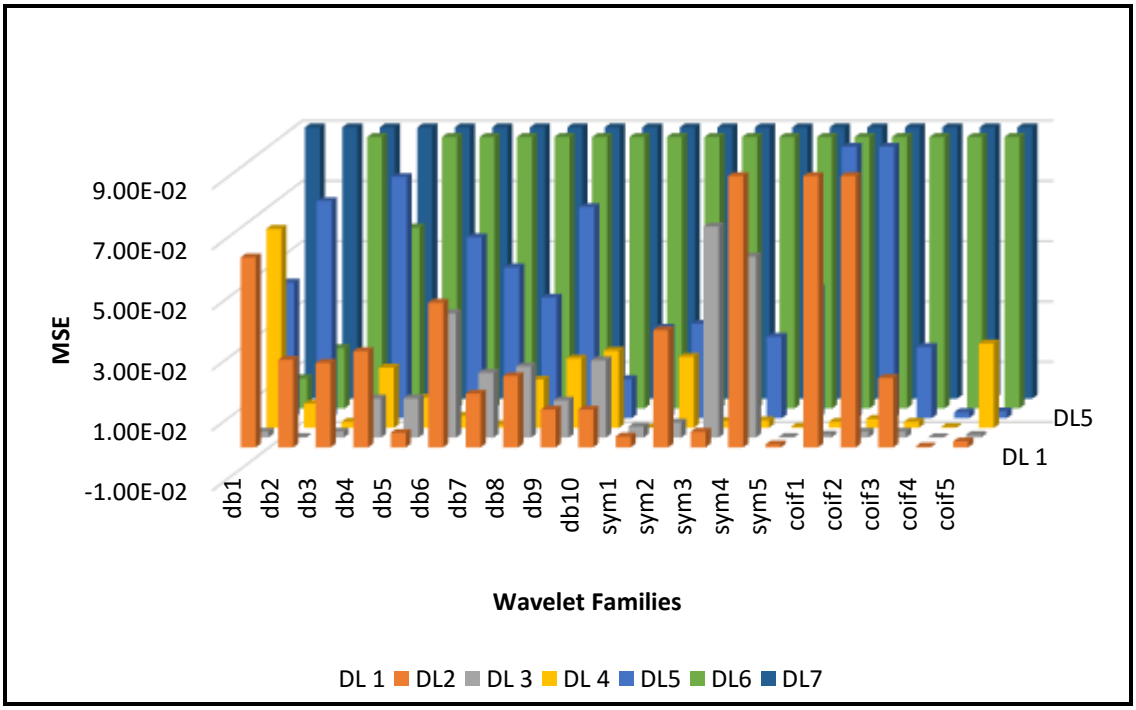

Figure 4.28: Optimal mother wavelet selection for pectoralis muscle

By the same process, the pectoralis and teres muscles were added with the same level of noise (white Gaussian noise with 5dB SNR) and then the signal was decomposed by different wavelet families. Figure 4.28 shows the calculated denoised MSE values of db, sym and c-oif mother wavelet families with different decomposition level DL1 to DL7 for the pectoralis muscles around the shoulder, with three upper limb movements to find out the optimal wavelet function with the optimal decomposition level and Figure 4.29 shows the MSE values for teres muscles. In the pectoralis muscles, the selected decomposition level was 3 and the wavelet family was db2, sym 1 with a DL4, sym 5 and coif 4 with DL3 with the MSE 2.00E-04,1.00E-04, 2.00E-04 and 1.5E-04 respectively. Afterwards, when we considered the teres muscles, then the condition was changed. In db family, db1 and db2 provided the error 1.00E-04 and 1.5E-04 with the third level of decomposition. With the same level of decomposition, sym 1 and sym 2 had MSE of 2.5 was 6E-08 and 5.56E-08 respectively. But in coif3, it produced the error as 2.3E-04 and 1.45E-04 with third and fourth decomposition level, respectively.

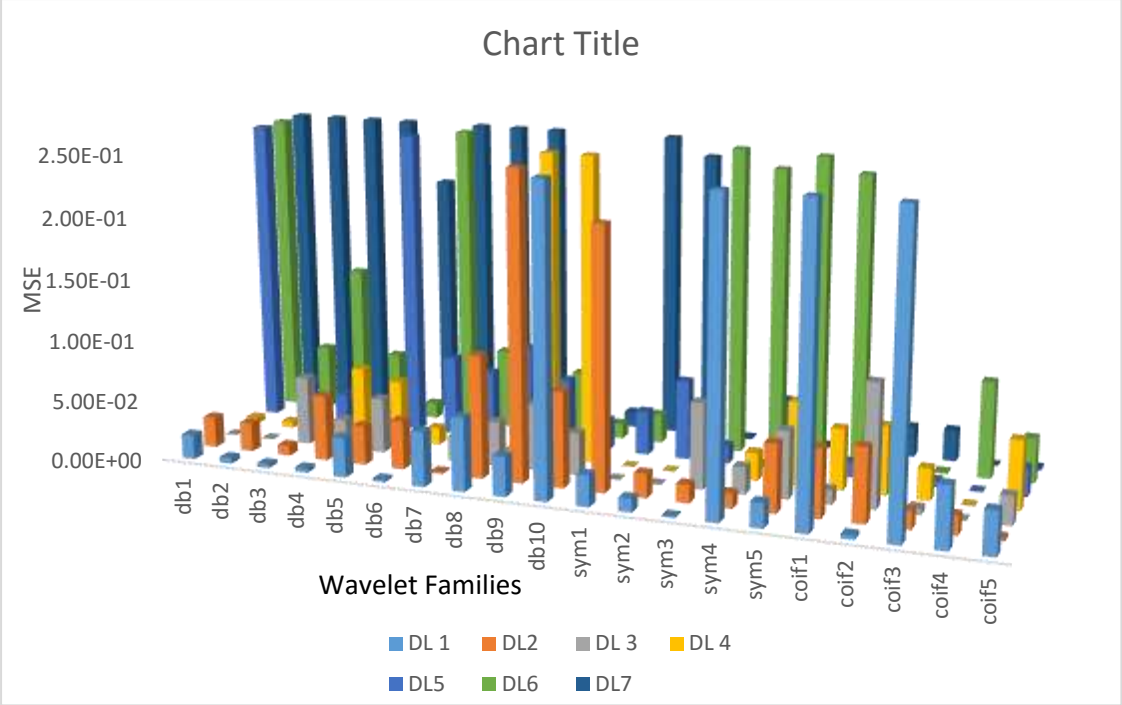

Figure 4.29: Optimal mother wavelet function selection in denoisisng for teres muscle.

During recording of the data signal from different muscles, noise or various types of artifacts contaminated the sEMG signal. In engineering and clinical application, noise is the main problem in the data signal. Due to the random nature of the sEMG signal, the conventional filters are not able to effectively remove the noise signal. But to choose the optimal wavelet method with the best decomposition level can help to eliminate the artifacts and that was the main aim of this work. Again, due to the stochastic nature of the sEMG signal, it was a challenge to select the best wavelet for the acquired signal from shoulder muscles.

The suggestion of different wavelet functions with the decomposition levels from four defined wavelet family with the universal thresholding level using soft thresholding function may be made as follows:

- Wavelet Functions: db3, db4, sym2, sym5, coif4
- Decomposition Levels: 3,4 and 5
- Threshold selection rule, rescaling method and function

These recommendations can be used for the sEMG shoulder muscles signal for different applications. For getting the best results from the wavelet, denoising method without adding or after adding the noise signal were also the part of the study. The main aim of this thesis to classify the different shoulder signal. For efficient classification of the signal , the various

features were extracted from the reconstructed coefficients of db3 with three level wavelet function to form a feature vector for the classifier described in next chapter.

Summary

A reliable and accurate method is necessary to appropriate maintain the rigour of scientific research. In this chapter, adaptive threshold method has been used to ignore the undesired signal in pre-processing stage. STFT analysis shown the comparison between the amputee and non-amputee persons. Then in analysis, the optimal wavelet method with the best decomposition level was used to eliminate the artifacts. The recommended decomposition level were Level 3,4 and 5 with db2,db4,sym2,sym5 and coif 4 wavelet functions.

Chapter 5
Surface Electromyography Signal Classification

5.1 Overview

Myoelectric signals offer critical perceptions in translating the motion intention in upper limb amputation with various feature extraction techniques. In the upper limb amputation, the initial step for controlling the prosthetic device is to extract the attributes from the sEMG signal and then classify the signal for driving the different arm/hand movements [139], [88] . With new approaches in signal processing techniques, sEMG signal analysis has become deterministic and reliable. Various methods of features extraction have been proposed by different researchers for obtaining an accurate classification [88], [140].

Feature extraction is a technique to extract the actual information hidden in the raw signal and convert it into a reduced set of features called the feature vector. Wavelet transform technique has gained importance as a feature extraction technique for the biomedical signals. Phinomark *et al.,* [35], [62], [69] extracted sixteen features from three classes using time domain, frequency domain and time-frequency domain techniques and also introduced the various white Gaussian noise to test the robustness of the system. Kevin Englehart [36], [55], [134] concluded that one or two channel data for the extraction of features is less efficient than the four channel data. Hargrove *et al.,* [142] used wavelet transform method as a feature extraction technique and then reduced the dimensions of the feature vectors with the PCA.

The time and frequency domain combined attributes were applied to increase the accuracy of classification of muscles-activity, for both non-amputeeand upper limb amputees [45], [131]. After attributes selection, the artificial neural network has been used for the pattern classification task [67]. Subasi *et al.,* classified the EMG signal with Multilayer Perceptron Neural Network (MLPNN) combined with Adaptive Neuro-Fuzzy Inference System [143]. Englehart *et al.,* used Support Vector Machine (SVM) classifier and achieved an efficiency of 95% [139]. Mattioli *et al.,* placed different electrode pairs on the arm to classify four different movements for virtual hand using the artificial neural network in real time with 95% success rate [144]. In another study on upper limb amputees, the electrodes were placed on the shoulder muscles [104], [105] and the muscles-activity of forearm were detected the motion of hand and wrist. Particle swarm optimization with SVM improves the accuracy of classification

[145]. Hlavac [143], used the wavelet neural network and feed forward error back propagation with a resulting efficiency of 90.7% and 88%, respectively. Machine learning is a relatively a new technique which is more reliable to identify and classify different arm and hand motions from the triceps and biceps muscles of trans-humeral amputee. Different decision tree methods have become the part of research in the classification of EMG signal by extracting the different attributes. Different machine learning algorithms like support vector machine, random forest, KNN *etc*. have used for the classification of EMG signal [146], [140]. The achievement of the classification methods depends on the type, nature of classifiers and input data to be classified [141], [142].

The main aim of this chapter is to describe the classification of different shoulder movements of the upper limb amputee using the various machine learning techniques. The different features extraction technique is defined in this chapter. The denoised signal obtained from the optimal wavelet transform function (Chapter 4) were introduced for the features extraction. The methodology of the motion classification is explained in (Section 5.2). The feature vector used for classification was selected from the combination of the recovered coefficients of the wavelet transform (Chapter 4) and the proposed transformation technique (Section 5.3). These features were used to classify the upper limb shoulder motions, especially for a transhumeral amputee person with zero muscles activation below the shoulder. Section 5.5 compares the different classifiers to choose the best one by using the performance metric parameters. After classification, the selected classifier output was checked with hardware by using the classified output for different rotations of three motors which are part of a complete prosthetic device for the amputee subjects.

5.2 Methodology to Classify the sEMG Signal

The complete flow graph of the analysis and classification of the sEMG signal, used to design more accurate and efficient controller for the upper-limb amputee shows in Figure 5.2. The raw sEMG signal is acquired from the four different shoulder muscles through a four-channel system (Chapter 3). To improve the quality of the signal, filtering and adaptive thresholding for peak detection was performed. Then the filtered signal was denoised by the wavelet transform function daubechies with three level of decomposition (Chapter 4). Analysis of the wavelet transform of signal was performed using different wavelet families with different decomposition levels. This procedure resulted in selection of optimal mother wavelet and

decomposition levels (Chapter 4). The features vector were obtained to convert the reconstructed signal coefficients from the wavelet transform to the new data coefficients by proposed transformation method described (Section 5.3).

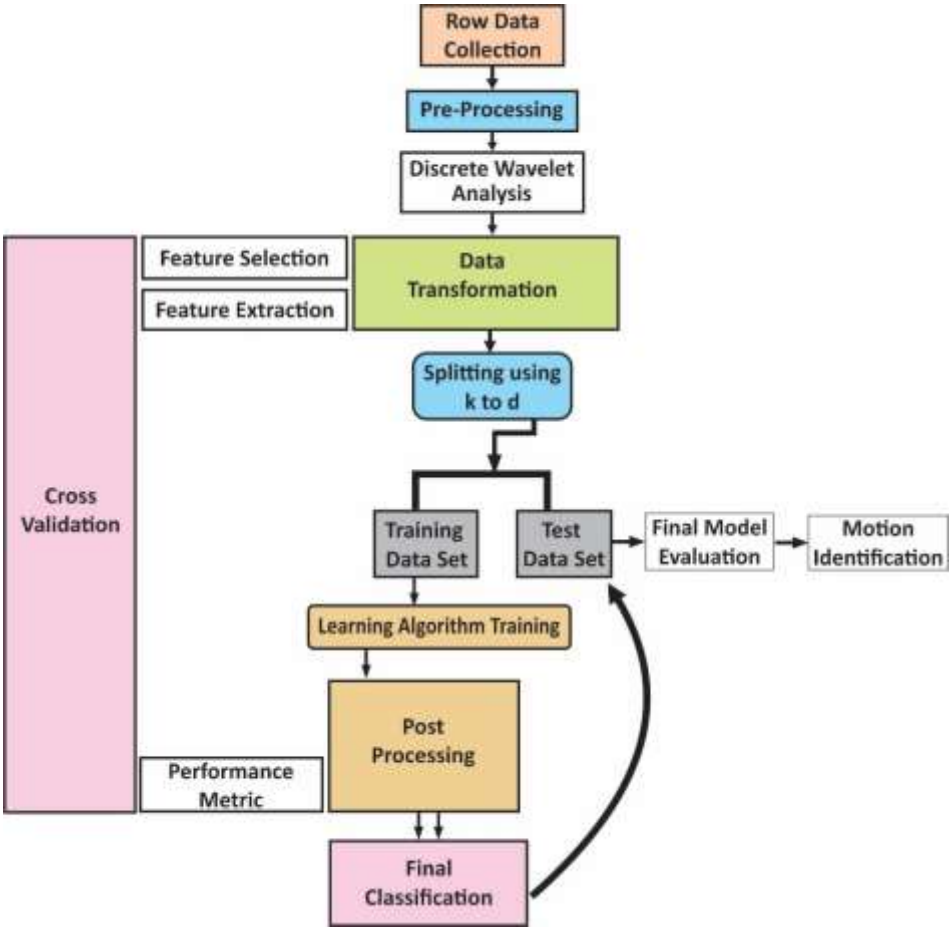

Figure 5.1: Methodology to classify the sEMG signal

The features vector obtained were split into the training set and testing set for further used for classification. After comparing different classifiers, the best classifiers were chosen to identify the motion of the shoulder.

5.3 Feature Extraction

Two methods namely *traditional method* [66], [65] and *new proposed method* for feature extraction are described. The section also provides a comparison of these two studies on the same data set of sEMG signal.

5.3.1 Traditional method for attributes extraction

Earlier feature extraction methods used for the signal, especially time and frequency domain [14], [35] for the classification of various hand movements. Zhang in 2011 *et al.,* [128], [143], [144] measured the signal from the upper limb (triceps and biceps) muscles and then used the DWT technique for extracting the features and concluded that the DWT method provided 98.9% recognition rate in classification of different hand movements. In this thesis, DWT technique was applied on the sEMG data set and provided five reconstructed coefficients D1+D2+D3+D4+A4 by using db3 with three decomposition levels (Chapter 4). Then the mean absolute value, mean absolute value slope, Median, Mean, Root Mean Square value and Variance (VAR) were extracted to make the feature vector space. The complete vector contains 30 features (5 decomposition levels * 6 features) for one motion value. Afterwards, this full feature vector was put on the machine learning models (Section 5.4) to classify different movements using the cross-validation technique.

5.3.2 Proposed method for attributes selection

In a time-frequency domain, the energy distribution of the signal is provided by the discrete wavelet transform. In this approach, five reconstructed coefficients D1+D2+D3+D4+A4 were produced from wavelet transform method. In which, D1 coefficients contains the maximum level of noise signal, D2 contains high-frequency signal and D3, D4 with approximate coefficients A4 contains the maximum information related to signal. Therefore, these three coefficients (D3, D4 and A4) were selected for feature extraction. The entire 6000 sample data set was used to extract the feature individually for each subject.

To classify the particular movement of the shoulder by acquiring the sEMG signal from the muscles is always typical and poses a significant challenge even to the best classifier. Due to the stochastic nature of the sEMG signal, the data values with a high degree of spread are tough to handle the classifier. For this, the data should be pre-processed before it is subjected to a classification. Therefore, the transformation method was used to preprocess the coefficients of the wavelet transformation. The data transformation technique[152] was evaluated to extract the features from the coeffcients for the classfication process.

The mean of the individual sensor is denoted as :

$$Y_{ij} = \frac{1}{m_{ij}} \sum_{k=1}^{m_{ij}} Y_{ijk} \quad 5.1$$

where Y_{ijk} is the response of the jth movement from the ith muscle at the kth data point, Y_{ij} is the mean value of the ith muscle response for the jth movement and m_{ij} is the total number of observations taken from the ith muscle for jth movement. The variance value is evaluated as:

$$V_{ij} = \frac{1}{m_{ij}} \sum_{k=1}^{m_{ij}} (Y_{ijk} - Y_{ij}) * (Y_{ijk} - Y_{ij}) \quad 5.2$$

Following equation gives the final transformation of data value

$$F_{ijk} = (Y_{ijk} - Y_{ij}) V_{ijk} \quad 5.3$$

F_{ijk} is the transformed value of the ith muscle for jth movement at the kth data point.

The feature vector obtained from the transformation method was used to classify the signal by using the machine learning models. Machine learning model used newly transformed values as the input to classify the four channel data with four different movements from the rest position.

5.4 Classification Technique for sEMG Shoulder Muscles Signal

5.4.1 Machine learning

In the era of technology, the human being is continuously increasing his knowledge on different topics in the world by collecting observations and realizations. Human learns these attitudes from experience. Practitioners collect various parameters from the patients like age, blood group, blood pressure for diagnosing the conditions of patients. It is clear that if a lot of information or observations regarding data set, drawing, graphs, sizes, colour, weight, shape and so forth are available for the human then by looking at this observation and by extracting the different attributes, the experts can easily predict the new model for observed data. The same behaviour is of machine learning.

Machine learning teaches the computer to learn from the experience naturally like a human, which means the *creation of an intelligent machine which can mimic the human mind.* So the machine learning is the study of a system that can learn from the data. The performance can be measured if the used tasks enhance the output [153]. Machine learning provides a number of algorithms for predicting the phenomenon inview of the past information. The programmer writes the code that does not have a predefined strategy, but it has a set of rules that need to be

learnt by the computer until it can classify the difference between the given data set and test data set. The two categories of the machine behavior are *classification* and *prediction*. In the *classification,* a machine can recognize and categorize the objects from the dataset, but in *prediction,* it can guess the value based on the previous values. The entire procedure of the machine learning is comprised by the three components: (i) *Experience* which implies the observation of data set that was acquired for classification (ii) *Task* refers the learning goal with different decision-making algorithms for the prediction of new observations, and (iii) *Performance* is to assess the system learning by comparing the observed and desired output. The machine learning is of two type viz. Supervised learning and Unsupervised learning.

5.4.2 Supervised learning

This technique teaches the system for every input task or input variable with corresponding output variables so that after sufficient learning of the system, it is able to generate the output response for the new input data set.

Values of input variables are called the input vector or samples and the output variables are known as the target. In supervised learning, corresponding to each input vector, value of the output variables is specified during the learning process. Supervised learning is further divided into *classification* and *regression* (Figure 5.2). *Classification* refers to sending the input data into the desired categories to form finite set discrete variables but the *regression* is to predict and then continue responses like fluctuation in power or temperature.

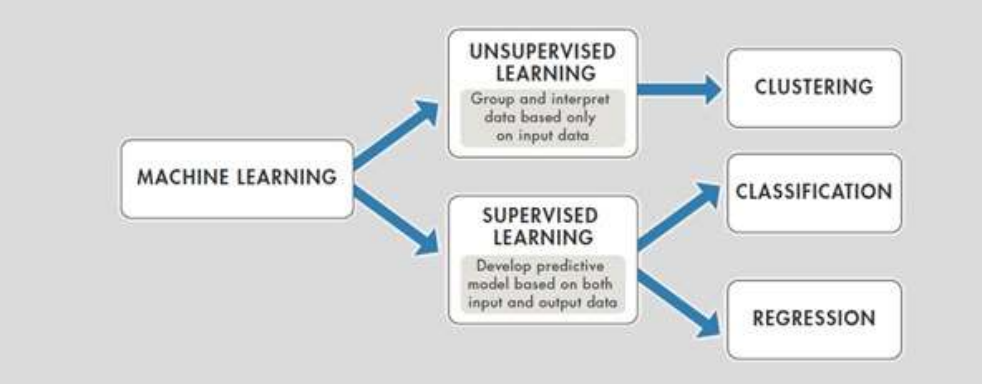

Figure 5.2: Different Machine Learning Techniques

Assume the training set with $\{A^{(n)}, B^{(n)}\}_{n=1}^{N}$ where B is the discrete labelled values in classifiers or in regression, it is a continuous labelled value. The prediction function is of the

form $\Psi(A) = B$ or as conditional probability P (B/A). During the training, different training sets are provided to get the predicted value for an unseen observation A using $\hat{A} = \Psi(A)$.

5.4.2.1 Unsupervised Learning

Here, no specific target output responses are provided with the input data sets. The algorithm interprets the input data set to find out its demarcating features based on which classification is to be carried out by the classifier. David Mass (1970) proposed the first unsupervised model [154]. Afterwards, the Boltzman machine learning algorithm was proposed by Geoffrey Hinton and Terrence Sejnowski for unsupervised learning [155]. This machine learning has two classes: density estimation and clustering. Density estimation is the distribution of the observations represented by $\{A^{(n)}\}_{n=1}^{N}$. Clustering discovers the different data sets (χ) and puts any of the new data in a particular cluster. The set of clusters is denoted by $\mathbb{C}_n = \{C_k\}_{k=1}^{K}$.

5.4.3 Classification Methods

Many techniques and methodologies have been developed for the machine learning task. Machine learning is a subfield of the artificial intelligence, which enables the computer to learn and perform the tasks and activities. The classifiers are the most significant part, to identify the different motion of a shoulder with commands. The different five classifiers are described in next section.

5.4.3.1 Support Vector Machine (SVM)

SVM is a kernel based supervised model used for classification and regression, to classify the binary function. It uses the machine learning theory to maximize prediction accuracy. SVM is a multi-class classifier where several binary classifiers are constructed to get the multi classifier performance. In the present work, we have used more than two classes by using the multiclass SVM classifier [153]. The multi-classifier can be built from the combination of the binary classifier in such a way that it does not degrade the performance of the classifier. For n classes, SVM requires $\frac{n(n-1)}{2}$ binary classifiers. Then with the voting mechanism, the class with most votes becomes the final output class. This method gives better measurement of the probability of each class. It has three phases namely, transformation in input, learning in middle and function in output. It maps the boundary for each class and uses a hyper plane to separate different classes. It is easily scalable to very large data set and can be used to classify the binary

as well as the multi class group function. It is designed to use all k classes by setting the kernel parameter with passing the function name. A number of kernel functions can be used for decision. The generally used kernel functions are linear, quadratic, polynomial and radial basis function. In this work, radial basis function with four different classes was used due to its high accuracy, less difficulties in mathematical computation and capability of classification [156].

5.4.3.2 Naive Bayes (NB)

It is a probabilistic approach based on Bayes' Theorem with an independent assumption among the attributes. In these type of classifiers, the value of a specific feature in a class variable is unrelated to the value of other attributes. In this study, each feature contributes independently and specifies the exact result irrespective of any correlation between the attributes. Supervised learning can efficiently train it. By finding the probability from each class, the classifiers are used to calculate the highest posterior probability [157]. The effect of predictor is independent from the other predictor which can be specified as class conditional independence. The classifier output of the NB is:

$$P(D/B) = \frac{P(B/D)*P(D)}{P(B)} \quad (4)$$

where P(D) is the prior probability of class,

P(D/B) is the posterior probability of class given predictor (attributes),

P(B/D) is the likelihood which is the probability of predictor given class,

P(B) is the prior probability of predictor.

$$Posterior = \frac{likelihood*prior}{normalizing\ constant} \quad (5)$$

The denominator value does not depend on D. Therefore; there is curiosity only about the numerator. The numerator in the posterior equation is equivalent to the joint probability model. By ignoring the normalizing constant, the joint distribution function was replaced by the individual conditional probability, which is our likelihood function.

5.4.3.3 K-Nearest Neighbor (KNN)

If Ts is a test sample from $[Ts1, Ts2, Ts3 \ldots . Tsn]$ and one of the sample from training set is KNN is a clustering algorithm most widely used in the classification problems with supervised learning, based on the closest training samples. It is also called the distance based learning. The training set samples have their values, and each feature corresponds to its attributes. Training data demarcates various features into different regions and form a class. In this algorithm, the

new classified data samples are compared with the training samples and these are put into different feature space by using the distance-based learning. Distance measured in the feature space and class is defined as the nearest class of the system. Nearest value is defined by the distance metric [158].

Xt describes as $[Xt1, Xt2, Xt3\ldots\ldots, Xtn]$, the Euclidean distance between these two samples Ts and Xt is defined as:

$$D(Ts, Xt) = \sqrt{(T_{s1}} - X_{t1})^2 + (T_{s2} - X_{t2})^2 + \cdots + (T_{sn} - X_{tn})^2 \quad 5.6$$

Equation (5.6) gives the Euclidean distance values. The decision is based on the small neighbors and it can be efficiently used with the multimodal classes. However, it does not work with the minor subset of the attributes for the proposed classification.

5.4.3.4 Decision Tree (DT)

It is a tree based algorithm under the category of supervised learning and is used in classification process. It consists of root node, representing the entire sample data and is further divided into different sub-nodes by a splitting process. The sub-nodes are called the decision nodes and the nodes that do not split in various nodes are called terminal or leaf nodes [159]. The internal node divided into different two parts depends on the input attributes value. The full tree structure is the combination of root>>Decision node >> Decision node>> Terminal node shown in Figure 5.3. Each leaf represents one class and each class has an appropriate target value. Different instances are classified by directing them from the tree according to the outcomes. Decision tree splits the data set record recursively using breadth-first or depth-first approach. It is utilized to classify the data records in the form of a structure and contains a root, interval and leaf nodes shown in the Figure 5.3. First, it constructs a tree based structure on the attributed values and then categorizes the attributes that distinguish the instances [160]. The decision tree is applied as a multistage problem solution.

In this method, a series of simple decisions are collected from a single complex decision. The classifier result is based on the knowledge of a full tree structure. The trained, classified trees predict the responses for a new data. It is easy to understand, useful in data exploration and a non-parametric method.

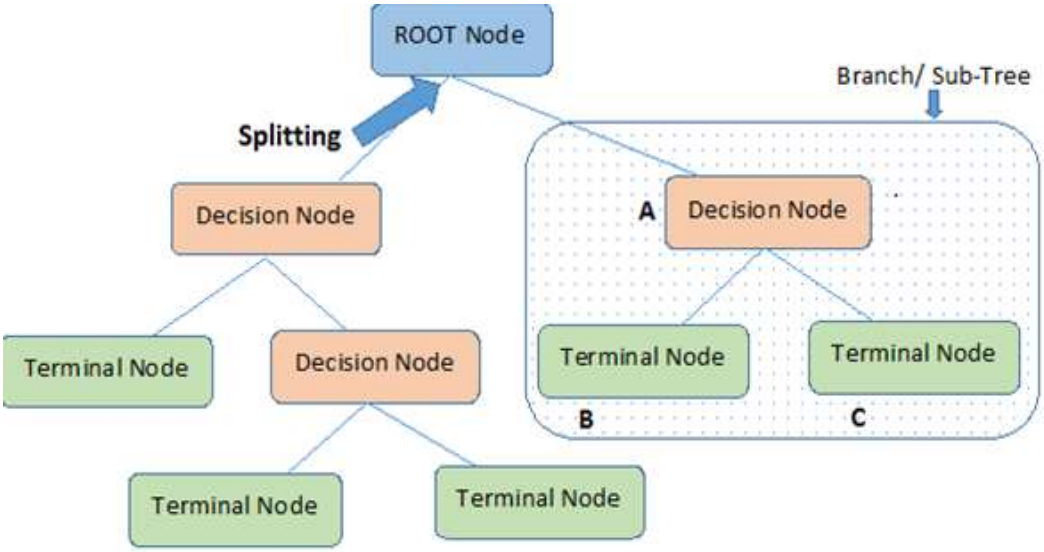

Figure 5.3: Structure of decision tree algorithm

5.4.3.5 Random Forest (RF)

Ensemble of decorrelated or independent decision trees provide good generalization called a random forest. Suppose T is the number of design trees with the random forest function $\mathcal{R}$. Then $\mathcal{R}$ =$R_1 . . R_2 . . R_3 \ldots R_n \ldots \ldots \ldots R_T$. Therefore random forest is a family that consists of the different decision trees with low bias and high variance used in several applications. It can also be used to solve the regression, clustering and density estimation task. Several approaches have been proposed to build the independent trees constructed from the same training set.

Beriman introduced the combination of bootstrap and aggregating to provide the concept of bagging [153], to reduce the variance and to improve the stability and accuracy of the algorithm. Suppose S_t is the subset of full training set $T = (Y(n) , Z(n))N$ where n = 1. Each independent tree R_n is trained with S_t which is randomly sampled using a uniform distribution. Then using averaging, an aggregate of all the individuals' trees in the forest is obtained.

Different researchers inserted different randomization in the optimization of the node and provides greater generalization by decreasing the degree of correlation between the trees because of an increased randomness. The set of splitting function has generated to choose the best of them by a predefined objective function.

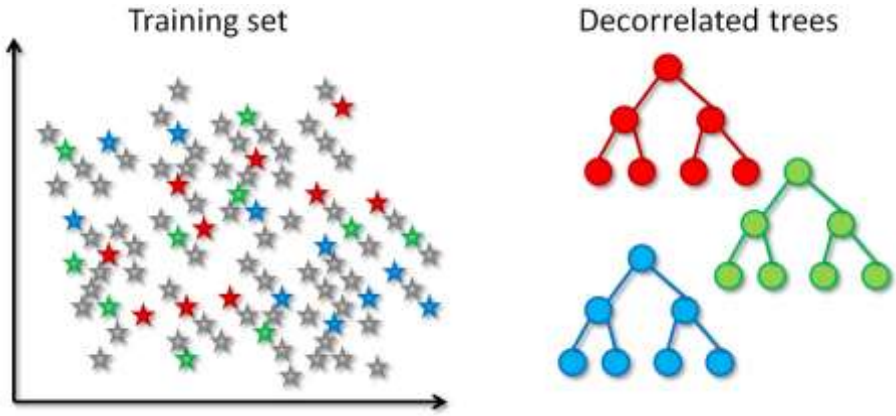

Figure 5.4: Bagging method for different data sets

In random forest, the main parameters are: (1) number of trees and (2) depth of trees. To decrease the prediction error, the number of trees should be more with maximal allowed depth that directly impacts on the ability of trees. As shown in Figure 5.5, prediction error curve is entirely dependent on the depth of the trees; it decreases with the depth, but after that, it again increases. Also, the prediction error decreases with the number of trees.

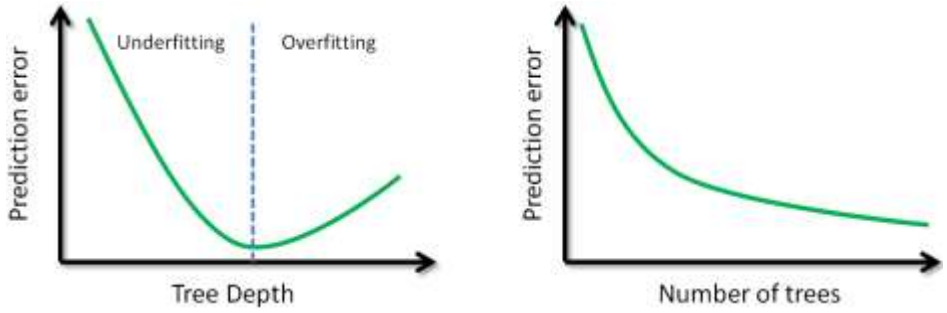

Figure 5.5: Forest parameters - Tree depth and number of trees are the two most important parameters

While increasing the number of trees corresponding to a decrease in the prediction error, tree depth needs to be carefully tuned as it controls the generalization ability of the forests.

For the random forest $\mathcal{R} = \{R_n\}_{n=1}^{T}$, R_n with the partition P_n with attributes space $\mathcal{F}$, the whole forest with ensemble of cells is defined as :

$$R(X) = \{L_1^{Z_1}, \dots \dots L_n^{Z_n}, \dots \dots \dots, L_T^{Z_T}\} \quad 5.7$$

where each tree is associated with an observation $\mathcal{F}\ \mathcal{E}\ F$ to a cell $L_n^{Z_n}$.

Then the forest prediction can be computed by averaging the trees and is defined as:

$$P(B/A) = \frac{1}{T}\sum_{n=1}^{T} P(B/A\ \mathcal{E}\ L_n^{Z_n}, P_n) \quad 5.8$$

It gives more weight to more certain trees thereby reducing the noise level contribution. Due to the vast generalization and scalability to large data set, random forest provides the ability of classification. In fact, it is a randomly trained set of various independent decision tree algorithms introducing both bagging and random variable selection for tree building [23]. Good performance and robustness are the great attributes of this algorithm. The sample of training data out of the bootstrap is called the out of bag (OBB). This OBB score can measure the prediction efficiency. The number of trees and the number of variables are the specified parameters for each split, and there is no specified rule to find out the optimal number of trees [154]. There should be some threshold limit on the number of trees, and this limit varies according to the usage and application. Increasing the number of trees does not always mean that error will be reducing continuously and will come down to a limit. Moreover, it increases the computational cost. One can select the trees by examining the OBB error rate values as will be explained in the results and discussion section.

5.5 Performance Metric

In the field of machine learning, confusion matrix permits the visualization and describes the performance of a supervised learning. It is also called contingency matrix or error matrix in which each row represents the instances in the actual class and each column represents the predicted class. Distinctive parameters are utilized to evaluate the performance of the classifiers [28]. There are four alternative parameters for the classifier. *True Positive* implies that the predicted and actual values are positive. If the predicted value is negative and the real value is also negative then the term is called the *true negative*. In other words, the true positive and true negative implies that the predicted class and actual class are of the same nature. However, if the predicted class and actual class have an inverse relationship, the nomenclature is different. If the predicted value is positive or true but actual is negative then that kind of class is called the *false positive,* also known as type 1 error. On the other hand, when we predict false and the actual is true then it is called as *false negative* and also called type II error. Table 5.1 represents these situations and it is called as a two-level matrix.

This two-level matrix is converted to the four-level to find the parameters for the four movements of the shoulder. A confusion matrix has been used to analyse the performance of the classifiers by calculating the different values like sensitivity, selectivity, and recall value

by using different equations related to the above recommemeded parameters (True positive, False Positive and False Negative) with the two level class, table shows in Table 5.1.

Table 5.1: Standard two-level matrix

	Actual Class	**Actual Class**
	(Condition Positive)	**(Condition negative)**
Predicted Class **(Condition Positive)**	True Positive (TP)	False Positive (FP)
Predicted Class **(Condition negative)**	False negative (FN)	True negative (TN)

Table 5.2 represented the four-level matrix for four different movement of shoulder. The different performance metric parameters were calculated for all the classifiers to find the best classifier of the study.

Table 5.2: Four level matrix for different movements of shoulder

	Predicted Class				
Actual Class		**A**	**B**	**C**	**D**
	A	TP_A	E_{AB}	E_{AC}	E_{AD}
	B	E_{BA}	TP_B	E_{BC}	E_{BD}
	C	E_{CA}	E_{CB}	TP_C	E_{CD}
	D	E_{DA}	E_{DB}	E_{DC}	TP_D

Various performance metric corresponding to 4-level matrix are as follows:

Accuracy: It is the total number of all correct predictions to the total number of data sets. Its value lies in 0-1 for lower to best accuracy. Accuracy can also be calculated by the 1-error rate where error rate is the ration of incorrect prediction to the total number of data sets. The equation of accuracy is:

$$\text{Accuracy} = \frac{TP_A + TP_B + TP_c + TP_D}{TP_A + TP_B + TP_C + TP_D + E_{AB} + E_{AC} + E_{AD} + E_{BA} + E_{BC} + E_{BD} + E_{CA} + E_{CB} + E_{CD}} \times 100\% \qquad 5.9$$

***Sensitivity*:** It provides the proportion of correctly identified positive rate. It is the ratio of the number of correct positive prediction to the total number of positives. It is called as recall or

true positive rate. The sensitivity values lie between 0-1. The sensitive nature of the four classes A, B,C,D are defined as:

$$\text{Sensitivity for A} = \frac{TP_A}{TP_{A+}E_{AB+}E_{AC+}E_{AD}} \times 100\% \quad 5.10$$

$$\text{Sensitivity for B} = \frac{TP_B}{TP_{B+}E_{BA+}E_{BC+}E_{BD}} \times 100\%$$

$$\text{Sensitivity for C} = \frac{TP_C}{TP_{C+}E_{CA+}E_{CB+}E_{CD}} \times 100\%$$

$$\text{Senstivity for D} = \frac{TP_D}{TP_{D+}E_{DA+}E_{DB+}E_{DC}} \times 100$$

Precision: Precision is the proportion of the correct positive predictive values. It is the ratio of the positive prediction to the sum of positive predictions. It is also called the predictive value. The value of the precision is lies between 0-1. It is calculated for four classes using the following equations:

$$\text{Precisions for A} = \frac{TP_A}{TP_{A+}E_{BA+}E_{CA+}E_{DA}} \times 100\% \quad 5.11$$

$$\text{Precisions for B} = \frac{TP_B}{TP_{B+}E_{AB+}E_{CB+}E_{DB}} \times 100\%$$

$$\text{Precisions for C} = \frac{TP_C}{TP_{C+}E_{AC+}E_{BC+}E_{DC}} \times 100\%$$

$$\text{Precisions for D} = \frac{TP_D}{TP_{D+}E_{AD+}E_{BD+}E_{CD}} \times 100\%$$

Specificity: Specificity is defined as the ratio of the correct negative prediction to the total number of negatives which means that it is the proportion of the negative cases. The range of the specificity lies between 0-1. It is also called the true negative rate. The specificity of the four classes can be represented as follows:

$$\text{Specificity for A} = \frac{TP_B+ E_{BC}+ E_{BD}+E_{CB+} TP_c+ E_{CD}+E_{DB}+E_{DC}+TP_D}{TP_B+ E_{BC}+ E_{BD}+E_{CB+} TP_c+ E_{CD}+E_{DB}+E_{DC}+T_{PD}+ E_{BA}+E_{CA}+E_{DA}} \times 100\% \quad 5.12$$

$$\text{Specificity for B} = \frac{TP_A+ E_{AC}+E_{AD}+ E_{CA+} TP_C+E_{CD}+E_{DA}+E_{DC}+TP_D}{TP_A+ E_{AC}+E_{AD}+ E_{CA+} TP_C+E_{CD}+E_{DA}+E_{DC}+TP_D+ E_{AB}+E_{CB}+E_{DB}+} \times 100\%$$

$$\text{Specificity for C} = \frac{TP_B+ E_{AB}+ E_{BA+} TP_A+ E_{DA}+E_{DB}+E_{CB}+E_{AD}+E_{BD}+ TP_D}{TP_B+ E_{AB}+ E_{BA+} TP_A+ E_{DA}+E_{DB}+E_{CB}+E_{AD}+E_{BD}+TP_D+ E_{AC}+E_{BC}+E_{DC}} \times 100\%$$

$$\text{Specificity for D} = \frac{TP_B+ E_{AB}+ E_{BA+} TP_A+ E_{DA}+E_{DB}+E_{CB}+E_{AD}+E_{BD}+ TP_D}{TP_B+ E_{AB}+ E_{BA+} TP_A+ E_{DA}+E_{DB}+E_{CB}+E_{AD}+E_{BD}+ TP_D+ E_{AC}+E_{BC}+E_{DC}} \times 100\%$$

5.6 Evaluation Method

After developing a classifier, the evaluation provided the error rate of the classifier and also an idea about the future performance of the classifier for an unseen data set. The evaluation is apparently necessary to choose a single classifier among the number of classifiers. Different testing methods have been adopted to decide the classifier. Different evaluation methods describe as follows:

5.6.1 Residual method

First of all, the divide the training data set into training set and test set. The training set is used to train the classifier while the remaining set (part of training set) applied as the test set and called the called the training error method. The actual output is then obtained by comparing the actual and the measured result. It provides the maximum efficiency of the classifier but there is no unknown data set for evaluating the performance. This method is not able to give the indications about the learning of the model.

5.6.2 Cross Validation

In this method, the evaluation of the classifier is obtained by dividing the whole data set into two subsets: one is used to train the model and the other subset is for the validation. The second subset evaluates the performance of the final model. The cross validation is very useful while comparing the different models and provides the estimate performance of the models. The thesis has covered the two types of the cross-validation methods:

5.6.2.1 Holdout Method

It is the simplest method of the cross-validation. In this approach, the data set is divide into the two separate non-overlapped sets called training and the testing set [116]. The training model is fit on the training set and afterwards, the model response is predicted by fitting the model on the testing set (Figure 5.6). An absolute error rate calculation between the actual value of the testing data set and the predicted value is performed for the evaluation of the test set. The results of the assessment are heavily dependent upon the division of the training and testing data set. An absolute error rate calculation between the actual value of the testing data set and the predicted value is performed for the evaluation of the test set. The results of the assessment are heavily dependent upon the division of the training and testing data set. Moreover, results are highly dependent on the choice of the test and the train split.

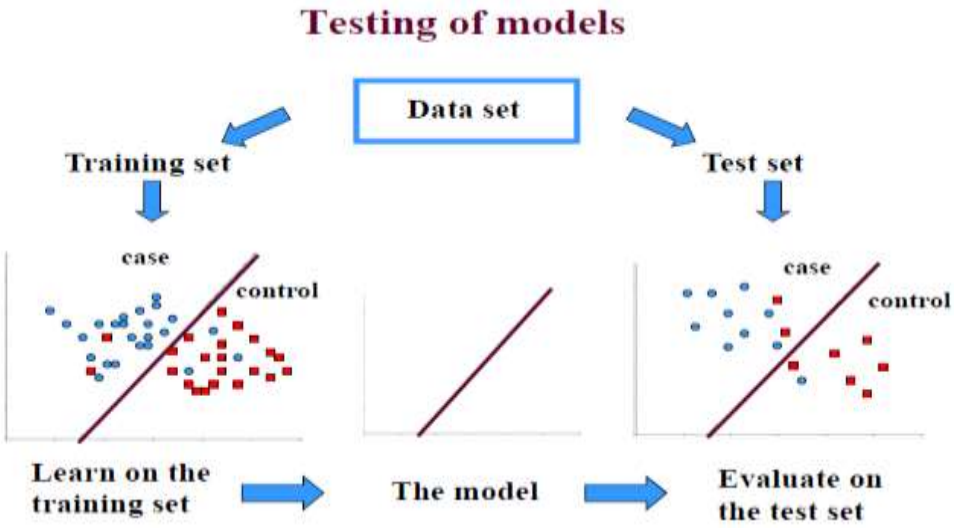

Figure 5.6: Hold out test for training and testing model of machine learning algorithm

If the data laid down in the test set is valuable for the training of the model then the performance of the prediction may suffer. Therefore, to solve this problem, the K-fold method is used.

5.6.2.2 K-fold cross-validation

It is an improvement over the holdout method. The data is divided into different subsets with an equal sized segment and denoted by *k*. One part of the k is for the training, and the remaining *k-1* set put together are used for testing.

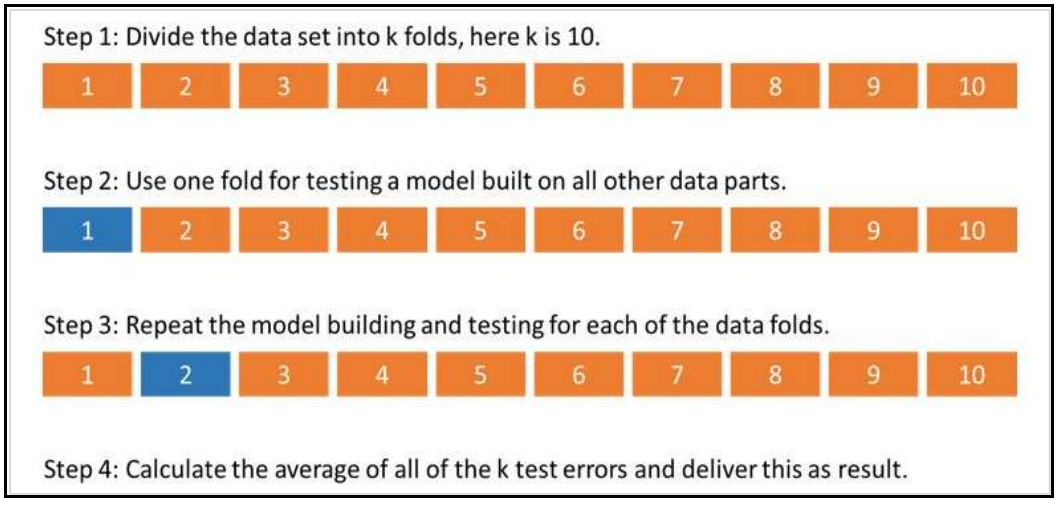

Figure 5.7: Technique of K-fold Test

Figure 5.7 shows the whole data set is divided in ten different partitions for k = 10 fold method. Afterwards, one data fold is used for testing while another part for training. This method is

repeated for the full data set. Then, an average error for all the trials is computed. In this approach, the division of the data set depends on the value of K that is an advantage over the holdout method. The other advantage is that anyone can independently choose the size of the test data and the number of trials required for the computation. This algorithm takes a total of k time computation to provide an optimal solution as it trains and tests at every point [163]

5.7 Results and Discussion

The classification of the different movements is a very cumbersome task due the stochastic nature of the sEMG signal. After the pre-processing of the signal, DWT wavelet transformation technique was chosen for the analysis of the signal. The traditional method and the proposed technique was applied to the coefficients for feature extraction (Section 5.3). Various results regarding feature extraction and classification of the four classes (retraction, protraction on one side of shoulder and elevation on both the sides of the shoulder) of shoulder movement is the next part of the study to classify the two degree of freedom of hand and elbow.

5.7.1 Traditional features extraction results

Total 30 features were extracted from the obtained DWT coefficients of the db3 wavelet transform with four level decomposition. The feature matrix contains the different channel data with different movements of an individual shoulder. The next step was to classify the attributes matrix data using different machine learning algorithms.

5.7.1.1 Hold out test

The training and testing partition was chosen to be 70-30 percent respectively. The results presented in Table 5.3 describe the performance of different machine learning algorithm for the hold-out test. It can be observed from these machine learning algorithms, RF and KNN were the best learning algorithm for shoulder muscles. Both provided the 98.49% efficiency with only 1.51% incorrect instances.

Table 5.3: Hold out test results for five classifiers

Classifiers →	RF	DT	KNN	NB	SVM
Accuracy	0.98±0.7	0.91±0.93	0.98±0.8	0.86%±0.17	0.78%±0.08
TP Rate/ Recall	0.98±0.02	0.91±0.03	0.98±0.07	0.86±0.01	0.77±0.04
FP Rate	0.007±0.03	0.043±0.05	0.007±0.02	0.82±0.02	0.70±0.02
Precision	0.98±0.0013	0.91±0.1	0.97±0.01	0.80±0.13	0.68±0.02

The next used model was the DT model with the efficiency of 91.3%. NB and SVM have very low value of effectiveness, therefore, these could not be considered for the training. The different parameters of the confusion matrix were calculated for the different movements of the shoulder to find out the accuracy rate of an individual movement. The standard deviation values show the various trials of each movement for the six subjects. The cross-validation or hold out was the simplest method to train the network, and its efficiency is better because it simply divides the data into 70-30 partition sets for training and testing.

5.7.1.2 K-fold test

During the K-fold test, the data set was split into different subsets. The value of k was taken as 10 which means the data set was divided into ten parts. Different machine learning algorithms were compared with the K-fold (Table 5.4).

Table 5.4: K-fold test results for five classifiers

Classifiers (K=10)	RF	DT	KNN	NB	SVM
Accuracy	0.61± 0.9	0.50±1.3	0.49±0.8	0.36%±0.97	0.38%±0.08
TP Rate or Recall	0.618±0.014	0.51±0.15	0.45±0.045	0.36±0.01	0.38±0.04
FP Rate	0.20±0.03	0.249±0.19	0.26±0.02	0.30±0.02	0.32±0.02
Precision	0.613±0.019	0.55±0.1	0.50±0.02	0.409±0.13	0.348±0.02

With this K-fold, the results introduced the profound change in the machine learning proficiency. The accuracy level of KNN and DT was close to each other (approx. 0.50) but was not adequate for any design. With holdout method, the efficiency of the RF was 0.98 and with the K-fold technique, achieved efficiency was 0.61. If the training data set is qualitatively better than the experimental data set then it provides a good classification result, but on the other hand, if test set is more complex than the training set, then it provides worst results. Therefore, the hold out test was not the technique to get the generalization of results. Data set partition may vary the outcomes in various trials. In K-fold technique the complete information is utilized for the training and testing shows that the RF outperformed all the listed classifiers, but its accuracy was not so good that it could be considered to design a prosthetic device. The recall value provided the correctly obtained events, and this was equal to the efficiency, i.e., approx. 0.618 for the RF model and the precision value was 0.613. There was a slight difference in both the cases. Even the false positive rate was only 0.2 in the case of RF learning algorithm. To enhance the proficiency of the K-fold method, we have to select combinations of the feature vector. The next section provides the best combination of features.

5.7.1.3 Attributes Selection

In this section, reduction of the number of attributes help to improve the performance of the K-fold technique.

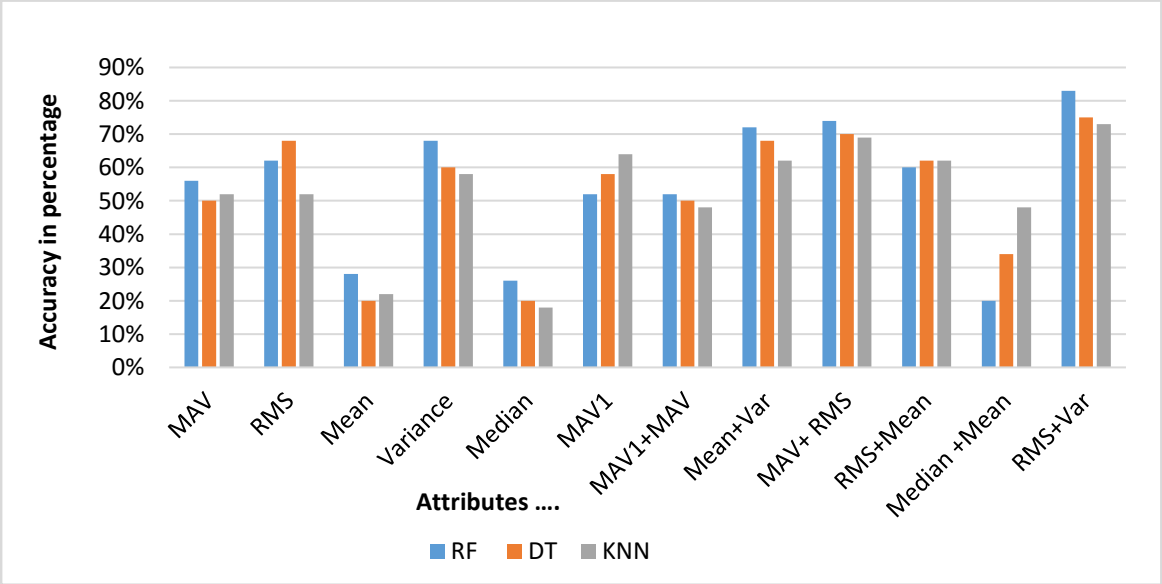

Figure 5.8: Selection of attributes with respect to the accuracy of the data set.

As seen from the last section, a large number of attributes reduced the efficiency of the model.

Secondly, NB and SVM have worst perforance with efficiency of not even 50%, therefore in this section, we have considered the three remaining algorithms - KNN, RF and DT. The individual features and the combination of different attributes were chosen to calculate the efficient parameters for the classification with K-fold technique.

In Figure 5.8 the results indicate the change in the accuracy due to the presence of the different attributes in three learning models. If we consider the individual attributes, then, in that case, RMS and variance individually have provided 68% efficiency for the DT and RF respectively. However, with the combination of different attributes, the result indicates that the three models provided the results with more than 72% accuracy with the RMS + VAR. The result shows that the combined attributes have provided better results than the single attributes. However, this RF model with 83% efficiency can also not be considered satisfactory for driving the prosthetic device. Therefore, a new proposed method was applied to improve the effectiveness of this model.

5.7.2 Proposed method

In classification process, proposed method is used to to classify the shoulder signal accurately so as to make a better prosthetic for the upper limb amputees by using the transformation method. The different features of wavelet transformed coefficients were extracted by transfromation method. Afterwards, different learning algorithms were provided with transformed data for calculating the performance of the models.

Table 5.5: K-10 fold test results for five classifiers using the proposed method

Classifiers ⇨	**RF**	**DT**	**KNN**	**SVM**	**NB**
Accuracy	0.985 %± .25	0.963%±1.25	0.952±1.29	0.74±0.24	0.72±0.25
TP Rate	0.997±0.004	0.932±0.005	0.94±0.005	0.745±0.025	0.728±0.02
FP Rate	0.003±0.002	0.029±0.07	0.005±0.007	0.272±0.015	0.7234±0.01
Precision	0.997±0.008	0.912±0.003	0.989±0.001	0.609±0.5	0.528±0.0127
Recall	0.997±0.002	0.932±0.004	0.989±0.002	0.745±0.028	0.723±0.002

Then the K-fold technique was applied with K=10 and evaluated the results for all the classifiers. Table 5.5 presents the evaluated results using different machine learning supervised algorithms (DT, RF, SVM, KNN and NB) with proposed method. The minimum obtained efficiency was 72% with NB and 74% with SVM. It is to be noted that in the case of a traditional method, it provided an efficiency of less than 40% for the same classifier. The results also show

that the RF model obtained the highest average classification accuracy with some value of standard deviation (98%± 0.25) trailed by the DT and KNN model (98.8%). TP rate, recall and precision provided almost the same result with the accuracy. The FP rate was also at a lower level (0.003) than previous. The classifiers' response was tested for different muscles signal due to the movement of the shoulder so that different muscles activation can be realized with the motion of the shoulder. Three selected classifiers (RF, DT and KNN) performance level was analyzed with different performance metric parameters.

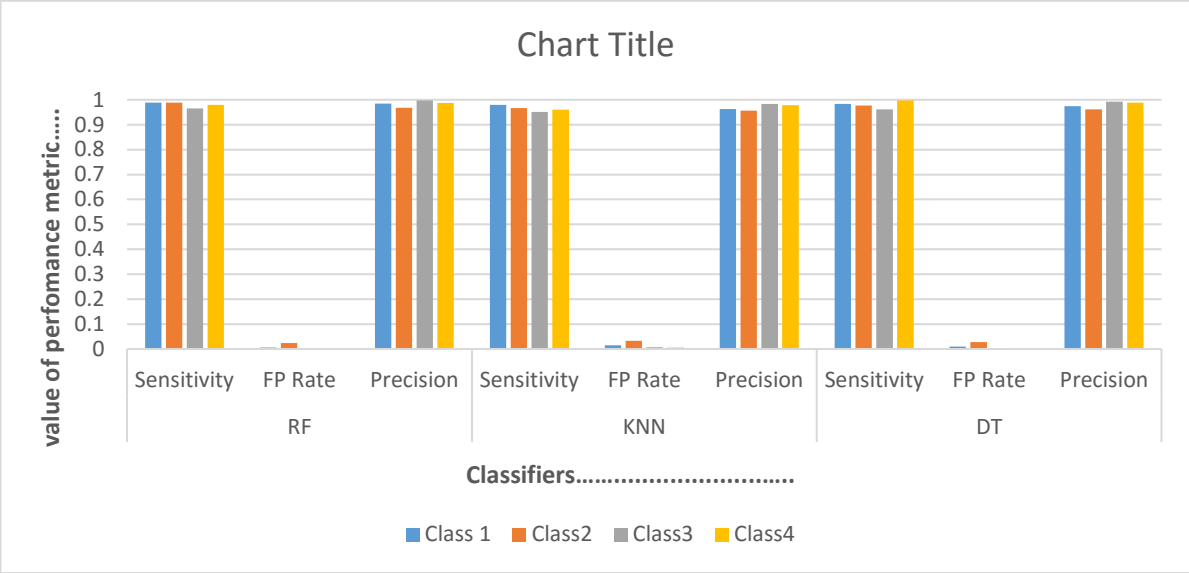

Figure 5.9: Performance of Random Forest, K-nearest neighbour and Decision tree Classifier.

The histogram displays (Figure 5.9) the graphical comparison of RF, DT and KNN models with various parameters for different four motions of the shoulder. The results were found to be better for the RF model than DT and KNN. DT classifier takes less time to classify the results as compared to RF and can be called better if we can compromise with the efficiency of the system. For a real-time system, DT can also be used for fast classification of the data set. The FP rate for all the classes was less than 0.1% and the precision value for RF was more than 98% value. The different subjects' data was provided to the RF classifier for further classification of individual shoulder movement of various participants. Table 5.6 shows the muscles vise resulted classiffication for six subjects. The trapezius muscles activation in elevation motion in various subjects provided more effcieincy than the other motion of shoulder.

Table 5.6: Perormance of Random Forest Classifiers with different subjects movement

Subjects	Protraction	Retraction	Elevation	Elevation 2
Subject 1	0.97±0.01	0.98±0.01	0.98±0.001	0.978 ±0.003
Subject 2	0.97±0.01	0.96±0.02	0.98±0.001	0.99±0.012
Subject 3	0.96±0.01	0.97±0.01	0.98±0.001	0.98±0.002
Subject 4	0.96±0.02	0.99±0.045	0.99±0.001	0.96±0.025
Subject 5	0.96±0.01	0.97±0.01	0.97±0.001	0.98±0.45
Subject 6	0.98±0.045	0.98±0.003	0.99±0.004	0.97±0.568

5.8 Validation of Results

A good prosthesis should ideally integrate with the user's body. The mechanical engineering and designing of devices has advanced rapidly, but the analysis of the muscles activation signal has to be done reliably to carry out the hand function successfully. It is a tough task to identify the location of the shoulder muscles that can produce signals which can directly control the elbow and hand.

The four different movements - hand open/close and the elbow up/down movement of the arm were validated from the acquired shoulder muscle signals. As described before, first, the acquired data was preprocessed to remove the noise signal, then analyzed and classified with the best classifier (Random Forest) that provided approx. 98% efficiency. The output of the RF classifier was interfaced with the hardware to check the prototype function with the movement of the shoulder. The prototype shows in Figure 5.10 involves designing and building a robotic arm capable of human-like motions. The arm and hand were designed to replicate motions similar to human arm. The translation of the signal from the body muscle to the prosthetic device is the combination of the high performance of the signal processing techniques with the new algorithm. A good classification was able to improve the accuracy of control of the dexterity of upper limb immensely.

For making the base of the robotic arm, a rectangular piece of wooden board was cut. It is supported by other two rectangular wooden pieces with the help of L-clamps; the DC servo motor is fixed in between. The servo motor is accompanied with a gear assembly. The gears drive the wooden arm upward or downward to mimic the elbow motion. The end part of the arm is attached with a wooden ply that has a servo motor fixed with a gear assembly. These gears are attached with two wooden ply pieces designed to grasp and hold objects.

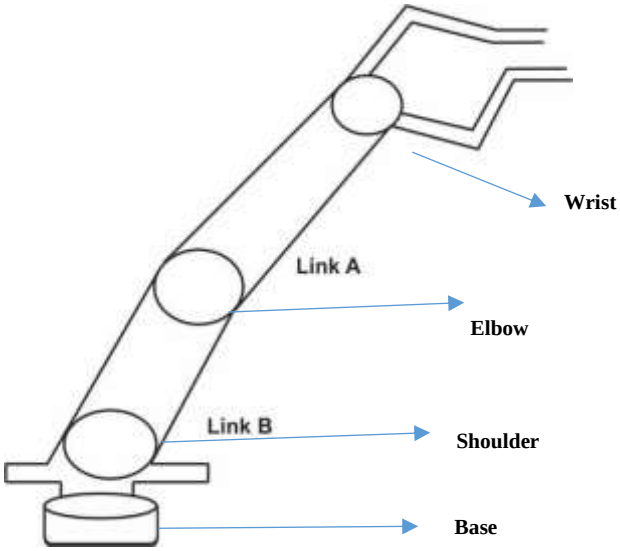

Figure 5.10: Design overview of prototype.

Figure 5.11: Validation of results through prototype

Servo motor is used for rotating the joints and moving the gripper for grasping the object. It has two degrees of freedom similar to that in a human arm. The four shoulder movement signals control two DC motors in the prototype. Protraction and retraction movement of the shoulder are used to open/close the hand while left/right trapezius motion controls the elbow up/down movement of the prosthetic arm. The host PC was connected to the Arduino board by using the serial port interface. The output signal from classifier was fed to the aurdino board which sent classified commands to the motors. One DC servomotor was attached to

hand (gripper) and the other to the elbow to provide the synergy function of hand and elbow as shown in the Figure 5.11.

For hardware validation, the detailed workflow of SEMG signal was performed. The data was acquired from six upper limb right-hand amputee persons who had lost their arm due to some accident. Different subjects were made a request to make the distinctive four activities with the right arm. After recording of the information from various muscles, the acquired data was sent for pre-processing stage which contains different filtering processes. To classify the different arm and hand motions, machine learning technique was used and then the output of classifier was directly given to hardware prototype to control the rotation of two motors corresponding to four movements of hand and elbow. The whole process was working by acquired EMG signal from shoulder muscles. For commercial purposes, the processors and the DSP chip system can be used to handle the large data set with MATLAB code downloaded on to the DSP chip. The use of energy efficient motors, driving circuits and couplings can further improve the degree of functionality of prosthetic device.

Summary

A reliable and accurate method of SEMG analysis is necessary to appropriately maintain the rigor of scientific research in the field of rehabilitation. Random Forest with proposed data transformation method was found to be a valid tool to classify different movements of upper limb amputee shoulder from the onset muscle activity. A hand-made prototype has been used to validate the output of the random forest through the Arduino board. The proposed method is relevant to other studies involving SEMG signal for different applications.

Chapter 6
Conclusion and Future Scope

6.1 Research Contributions

Upper limb amputation causes the greatest disruption in the daily life function and can lead individuals to lose their confidence and autonomy. Prosthetic devices can give alleviation by replacing the function of missing limb which can bring a sea change in the life of the amputees. A prosthetic device is an artificial limb that can upgrade and deal with the daily activities of life by replacing the function of the missing limb. Myoelectric devices promise natural appearance of the arm with extreme functionality. The control of myoelectric devices is highly dependent upon the SEMG signal acquired from the muscles-activity of the human body. These signals are acquired from the body by the surface electrodes, processed by a suitable combination of hardware and software to control the hand, arm or elbow of the artificial limb using actuators.

The primary contribution of this work was to demonstrate a successful prototype with the independent motion of two motors in both directions corresponding to the functionality of elbow and hand of around-shoulder myoelectric arm for upper limb amputees. Recording and interoperating the signal from the shoulder muscle of an amputee was a challenging task because of the difference between the muscles-activity of amputees and the non-amputeebody person. The placement of the electrode on shoulder must be accurate to avoid cross talk and the extra force exertion by the individual subject. With the movement of the shoulder, muscles get activated and generate the electrical signals with different amplitude levels. This amplitude level is directly proportional to the force exerted by subjects to move the shoulder. During the acquisition of the signal, a variety of variations (amplitude, frequency and noise) were introduced into the acquired signal which could misguide in the prediction of motion of the shoulder. Therefore, a novel approach has been aimed to adaptively adjust the threshold of Teager energy operator to filter the unwanted peaks in the pre-processing stage of the SEMG signal (Chapter 3).

Many different sets of tools exist to analyze the SEMG signal. In this case, the Discrete Wavelet Transform was used for analyzing the non-stationary signal. A wavelet-based algorithm was

developed to find the suitable wavelet function for the shoulder muscles signal. There are mainly four types of noise such as motion artifacts, inherent instability, ambient noise and thermal noise in electronic components. First three noise can be reduced with the help of different filters but the fourth noise lies is in the range of the SEMG frequency band. Wavelets are a powerful statistical tool mostly used for the de-noising process, to compress and smoothen the data signal. It can maintain the characteristic of the signal while reducing the random noise in the non-stationary signal.

The main objective of this thesis was to classify the acquired SEMG signal from the shoulder muscles. Worldwide, various methods of extraction of features from the coefficients of the wavelet transform have been used. Like the traditional methods, the six features i.e. Mean absolute value, Mean absolute value slope, Median, Mean, Root Mean Square value and Variance (VAR) were calculated to make the feature vector space. The complete vector contains 30 features (5 decomposition levels * 6 features) for one motion value. The five classifiers Random Forest, Decision Tree, K-nearest Neighbour, Naïve Bayes and Support Vector Machine were implemented and compared for performance based on these features. The random forest provided 61% efficiency using K-fold methods with K=10. Afterwards, reduction in the number of attributes was done to improve the performance of classification. Reduced set of features produced 83% efficiency by the random forest classifier. Even then this method was not reliable to drive the prosthetic device which was the main goal of this work. The proposed method was used to extract the features before applying to classifiers. During the comparison of the classifier proficiency, random forest outperformed others with 99.7% accuracy using K-fold method with k=10 (chapter 5). The four different movements - hand open/close and the elbow up/down movement of the arm were validated from the acquired shoulder muscle signals. The host PC was connected to the Arduino board UNO/MEGA by using the serial port interface to test the results. The output signal was fed to the Arduino board to send the classified commands to the motors. One DC servomotor was attached to hand and the other to the elbow to provide the synergy function of hand and elbow. The relevance of this method to other clinical populace establish its feasibility for are commendation on its use in the prosthetic design by extracting the accurate and efficient SEMG signal.

6.2 Future Work & Suggestions

- The main requirement of the prosthetic devices is less weight and natural appearance. The present heavy weight of the prosthetic is due to the use of data acquisition system, motors and battery system. With the development of technology, the active electrode can be used having in-built pre-processing system contain filtering and adaptive peak detection. Polymer/magnesium composites materials can be the better solution for the light weight real-time prosthetic device.
- The implantable myoelectric sensors comprised of multiple channel which provide the various degrees of freedom to improve the degree of functionalities of prosthetic devices further.
- Performance of the entire framework can be improved by smoothening of the hand grip and use of the high torque motor so that it can lift heavy objects.
- Data from more number of amputee subjects would increase the authenticity of results.
- The used algorithm is for the upper limb amputee person having no muscles activation below the shoulder. This algorithm can further be used for the shoulder disarticulation amputees.
- The hardware based machine learning system composed of electronic representation of the output of classifier in online mode can be designed for the motion recognition. It should be like a system on chip platform implementation to decrease the detection delay and make the real time reliable prosthetic for amputees for daily life activity.
- The prosthetic device fabrication using 3D printing by using low weight fiber material can be quite comfortable to wear.
- Degree of freedom can be improved by using the hybrid classification method which is based on the combination of EEG and SEMG signal for the classification of arm and hand motion.

References

[1] Y. C. Kim, C. I. Park, D. Y. Kim, T. S. Kim, and J. C. Shin, "Statistical analysis of amputations and trends in Korea.," *Prosthetics and orthotics international*, vol. 20, no. 2, pp. 88–95, 1996.

[2] F. Cordella and Ciancio, "Literature review on needs of upper limb prosthesis users," *Frontiers in Neuroscience*, vol. 10, pp. 1–14, 2016.

[3] G. Das Pooja and L. Sangeeta, "Prevalence and aetiology of amputation in Kolkata, India: A retrospective analysis," *Hong Kong Physiotherapy Journal*, vol. 31, no. 1, pp. 36–40, 2013.

[4] F. Cordella *et al.*, "Literature review on needs of upper limb prosthesis users," *Frontiers in Neuroscience*, vol. 10, no. MAY, pp. 1–14, 2016.

[5] P. Hernigou, "The early history of artificial limbs (from robotic to prostheses)," *International Orthopaedics*, vol. 37, no. 6, pp. 1195–1197, 2013.

[6] N. Krishnamurthi Jellish, James J. Abbas, Todd M. Ingalls , Padma Mahant, Johan Samanta , Maria Cristina Ospina, "A System for Real-Time Feedback to Improve Gait and Posture in Parkinson's Disease," *IEEE Journal of Biomedical and Health Informatics*, vol. vol.19, no. 6, pp. 1809–1819, 2015.

[7] S. Ong, J. Wu, S. M. Moochhala, M. Tan, and J. Lu, "Biomaterials Development of a chitosan-based wound dressing with improved hemostatic and antimicrobial properties," *Biomaterials*, vol. 29, pp. 4323–4332, 2008.

[8] C. Toledo, L. Leija, R. Muñoz, A. Vera, and A. Ramírez, "Upper limb prostheses for amputations above elbow: A review," *2009 Pan American Health Care Exchanges - PAHCE 2009*, no. April, pp. 104–108, 2009.

[9] C. L. Taylor, "The biomechanics of control in upper-extremity prostheses.," *Artificial limbs*, vol. 2, no. 3, pp. 4–25, 1955.

[10] K. Talbot, "Using Arduino to Design a Myoelectric Prosthetic," 2014.

[11] A. Muzumdar, *Powered Upper Limb Prostheses*. 2004.

[12] "Disposal EMG Electrode." [Online]. Available: http://www.sieso-ergo.eu/en/product-info/disposable-emg-electrodes-suited-for-bf001-10x50-pcs/334.

[13] J. Muthuswamy, "Standard Handbook of Biomedical Engineering and Design," in *Chapter 18 Biomedical Signal Analysis*, 2004, pp. 1–34.

[14] B. S. Day, "Important Factors in Surface EMG Measurement," *Measurement*, pp. 1–17, 2002.

[15] F. Duan, L. Dai, W. Chang, Z. Chen, C. Zhu, and W. Li, "SEMG-Based Identification of Hand Motion Commands Using Wavelet Neural Network Combined with Discrete Wavelet Transform," *IEEE Transactions on Industrial Electronics*, vol. 63, no. 3, pp. 1923–1934, 2016.

[16] B. Chakrabarti, S. Maity, S. Barui, S. Palbhowmik, S. Das, and B. Neogi, "Overview on Literature Survey towards EMG Interpretations Technique in Addition," *International Journal of Scientific and Engineering Research*, vol. 6, no. 5, pp. 4119–424, 2015.

[17] D. Blana, T. Kyriacou, J. M. Lambrecht, and E. K. Chadwick, "Feasibility of using combined EMG and kinematic signals for prosthesis control: A simulation study using a virtual reality environment," *Journal of Electromyography and Kinesiology*, vol. 29, pp. 21–27, 2016.

[18] A. Phinyomark, P. Phukpattaranont, and C. Limsakul, "The Usefulness of Wavelet Transform to Reduce Noise in the SEMG Signal," in *EMG methods for evaluating muscle and nerve function*, 2012, pp. 107–132.

[19] A. Phinyomark, C. Limsakul, and P. Phukpattaranont, "Optimal Wavelet Functions in

Wavelet Denoising for Multifunction Myoelectric Control," *Proceedings of the Electrical Engineering/Electronics, Computer, Telecommunications and Information Technology*, vol. 8, no. 1, pp. 43–52, 2010.

[20] W. K. Ngui, M. S. Leong, L. M. Hee, and A. M. Abdelrhman, "Wavelet Analysis: Mother Wavelet Selection Methods," *Applied Mechanics and Materials*, vol. 393, no. January, pp. 953–958, 2013.

[21] Y. Narayan, L. Mathew, and S. Chatterji, "sEMG signal classification using Discrete Wavelet Transform and Decision Tree classifier," *International journal of control theory and applications*, vol. 10, no. 6, pp. 511–517, 2017.

[22] K. R. Foster, R. Koprowski, and J. D. Skufca, "Machine learning, medical diagnosis, and biomedical engineering research - commentary," *BioMedical Engineering OnLine*, vol. 13, no. 1, p. 94, 2014.

[23] S. Jadhav, H. Hongmei, and K. Jenkins, "An Academic Review: Applications of Data Mining Techniques in Finance Industry," *International Journal of Soft Computing and Artificial Intelligence*, vol. 4, no. 1, pp. 79–95, 2016.

[24] M. Perez-Ortiz, S. Jimenez-Fernandez, P. Gutierrez, E. Alexandre, C. Hervas-Martinez, and S. Salcedo-Sanz, "A Review of Classification Problems and Algorithms in Renewable Energy Applications," *Energies*, vol. 9, no. 8, p. 607, 2016.

[25] D. F. Stegeman and H. J. Hermens, "Standards for suface electromyography : The European project Surface EMG for non-invasive assessment of muscles," 2007.

[26] S. Kusukawa, *Picturing the book of nature : Image Text and Arguments in sixteenth century human Anatomy and medical botony*. The university of Chicago, 2012.

[27] U. D. Yves Blanc, "History of the Study of Skeletal Muscle Function with Emphasis on Kinesiological Electromyography," *The Open Rehabilitation Journal*, vol. 8, no. 3, pp. 84–93, 2010.

[28] C. J. De Luca, " 'The use of surface electromyography in biomechanics," *J Appl Biomech*, vol. 13, no. 2, pp. 135–163, 1997.

[29] M. R. Bennett, *History of the Synapses*. harwood academic publisher, 2001.

[30] F. A. Navarro, "Archives Italiennes de biologie," *Panacea*, vol. 14, no. 38, p. 279, 2013.

[31] P. Brown, S. Salenius, J. C. Rothwell, and R. Hari, "Cortical correlate of the piper rhythm in humans," *Journal of Neurophysiology*, vol. 80, no. 6, pp. 2911–2917, 1998.

[32] Hill, "The tetanic nature of the voluntary contraction in man," *J. Physiol. (Lond.)*, vol. 351, pp. 1801–1804, 1998.

[33] P. Brown, "Muscle sounds in Parkinson's disease.," in *Lancet*, vol. 349, 1997, pp. 533–535.

[34] H. Davis, "Joseph erlanger," *National Academy of Sciences*, pp. 110–139, 1970.

[35] J. R. Cram and G. S. Kasman, "The basics of surface myoelectrography," in *Jones and Bartlett publication*, 2005, pp. 1–8.

[36] C. Hardyck, L. Pentrincovich, and D. Elseworth, "Feedback of sppech signal muscles activity during silent reading- Rapid Extension," *Science*, vol. 154, pp. 1467–1468, 1966.

[37] H. . Booker, R. Robow, and C. PJ, "Simplified feedback in neuromuscular retraining, an automated approach using EMG signal.," *Arch Phys Med*, vol. 50, pp. 621–625, 1969.

[38] J. Cram and J. Steger, "Muscles Scanning and diagonsis of chronic pain," *Biofeedback Self - Regul.*, vol. 8, pp. 229–241, 1983.

[39] A. Phinyomark, F. Quaine, S. Charbonnier, C. Serviere, F. Tarpin-Bernard, and Y. Laurillau, "EMG feature evaluation for improving myoelectric pattern recognition robustness," *Expert Systems with Applications*, vol. 40, no. 12, pp. 4832–4840, 2013.

[40] K. Englehart, B. Hudgins, and P. Parker, "A wavelet-based continuous classification scheme for multifunction myoelectric control," *IEEE Trans Biomed Eng.*, vol. 48, no.

3, pp. 302–311, 2001.
[41] U. Yeom, H.; Yoon, "ECG Artifact Removal from Surface EMG Using Adaptive Filter Algorithm," *Int. J. Multimed. Ubiquitous Eng.*, vol. 1, pp. 533–538, 2012.
[42] S. Lu, G.; Brittain, J.S.; Holland, P.; Yianni, J.; Green, A.L.; Stein, J.F.; Aziz, T.Z.; Wang, "Removing ECG noise from surface EMG signals using adaptive filtering.," *Neurosci. Lett.*, vol. 462, pp. 14–19, 2009.
[43] G. Balbinot, A.; Favieiro, "A Neuro-Fuzzy System for Characterization of Arm Movements," *Sensors*, vol. 13, pp. 2613–2630, 2013.
[44] B. Kendell, C.; Lemaire, E.D.; Losier, Y.; Chan, A.; Hudgins, "A novel approach to surface electromyography: An exploratory study of electrode-pair selection based on signal characteristics," *J. Neuro Eng. Rehabil.*, vol. 9, 2012.
[45] A. Kaur, R. Agarwal, and A. Kumar, "Comparison of muscles activity of abled bodied and aputee subjects for around shoulder movement," *Biomed Mater Eng.*, vol. 27, pp. 29–37, 2016.
[46] Gotman, J. and L.Y. Wang, "State dependent spike detection: Validation, Electroencephalogram and Clinical Neurophysiology neoralnetwork classifier," *IEEE Trans. on Boimed. Eng.*, vol. 47, no. 10, pp. 1400–1406, 2000.
[47] Mukhopadhyay, S. and G.C. Ray, "A new interpretation of nonlinear energy operator and its efficiency in spike detection," *IEEE Trans. on Biomedical Engineering*, vol. 45, no. 20, pp. 180–187, 1998.
[48] J.F. Kaiser, "On a simple algorithm to calculate the energy of a signal," in *IEEE Int. Conf Acoustic, Speech and Signal Processing, Albuquerque*, 1990, pp. 381–384.
[49] R.Q. Quiroga, Z. Nadasday and Y. Ben-shaul, "Unnsupervised spike detectionand sorting with wavelets and superparamagnetic clustering," *J. Neural Comput.*, vol. 10, pp. 1661–1687, 2004.
[50] N.M. López, E. Orosco and F. di Sciascio, "Surface electromyographic onset detection based on statistics and information content," in *J. Phys: Conf. Ser.*, 2011, pp. 12043–12050.
[51] R. Lauer and L. Prosser, "Use of the Teager–Kaiser energy operator for muscle activity detection in children," *Ann Biomed Eng.*, vol. 37, pp. 1584–1593, 2009.
[52] J. Kaiser, P. Maragos, and T. F. Quatieri, "Speech nonlinearities, modulations, and energy operators," in *Acoustics, Speech, and Signal Processing, 1991. ICASSP-91.*, 1991, p. 421--424.
[53] H. Semmaoui, J. Drolet, A. Lakhssassi, and M. Sawan, "Setting adaptive spike detection threshold for smoothed TEO based on robust statistics theory.," *IEEETrans. Biomed. Eng.*, vol. 59, pp. 836–841, 2012.
[54] P. Maragos, J. . Kaiser, and T. . Quatieri, "On amplitude and frequency demodulation using energy operators," *IEEE Transactions on Signal Processing*, vol. 41, no. 4, pp. 1532–1550, 1993.
[55] R. Hamila, R. M, M. Gabbouj, and J. Astola, "Time–frequency signal analysis using Teager Energy," in *Proceeding of fourth international conference on electronics, circuits and systems*, 1997, pp. 911–914.
[56] Z. Lin and J. Chen, "Advances in time-frequency analysis of biomedical signals, Crit.," *Rev. Biomed. Eng.*, vol. 24, pp. 1–72, 1996.
[57] S. Solnik, P. Rider and T. Hortobágyi, "Teager–Kaiser energy operator signal conditioning improves EMG onset detection," *Eur. J. Appl. Physol*, vol. 110, no. 3, p. 489--498., 2010.
[58] M. A. Dayan O, Spulber I, Eftekhar A, Georgiou P, Bergmann J, "Applying EMG Spike and Peak Counting for a Real-Time Muscle Fatigue Monitoring System," in *IEEE Biomedical Circuits and Systems Conference (BioCAS)*, 2012, pp. 41–44.

[59] K. Englehart, B. Hudgins, P. A. Parker, and M. Stevenson, "Classification of the Myoeletric Signal using Time-Frequency Based Representations.," *Medical Eng. {&} Physics*, vol. 21, pp. 431–438, 1999.
[60] M. R. Hogan N, "Myoelectric signal processing: optimal estimation applied to electromyography, Experimental demonstration of optimal myoprocessor performance.," *IEEE Trans Biomed Eng.*, vol. 27, no. 7, pp. 396–410, 1980.
[61] R. Hudgins, B.; Parker, P.; Scott, "A new strategy for multifunction myoelectric control.," *IEEE Trans. Biomed. Eng.*, vol. 1, p. 82--94., 1993.
[62] M. Hashemi, Zardoshti-Kermani, B. C. Wheeler, and K. Badie, "EMG feature evaluation for movement control of upper extremity prostheses," *IEEE Transactions on Rehabiliation Engineering.*, vol. 3, no. 4, pp. 324–333, 1995.
[63] I. O. Khalifa Md, R Ahsan M. I, "Neural Network Classifier for Hand Motion Detection from EMG Signal," in *5th Kuala Lumpur International Conference on Biomedical Engineering*, 2011, pp. 536–541.
[64] A. Phinyomark, F. Quaine, S. Charbonnier, C. Serviere, F. Tarpin-Bernard, and Y. Laurillau, "EM G Feature Evaluation for Improving Myoelectric Pattern Recognition Robustness," vol. 33, no. 0.
[65] A. Phinyomark, C. Limsakul, and P. Phukpattaranont, "A Novel Feature Extraction for Robust EMG Pattern Recognition," *Journal of Computing*, vol. 1, no. 1, pp. 71–80, 2009.
[66] W. M. Daud, A. B. Yahya, C. S. Horng, M. F. Sulaima, and R. Sudirman, "Features Extraction of Electromyography Signals in Time Domain on Biceps Brachii Muscle," *International Journal of Modeling and Optimization*, vol. 3, no. 6, pp. 515–519, 2013.
[67] A. Balbinot and G. Favieiro, "A neuro-fuzzy system for characterization of arm movements," *Sensors (Switzerland)*, vol. 13, no. 2, pp. 2613–2630, 2013.
[68] M. R. Al-Mulla, F. Sepulveda, and M. Colley, "A review of non-invasive techniques to detect and predict localised muscle fatigue," *Sensors*, vol. 11, no. 4, pp. 3545–3594, 2011.
[69] L. C. Merletti, "Surface EMG signal processing during isometric contractions," *J. Electromyogr. Kinesiol.*, vol. 7, p. 241--250., 1997.
[70] W. Z. Li, X.; Shin, H.; Zhou, P.; Niu, X.; Liu, J.; Rymer, "Power spectral analysis of surface electromyography (EMG) at matched contraction levels of the first dorsal interosseous muscle in stroke survivors.," *Clin. Neurophysiol*, vol. 125, pp. 988–994.
[71] H. Oskoei, M.; Hu, "GA-based feature subset selection for myoelectric classification," in *IEEE Int. Conf.*, 2006, pp. 1465–1470.
[72] A. Phinyomark, P. Phukpattaranont, and C. Limsakul, "Feature reduction and selection for EMG signal classification," *Expert Systems with Applications*, vol. 39, no. 8, pp. 7420–7431, 2012.
[73] T. T. Tsai, A.C.; Hsieh, T.H.; Luh, J.J.; Lin, "A comparison of upper-limb motion pattern recognition using EMG signals during dynamic and isometric muscle contractions.," *Biomed. Signal Process. Control*, vol. 11, p. 17--26., 2014.
[74] P. Bonato, S. H. Roy, M. Knaflitz and C. J. De Luca, "Time-frequency parameters of the surface myoelectric signal for assessing muscle fatigue during cyclic dynamic contractions," *IEEE Trans Biomed Eng*, vol. 48, no. 7, pp. 745–753, 2001.
[75] J. J. M. Sparto PJ1, Parnianpour M, Barria EA, "Wavelet analysis of electromyography for back muscle fatigue detection during isokinetic constant-torque exertions.," *Spine*, vol. 24, no. 17, pp. 1791–1798, 1999.
[76] R. Alexandre, "in cyclists and non-cyclists using Fourier," no. May, pp. 660–670, 2012.
[77] S. R. Dorcas D, "A three state myoelectric control," *Medical and Biological Engineering*, vol. 4, pp. 367–372, 1966.

[78] Hudgins, B., K. Englehart, P.A. Parker and R. N. Scott, "A microprocessor-based multifunction myoelectric control system," in *23rd Canadian Medical and Biological Engineering Society Conference*, 1997.

[79] T. Altimari, J. Dantas, T. Abrão, M. O, A. Moraes, and L. R, "Fourier and wavelet spectral analysis of EMG signals in supramaximal constant load dynamic exercise," in *Annual International Conference of the IEEE Engineering in Medicine and Biology*, 2010, pp. 1364–1367.

[80] M. R. Canal, "Comparison of wavelet and short time Fourier Transform methods in the analysis of EMG signals," *Journal of Medical Systems*, vol. 34, no. 1, pp. 91–94, 2010.

[81] R. Boostani and M. H. Moradi, "Evaluation of the forearm EMG signal features for the control of a prosthetic hand," *Physiological Measurement*, vol. 24, no. 2, pp. 309–319, 2003.

[82] M. G. Alkan, Ahmet, "Identification of EMG signals using discriminant analysis and SVM classifier," *Expert Systems with Applications*, vol. 39, no. 1, pp. 44–47, 2012.

[83] C. C. Kim and Jung, "A Real-time EMG-based Assistive Computer Interface for the Upper Limb Disabled. In , Noordwijk, The Netherlands.," in *Proceedings of the 2007 IEEE 10th International Conference on Rehabilitation Robotics*, 2007, pp. 459–462.

[84] F. Reaz, M. B. I.; Hussain, M. S. & Mohd-Yasin, "Techniques of EMG Signal Analysis: Detection, Processing, Classification and Applications," *Biological Procedures Online*, vol. 8, no. 1, pp. 11–35, 2006.

[85] A. Phinyomark, C. Limsakul and P. Phukpattaranont, "EMG Denoising Estimation Based on Adaptive Wavelet Thresholding for Multifunction Myoelectric Control," in *Proc. Conf. Innovative Technologies in Intelligent Systems and Industrial Applications*, 2009, pp. 171–176.

[86] M. Khezri, M. & Jahed, "Surface Electromyogram Signal Estimation based on Wavelet Thresholding Technique.," in *Proceedings of EMBS 2008 30th Annual International Conference of the IEEE Engineering in Medicine and Biology Society*, 2008, pp. 4752–4755.

[87] J. Rafiee, P. W. Tse, A. Harifi, and M. H. Sadeghi, "A novel technique for selecting mother wavelet function using an intelli gent fault diagnosis system," *Expert Systems with Applications*, vol. 36, no. 3 PART 1, pp. 4862–4875, 2009.

[88] S. Amsuess, P. Goebel, B. Graimann, and D. Farina, "A Multi-Class Proportional Myocontrol Algorithm for Upper Limb Prosthesis Control : Validation in Real-Life Scenarios on Amputees," *IEEE Transactions on Neural Systems and Rehabilitation Engineering*, vol. 23, no. 5, pp. 827–836, 2015.

[89] Y. Geng, P. Zhou, and G. Li, "Toward attenuating the impact of arm positions on electromyography pattern-recognition based motion classification in transradial amputees," *Journal of NeuroEngineering and Rehabilitation*, vol. 9, no. 1, p. 74, 2012.

[90] B. E. Boser, I. M. Guyon, and V. N. Vapnik, "A Training Algorithm for Optimal Margin Classiiers," *Proceedings of the fifth annual workshop on Computational learning theory*, pp. 144–152, 1992.

[91] K. T. Masahiro Yoshikawa, Masahiko Mikawa, "Real-time hand motion estimation using EMG signals with support vector machines," in *SICE-ICASE International Joint Conference*, 2006, pp. 593–598.

[92] H. Oskoei, Mohammadreza Asghari ; Huosheng, "Support Vector Machine-Based Classification Scheme for Myoelectric Control Applied to Upper Limb," *IEEE Transactions on Biomedical Engineering*, vol. 55, no. 8, pp. 1956–1965, 2008.

[93] N. S. Rekhi, A. S. Arora, S. Singh, and D. Singh, "Multi-Class SVM Classification of Surface EMG Signal for Upper Limb Function," in *3rd International Conference on Bioinformatics and Biomedical Engineering*, 2009, pp. 1–4.

[94] S. Guo, M. Pang, B. Gao, H. Hirata, and H. Ishihara, "Comparison of sEMG-based feature extraction and motion classification methods for upper-limb movement," *Sensors (Switzerland)*, vol. 15, no. 4, pp. 9022–9038, 2015.
[95] M. Leon and J. Gutierrez, "EMG pattern recognition using Support Vector Machines classifier for myoelectric control purposes," in *Health Care Exchanges*, 2011, pp. 175–178.
[96] K. Hosseini and H. Gholam, "Wavelet analysis of surface electromyography signals," in *26th Annual International Conference of the IEEE on Engineering in Medicine and Biology Society*, 2004, pp. 3832–3835.
[97] F. AlOmari and G. Liu, "Analysis of extracted forearm sEMG signal using LDA, QDA, K-NN classification algorithms," *Open Automation and Control Systems Journal*, vol. 6, no. 1, pp. 108–116, 2014.
[98] A. E. Kim Jonghwa, Mastnik Stephan, "EMG based hand gesture recognition for realtime biosignal interfacing," in *Proceedings of the 13th international conference on Intelligent user interfaces* ., 2008, p. 30.
[99] X. Wu *et al.*, *Top 10 algorithms in data mining*, vol. 14, no. 1. 2008.
[100] P. A. Alison E. Gibson, Mark R. Ison, "User independent hand motion classification with electromyography," in *Dynamic Systems and Control Conference*, 2013.
[101] E. Gokgoz and A. Subasi, "Comparison of decision tree algorithms for EMG signal classification using DWT," *Biomedical Signal Processing and Control*, vol. 18, pp. 138–144, 2015.
[102] A. A. Abdullah, A. Subasi, and S. M. Qaisar, "Surface EMG Signal Classification by Using WPD and Ensemble Tree Classifiers," in *IFMBE Proceedings*, 2017, pp. 475–481.
[103] M. Fernandez Delgado, E. Cernadas, S. Barro, D. Amorim, and D. Amorim Fernandez Delgado, "Do we Need Hundreds of Classifiers to Solve Real World Classification Problems?," *Journal of Machine Learning Research*, vol. 15, pp. 3133–3181, 2014.
[104] H. Soma, Y. Horiuchi, J. Gonzalez, and W. Yu, "Classification of Upper Limb Motions from Around Shoulder Muscle Activities," in *Advances in Applied Electromyography*, 2012.
[105] J. Gonzalez, "Classification of Upper Limb Motions from Around-Shoulder Muscle Activities: Hand Biofeedback{~}!2009-10-08{~}!2009-11-25{~}!2010-05-28{~}!," *The Open Medical Informatics Journal*, vol. 4, no. 2, pp. 74–80, 2010.
[106] H. Soma, Y. Horiuchi, and J. Gonzalez, "Preliminary Results of Online Classification of Upper Limb Activities," *Robotics (ICORR), 2011*, pp. 310–315, 2011.
[107] A. Araujo, F. Adson, dos S. Icaro, G. S. Iwens, and S. Sauro, "Development of a microcontrolled bioinstrumentation system for active control of leg prostheses," in *IEEE International Conference of the Engineering in Medicine and Biology Society*, 2008, pp. 2393–2396.
[108] P. Pandis, "Musculoskeletal Biomechanics of the Shoulder in Functional Activities," 2013.
[109] "Shoulder Anatomy." [Online]. Available: https://www.shoulderdoc.co.uk/section/342.
[110] P. Walia, "a Theoretical Model of the Effect of Bone Defects on Anterior Shoulder Instability : a Finite Element Approach," 2010.
[111] R. D. Dambrosia, "Shoulder Muscles," in *Musculoskeletal Disorders*, 1986, pp. 366–380.
[112] M. S. B. M. . Joel D. White, "Optimization of Muscle Physiological Parameters for a Computer Model," 2011.
[113] O. Lipploid, "The relation between integrated action potentials in the human muscle and its isometric tension," *J Physiol*, vol. 112, pp. 492–499, 1950.

[114] C. J. De Luca, “Description and Analysis of the EMG Signal,” in *Muscles Alive*, 1985, pp. 65–101.
[115] C. J. De Luca, “Surface Electromyography : Detection and Recording,” *DelSys Incorporated*, 2002. .
[116] J. M. WILLIAMS, “Surface Electromyography with in Equine Performance Analysis,” 2014.
[117] “Shoulder Joint.” [Online]. Available: https://www.pinterest.com/explore/shoulder-joint/.
[118] P. Heuberer, A. Kranzl, B. Laky, W. Anderl, and C. Wurnig, “Electromyographic analysis: shoulder muscle activity revisited,” *Archives of Orthopaedic and Trauma Surgery*, vol. 135, no. 4, pp. 549–563, 2015.
[119] J. C. De Luca, A. Adam, R. Wotiz, L. D. Gilmore, and S. H. Nawab, “Decomposition of surface EMG signals,” *J Neurophysiol*, vol. 96, no. 3, pp. 1646–1657, 2006.
[120] F. P. Analysis and A. L. Sclerosis, “Detailed Analysis of Clinical Electromyography Signals,” 2001.
[121] Z. Nenadic and J. W. Burdick, “Spike detection using the continuous wavelet transform.,” *Ieee Tbme*, vol. 52, no. 1, pp. 74–87, 2005.
[122] S. Kadambe, R. Murray and G. F. Boudreaux-Bartels, “Wavelet transform-based QRS complex detector,” *IEEE Trans. Biomed. Eng.*, vol. 46, pp. 838–848, 1999.
[123] I. N. Bankman, K. O. Johnson, and W. Schneider, “Optimal Detection, Classification, and Superposition Resolution in Neural Waveform Recordings,” *IEEE Transactions on Biomedical Engineering*, vol. 40, no. 8. pp. 836–841, 1993.
[124] L. Tang, F. Li, S. Cao, X. Zhang, and X. Chen, “Muscle synergy analysis for similar upper limb motion tasks,” *Conference proceedings : ... Annual International Conference of the IEEE Engineering in Medicine and Biology Society. IEEE Engineering in Medicine and Biology Society. Annual Conference*, vol. 2014, pp. 3590–3593, 2014.
[125] M. Rizk and P. Wolf, “Optimizing the automatic selection of spike detection thresholds using a multiple of the noise level,” *Medical & biological engineering & computing*, vol. 47, no. 9, pp. 955–966, 2009.
[126] R. Lauer and L. Prosser, “Use of the teager-kaiser energy operator for muscle activity detection in children,” *Annals of Biomedical Engineering*, vol. 37, no. 8. pp. 1584–1593, 2009.
[127] J. Drapała, K. Brzostowski, A. Szpala, and A. Rutkowska-Kucharska, “Two stage EMG onset detection method,” *Archives of Control Sciences*, vol. 22, no. 4, pp. 427–440, 2012.
[128] S. Solnik, P. Rider, K. Steinweg, and P. Devita, “Teager-Kaiser energy operator signal conditioning improves EMG onset detection,” *European Journal of Applied Physiology*, vol. 110, no. 3, pp. 489–498, 2010.
[129] P. Zhang, X.; Zhou, “Sample entropy analysis of surface EMG for improved muscle activity onset detection against spurious background spikes,” *J. Electromyogr. Kinesiol.*, vol. 22, pp. 901–907, 2012.
[130] A.L. Jacobsen, “Auto-threshold peak detection in physiological signals,” in *IEEE,Proceeding of the 23rd annual international conference of the Arab Emirates*, 2001, p. 2194–2195.
[131] A. Kaur, R. Agarwal and A. Kumar, “A combined statistical and time–frequency approach to the analysis of electromyography signals, InNational conferenceonadvances inmetrology, Springer,” in *National conference on advances inmetrology, Springer*, 2014, pp. 19–21.
[132] T. N. S. T. Zawawi, A. R. Abdullah, E. F. Shair, I. Halim, and O. Rawaida, “Electromyography signal analysis using spectrogram,” *Proceeding - 2013 IEEE*

Student Conference on Research and Development, SCOReD 2013, no. December, pp. 319–324, 2015.

[133] H. Moshou, D.; Hostens, I.; Papaioannou, G. & Ramon, "Wavelets and Self-organising Maps in Electromyogram (EMG) Analysis," in *Proceedings of ESIT 2000 European Symposium on Intelligent Techniques*, 2000, pp. 186–191.

[134] Z. Z. Zhang, Q. J. & Luo, "Wavelet De-noising of Electromyography," in *Proceedings of ICMA 2006 IEEE International Conference on Mechatronics and Automation*, 2006, pp. 1553–1558.

[135] P. Phinyomark, A. ; Limsakul, C. & Phukpattaranont, "EMG Feature Extraction for Tolerance of White Gaussian Noise," in *Proceedings of I-SEEC 2008 International Workshop and Symposium Science Technology*, 2008, pp. 178–183.

[136] "Spectral Approach for Emg Feature Extraction," pp. 60–101.

[137] A. I. Megahed, A. M. Moussa, H. B. Elrefaie, and Y. M. Marghany, "Selection of a suitable mother wavelet for analyzing power system fault transients," *IEEE Power and Energy Society 2008 General Meeting: Conversion and Delivery of Electrical Energy in the 21st Century, PES*, pp. 1–7, 2008.

[138] N. Al-Qazzaz, S. Hamid Bin Mohd Ali, S. Ahmad, M. Islam, and J. Escudero, "Selection of Mother Wavelet Functions for Multi-Channel EEG Signal Analysis during a Working Memory Task," *Sensors*, vol. 15, no. 12, pp. 29015–29035, 2015.

[139] M. Zecca, S. Micera, M. C. Carrozza, and P. Dario, "Control of Multifunctional Prosthetic Hands by Processing the Electromyographic Signal," *Critical Reviews? in Biomedical Engineering*, vol. 30, no. 4–6, pp. 459–485, 2002.

[140] H. S. Rayait, A. Shatru, and R. Agarwal, "Interpretations of Wrist/Grip Operations From SEMG Signals at Different Locations on Arm," *IEEE Transactions on Biomedical Circuits and Systems*, vol. 42, no. 2, pp. 101–111, 2010.

[141] K. Englehart, B. Hudgins, and A Parker Philip, "A Wavelet Based Continuous Classification Scheme for Multifunction Myoelectric Control," pp. 1–31.

[142] L. Hargrove, S. Member, G. Li, K. Englehart, and L. Hargrove, "Principal Components Analysis Preprocessing to improve Classification Accuracies in Pattern Recognition Based Myoelectric Control Corresponding author," vol. 56, no. 506, pp. 1–28, 2009.

[143] A. Subasi, "Classification of EMG signals using combined features and soft computing techniques," *Applied Soft Computing Journal*, vol. 12, no. 8, pp. 2188–2198, 2012.

[144] A. O. Andrade, Fernando E. R. Mattioli , Edgard A. Lamounier, Alexandre Cardoso, Alcimar B. Soares, "Classification of EMG signals using artificial neural networks for virtual hand prosthesis control," in *Annual International Conference of the IEEE Engineering in Medicine and Biology Society*, 2011, pp. 7354–7357.

[145] V. Hlavac, "Classifier performance evaluation." [Online]. Available: http://cmp.felk.cvut.cz/˜hlavac, hlavac@fel.cvut.cz.

[146] A. Fadlalla, "An experimental investigation of the impact of aggregation on the performance of data mining with logistic regression," *Journal Information and Management archive*, vol. 42, no. 5, pp. 695–707, 2005.

[147] Y. D. Hüseyin Eristi, Aysegül Ucar, "Wavelet-based feature extraction and selection for classification of power system disturbances using support vector machines," *Electric Power Systems Research*, vol. 80, no. 7, pp. 743–752, 2010.

[148] M. Weis, T. Rumpf, R. Gerhards, and L. Plymer, "Comparison of different classification algorithms for weed detection from images based on shape parameters," *Image analysis for agricultural products and processes*, vol. 69, no. 2005, pp. 53–64, 2009.

[149] A. A. Adewuyi, L. J. Hargrove, and T. A. Kuiken, "Evaluating EMG Feature and Classifier Selection for Application to Partial-Hand Prosthesis Control," *Frontiers in Neurorobotics*, vol. 10, no. October, pp. 1–11, 2016.

[150] F. Zhang *et al.*, “SEMG Feature Extraction Methods for Pattern Recognition of Upper Limbs,” pp. 222–227, 2011.
[151] R. P. S. Zhang X, Wang Yaan, “Wavelet Transform Theory and its Application in EMG Signal Processing,” in *Proceedings 7th International Conference on Fuzzy Systems and Knowledge Discovery*, 2010, pp. 2234–2238.
[152] R. Kumar, R. R. Das, V. N. Mishra, and R. Dwivedi, “A radial basis function neural network classifier for the discrimination of individual odor using responses of thick-film tin-oxide sensors,” *IEEE Sensors Journal*, vol. 9, no. 10, pp. 1254–1261, 2009.
[153] Tom Mitchell, *Machine Learning*. McGraw Hill, 2013.
[154] S. Shalev-Shwartz and S. Ben-David, *Understanding Machine Learning: From Theory to Algorithms*. 2014.
[155] Z. Ghahramani, “Learning : The view from different fields,” 2005.
[156] X. Zhu and A. B. Goldberg, “Introduction to Semi-Supervised Learning,” *Synthesis Lectures on Artificial Intelligence and Machine Learning*, vol. 3, no. 1, pp. 1–130, 2009.
[157] X. Li, “Hierarchical Classification and Its Application in University Search,” no. August, 2013.
[158] O. Sutton, “Introduction to k Nearest Neighbour Classification and Condensed Nearest Neighbour Data Reduction,” *Introduction to k Nearest Neighbour Classification*, pp. 1–10, 2012.
[159] T. G. Dietterich, *Machine learning in ecosystem informatics and sustainability*. 2009.
[160] P. Flach, *Machine Learning :The Art and Science of Algorithms that Make Sense of Data*. Cambridge university press, 2015.
[161] B. D. Shai and Shalev Shwartz Shai, *Understanding Machine Learning: From Theory to Algorithms*. 2014.
[162] T. Shaikhina, D. Lowe, S. Daga, D. Briggs, R. Higgins, and N. Khovanova, “Decision tree and random forest models for outcome prediction in antibody incompatible kidney transplantation,” *Biomedical Signal Processing and Control*, pp. 1–7, 2015.
[163] L. Camelia, “Strategies for Dealing with Real world Classification Problems,” 2010.

Publications in Refereed Journals and Conferences

[1] A. Kaur, R. Agarwal, and A. Kumar, “A combined statistical and time–frequency approach to the analysis of electromyography signals”, Proceedings of Third National Conference on Advances in Metrology, Metrology Society of India, 2014, pp. 107–108.

[2] A Kaur, R Agarwal and A Kumar, “Comparison of muscles-activity of non-amputee bodied and amputee subjects for shoulder movement”, Biomed Mater Eng., Vol. 27(1), 2016, pp. 29-37. (SCIE Impact Factor 0.99)

[3] A Kaur, R Agarwal and A Kumar, “Adaptive Threshold method for Peak Detection of Surface Electromyography Signal from Shoulder Muscle”, Journal of Applied Statistics, Vol. 21(6), 2017, pp. 1-13. (SCIE Impact Factor 0.6649)

[4] A. Kaur, A. Kumar, R. Agarwal, "Wavelet Based Machine Learning Technique to Classify the Different Shoulder Movement of Upper Limb Amputee", Journal of Biomimetic, Biomaterials and Biomedical Engineering, Vol. 31, 2017, pp. 32-43. (Scopus)

[5] A Kaur, R Agarwal and A Kumar, “Investigation of Surface Electromyography Signal Acquired from the shoulder Muscles of Upper Limb Amputees" [Accepted in ICBIR 2017: International Conference on Biomedical and Interdisciplinary Research, Singapore].

[6] A Kaur, R Agarwal and A Kumar, “Investigation of Surface Electromyography Signal for an Upper Limb Amputee”. Current Trends in Signal processing, Vol 7, No.1, 2017. (Accepted)

[7] A Kaur and A Kumar “SEMG Based Classification Using Wavelet Function for Around Shoulder Muscles”. Journal of Engineering Science and Technology Review.2017, Scopus. (Accepted).